Hydrodynamics with a Wall-Slip Boundary Condition for a Particle Moving Near a Plane Wall Bounding a Semi-Infinite Viscous Fluid

by

Michael Tevriz Kezirian

Bachelor of Science, Brown University
Division of Engineering

Submitted to the Department of Chemical Engineering
in partial fulfillment of the requirements for the degree of

Master of Science in Chemical Engineering

at the

MASSACHUSETTS INSTITUTE OF TECHNOLOGY

June 1992

Author .....
Department of Chemical Engineering
February 29, 1992

Certified by .....
Howard Brenner
Willard Henry Dow Professor of Chemical Engineering
Thesis Supervisor

Accepted by .....
William M. Deen
Chairman, Committee on Graduate Students
Department of Chemical Engineering

Hydrodynamics with a Wall-Slip Boundary Condition for a Particle Moving Near a Plane Wall Bounding a Semi-Infinite Viscous Fluid

by

Michael Tevriz Kezirian

Submitted to the Department of Chemical Engineering
on February 29, 1992, in partial fulfillment of the
requirements for the degree of
Master of Science in Chemical Engineering

Abstract

An analytical attempt is presented aimed at modelling the experimentally observed anomalous hydrodynamic behavior of a small spherical particle translating and/or rotating in 'contact' with a plane wall bounding a viscous fluid, at small Reynolds number. In particular, when the gap between the particle and wall is sufficiently small, non-continuum behavior becomes theoretically possible in the form of cavitation or 'Knudsen-like' flow. This may be the source of the known disparity existing between theoretical predictions and the experimental observations of Carty (1957). An 'empirical' attempt is made here to model such non-continuum behavior by relaxing the traditional no-slip boundary condition on the wall in the course of solving Stokes' equations for a sphere moving in very close proximity to a plane wall.

In particular, the results of exact (bipolar coordinate) creeping-flow calculations are presented for a sphere translating and rotating parallel to a plane wall bounding a semi-infinite viscous fluid for the case where a linear slip boundary condition is applied (uniformly) on the wall. These calculations reveal that the singular behavior one obtains for the classical no-slip case (in the limit where the sphere contacts the wall), is eliminated entirely by any degree of slip, however small. Thus, no-slip constitutes a singular boundary condition for the creeping flow equations. In the traditional no-slip case, the singularity is of order $\ln \epsilon$ where ϵ ($\ll 1$) is the sphere/plane-wall gap width, non-dimensionalized with the particle radius. In this slip scenario, nonzero translational and rotational motions of the sphere along the wall under the action of a finite force (and zero torque) (acting parallel to the wall) become possible.

The introduction of the slip coefficient on the plane presents a physical interpretation of what is happening hydrodynamically near points of contact between solid surfaces in relative motion. The matching of experimental data to the analytical model can be effected by a dimensionless slip coefficient, $\beta^{-1} = 2.88 \times 10^{-7}$, which is hardly distinguishable from the classical no slip case, $\beta^{-1} = 0$.

Based on the physical parameters in Carty's experiments, the dimensional slip

coefficient β' was found to range from 2.27×10^7 to 1.03×10^8 kg/(m^2 s) for experiments in oil, from 2.05×10^5 to 3.13×10^6 kg/(m^2 s) for experiments in water and to be 272 kg/(m^2 s) for the experiment in air.

Thesis Supervisor: Howard Brenner
Title: Willard Henry Dow Professor of Chemical Engineering

Acknowledgements

Numerous individuals have contributed to the development of this thesis. I wish to thank my research advisor Howard Brenner for his guidance in the direction of this project. The technical assistance of Professors Tony Davis and Howard Stone are also greatly appreciated. My course instructors, and in particular, Professors Kenny Breuer, Bob Brown and Jeff Tester have shown a personal interest and provided encouragement. Fellow members of the Macrotransport Research Centre, especially my good friend Rick Batycky, served as a sounding board for ideas and suggestions.

I am forever indebted to my family: my parents and four brothers, Peter, Eric, Stephen and Douglas, who have inspired and motivated me throughout my academic career.

Numerical computations in this thesis were performed, in part, on a CRAY X-MP at the MIT Supercomputer facility.

Support for this project was provided by the Office of Basic Energy Sciences of the United States Department of Energy and through a TRW Space and Technology Group Doctoral Fellowship.

Contents

List of Figures

List of Tables

Chapter 1

Background

Numerous engineering and physical applications rely on knowledge of the hydrodynamic resistance of particles near a wall bounding a viscous fluid. This thesis contributes to this field of research, an area which has been developing over the past 30 years. Practical applications include rheological measurements of neutrally buoyant suspensions in viscometers (Li *et al* 1988) and in a rolling ball viscometer (King *et al* 1991 and Maude 1961), adhesion of biological cells (Mege *et al* 1986) and flucculation of suspended particles in soil-liquid separation processes (Muhle 1985). More recently, attention has focused on particle removal from semiconductor chips in the context of clean-room environments (Turner *et al* 1989 and Ye *et al* 1991). A possible limiting factor in removing minute particles from computer chips has been the degree to which submicron particles adhere to surfaces. Understanding the hydrodynamic forces involved in such problems is an important step in the design of such clean rooms.

The motion of a spherical particle in a viscous fluid–and in particular the hydrodynamic force exerted on such particle in an otherwise quiescent fluid–is a fundamental application of the equations of viscous fluid motion.

The motion of a particle in an *unbounded* fluid has long been understood. According to Stokes' Law, a spherical particle translating at small Reynolds number through

an otherwise quiescent fluid will experience a force F_∞ of magnitude given by,

$$F_\infty = 6\pi\mu U a, \tag{1.1}$$

where μ is the viscosity of the fluid, U the particle velocity, and a the sphere radius. Likewise, a spherical particle rotating in an otherwise unbounded quiescent fluid will experience a couple of magnitude T_∞ given by

$$T_\infty = 8\pi\mu a^3\Omega, \tag{1.2}$$

where Ω is the angular velocity of the particle. In these unbounded fluid cases there are no 'cross' (coupling) terms. In other words, there is no torque exerted on a purely translating sphere, and no force on a purely rotating sphere. The principle of superposition, due to the linearity of the constituent equations, allows us to separate the distinct translational and rotational hydrodynamic resistance characteristics of a sphere in a combined state of translational and rotational motions in a quiescent (generally bounded) fluid.

For a spherical particle moving near a plane wall, the principle of superposition enables one to separately consider the two constituent motions, one parallel and one perpendicular to the plane. These two isolated motions are illustrated in Figures 1-1and 1-2. The diagrams show that the axes of rotation for the two cases are different. The principle of superposition enables the pure rotation and pure translation components to be isolated for both the parallel and perpendicular cases. Thus, to describe the arbitrary composite translational and rotational motions of a spherical particle through a viscous fluid bounded by a plane wall, one need only consider four composite motions–namely translation and rotation of a sphere moving parallel to and perpendicular respectively to a plane wall. As subsequently discussed, theoretical and experimental studies have been conducted to establish the hydrodynamic resistance to motion of a spherical particle proximate to a plane wall bounding an effectively semi-infinite viscous fluid medium.

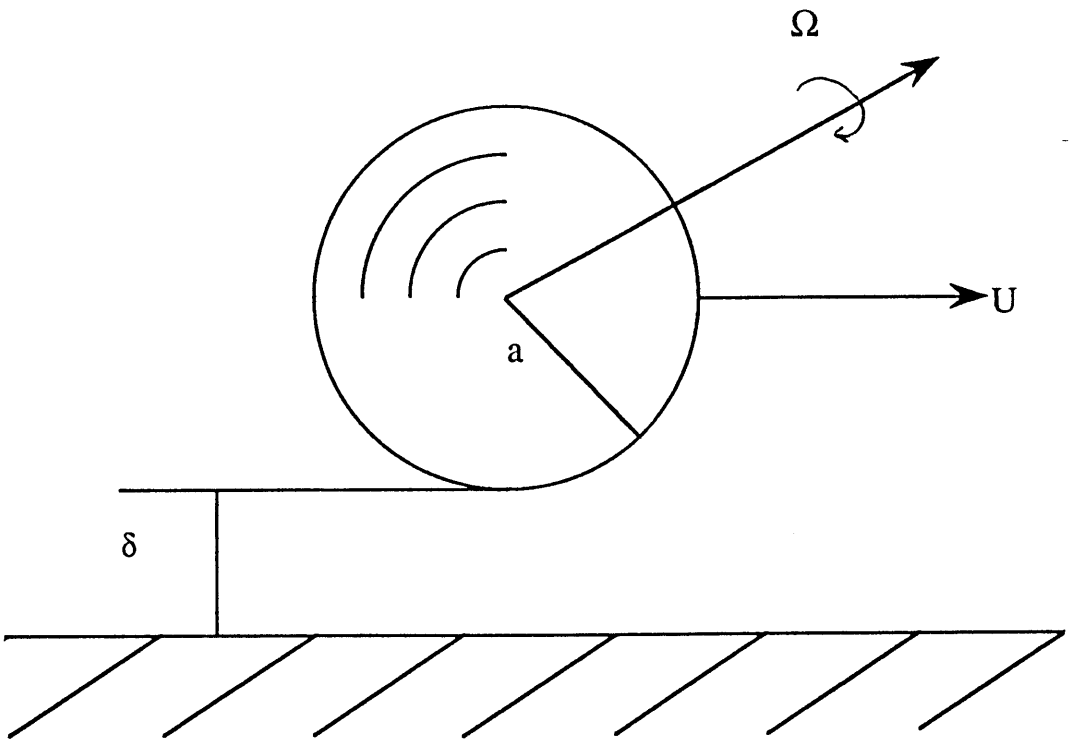

Figure 1-1: The motion of a sphere parallel to a plane wall

1.1 Exact Studies

The dimensionless separation distance ϵ is given by,

$$\epsilon = \frac{\delta}{a}. \tag{1.3}$$

The ϵ = O(1) case been fully described both analytically and numerically in the literature. Utilizing the principles of superposition, the perpendicular and parallel motion cases will be considered separately.

Sphere Moving Perpendicular to a Plane Wall

The solution for a sphere approaching a plane wall, i.e. the transverse or perpendicular case, was initially presented by Brenner (1961). In general this problem is axi-symmetric and therefore can be solved by introducing stream functions into the problem. The streaming flow equations in spherical bipolar coordinates are solved

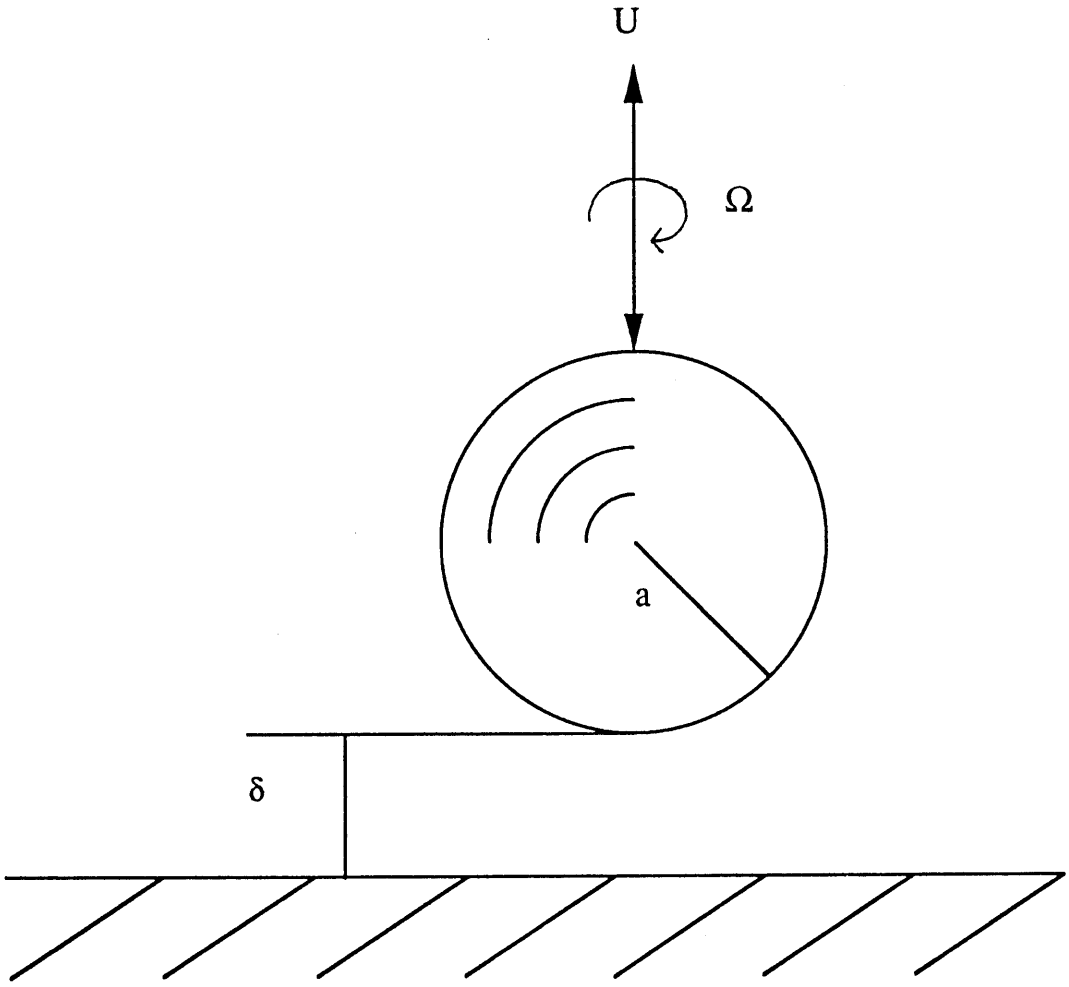

Figure 1-2: The motion of a sphere perpendicular to a plane wall.

for the case of zero Reynolds number flow. In general, the Stokes' Law correction for a particle moving towards a plane wall are given for all separation distances. When the sphere is far from the wall, the hydrodynamic force F_z, normalized with respect to the force that would exist in the absence of the plane given by F_∞ is given by,

$$\frac{F_z}{F_\infty} \simeq 1 + \frac{9}{8}\frac{a}{h}. \tag{1.4}$$

As pointed out by Brenner, this result agrees with the earlier work of Lorentz who obtained his value by the method of "reflexions".

As the sphere approached the wall, the hydrodynamic force tended towards infinity with order $1/\epsilon$.

Cox & Brenner (1967) developed this model further by evaluating the Reynolds Number correction terms, giving the distinct values for the motion of a sphere moving towards and away from a plane wall. By evaluating the sum of the infinite series, the order of the singularity inherent in the force terms was found to be $1/\epsilon$.

Experiments measuring the force exerted on a sphere as it approached a plane wall were performed by MacKay, Suzuki and Mason (1961 and 1963). In their experiments, the velocities of solid nylon spheres immersed in oil were measured for particles 2.0 to 2.7 mm in radius. Measurements were taken for separation distances less then 1.0 mm, corresponding to dimensionless distances less then 0.2.

Mackay *et al* (1961 and 1963) found their results to be in good agreement with Brenner's (1961) theoretical predictions over their entire range of experiments, including the small separation distances.

Ambari, Gauthier-Manuel and Guyon (1984) measured by magnetic levitation the force on a sphere whose position was kept fixed by an optical feedback system. For the case of a sphere approaching a wall they found their results to agree qualitatively with Brenner (1961). They also considered the case of sphere falling along the axis of a cylindrical tube in order to determine curvature effects to the parallel motion case.

Sphere Moving Parallel to a Plane Wall

The analytic solution describing the motion of a sphere moving parallel to a plane wall has been presented in the literature. It utilized spherical bipolar coordinates, as did the axi-symmetric, perpendicular motion case; however, the extent of symmetry was significantly less. Thus, a more complicated solution scheme was employed.

The solution in spherical bipolar coordinates was found by separation of variables following a standard transformation. A general series solution of the differential equations was obtained, one whose coefficients were calculated numerically for the prescribed set of boundary conditions. This problem was initially solved by Dean & O'Neill (1963) for the case of pure rotation and by O'Neill (1964) for the case of pure translation.

Goldman, Cox and Brenner (1967), extended the O'Neill model by considering the complete motion of the sphere, including 'coupling' effects. In addition an oversight was detected in Dean & O'Neill's numerical solutions.

Małysa & Van de Ven (1986) measured the rotational and translational velocities of a sphere moving at small Reynolds numbers parallel to a plane wall at dimensionless separation distances ϵ ranging from 0.006 to 1.8.

Carty (1957) measured the steady-state translational velocities of lucite, glass, steel and cellulose acetate spheres rolling down a smooth incline, under the influence of gravity, submerged in fluids of different viscosity. In each case the velocity was measured and the Reynolds number and resistance coefficient were measured. The range of sphere diameter based Reynolds numbers for these experiments was 2×10^{-2} - 9×10^{3}. Separate experiments were conducted in water, oil and air. Carty's correlation between the hydrodynamic resistance on the particle and the Reynolds number was independent of experimental parameters including the size of the particles and the nature of the materials. Carty did not measure the rotational velocities in his experiments but indicated that the spheres actually did roll. 'The spheres were allowed to roll several diameters before time was taken so as to be sure a steady velocity had been reached.'

Ambari *et al* (1983 and 1984) measured the translational velocity of a sphere falling

along the axis of a cylindrical tube, and they reported good agreement with O'Neill's (1964) exact studies for large separations ($4 \times 10^{-2} < \epsilon < 0.4$). The discrepancy between experiments and theory at close separations was attributed to the effect of curvature of the cylindrical tube wall.

The studies described above showed that for the case of $\epsilon = O(1)$, experimental observations and theoretical predictions were in good agreement.

1.2 Lubrication Studies

In the limit when the sphere touches the wall, in the limit $O(\epsilon \ll 1)$ lubrication techniques were used to evaluate the singular and order one terms in the force and torque expansions. Computations performed in this thesis are consistent with the earlier lubrication results.

Sphere Moving Perpendicular to a Plane Wall

Asymptotic methods have been used to study the problem of a sphere approaching a plane wall, in the limit when the separation distance goes to zero. G. I. Taylor's 'lubrication-theory' formula for a sphere approaching a wall gives the leading order term in the force expansion as

$$\frac{F_z}{F_\infty} \sim \frac{a}{(\delta - a)} \quad as\ a/h \to 1. \tag{1.5}$$

Cox & Brenner (1967) evaluated the leading order singular terms for a sphere with a small but non-zero velocity for a sphere approaching a wall. The wall correction factor is given by,

$$\frac{F_z}{F_\infty} = \frac{1}{\epsilon} + \frac{1}{5}\left(1 \pm \frac{1}{2}|Re| \ln \frac{1}{\epsilon}\right) + O(1). \tag{1.6}$$

Here Re is the Reynolds number based on the sphere radius given by,

$$|Re| = \frac{a|U|\rho}{\mu}. \tag{1.7}$$

The source of the $\pm|Re|$ term in the force expression is that the magnitude of the first order Reynolds number correction term depends on the direction of the sphere's motion. It takes a greater force to place a particle on a plane wall than it does to remove a particle from a plane wall.

To evaluate the nonsingular terms, tangent sphere coordinates were used to solve the problem when the sphere and wall were in contact. Cox & Brenner (1967) presented the solution to the axi-symmetric problem of a sphere rotating above a plane wall. In the limit when the sphere touches the wall, the hydrodynamic torque, T_z, was found to be finite and related by,

$$\frac{T_z}{T_\infty} = 1.202. \tag{1.8}$$

Experiments for the perpendicular motion case of a single sphere approaching a plane wall in the limit when the sphere touches the wall have not been reported in the literature. However, Małysa and Van de Ven (1985) have measured the hydrodynamic resistance of aggregates of spherical particles approaching a plane solid surface. They observed a tendency for the aggregates to rotate when they approached the surface. This agrees with the Cox & Brenner (1967) result giving a finite torque for small separations. Correlations of force to separation distance and orientation matched experimental observations except when the particle's orientation was nearly parallel to the wall, corresponding to the parallel case motion.

Sphere Moving Parallel to a Plane Wall

O'Neill & Stewartson (1967) utilized tangent sphere coordinates to represent the velocity field for the parallel motion case at small separation distances. Far from the point of contact, an 'outer' solution was constructed satisfying the boundary conditions, assuming no sphere-wall separation, ie $\epsilon = 0$. Near the point of contact, the 'inner' solution was generated, satisfying lubrication theory equations, and knowing the velocity gradients and pressure to be large. The 'inner' and 'outer' solutions were matched, fully describing the velocity field and enabling the hydrodynamic force and

torque to be computed. Goldman *et al* (1967) used lubrication theory to obtain the singular terms.

The force and torque on a sphere translating above a plane wall without rotating are given by,

$$\frac{F_x}{F_\infty} \simeq \frac{8}{15}\ln\frac{1}{\epsilon} + O(1), \tag{1.9}$$

$$\frac{T_y}{8\pi\mu U a^2} \simeq -\frac{1}{10}\ln\frac{1}{\epsilon} + O(1). \tag{1.10}$$

The force and torque exerted on a sphere rotating above a plane wall are given by,

$$\frac{F_x}{8\pi\mu a^2\Omega} \simeq -\frac{1}{10}\ln\frac{1}{\epsilon} + O(1), \tag{1.11}$$

$$\frac{T_y}{T_\infty} \simeq -\frac{2}{5}\ln\frac{1}{\epsilon} + O(1). \tag{1.12}$$

These results indicate that a sphere rolling down an inclined plane would actually not move. Both the translational velocity and its angular velocity would tend to zero as the sphere approached the wall. Balancing the torque on the sphere and noting the absence of external torques, the ratio of rotation to translation given by,

$$\frac{a\Omega}{U} \rightarrow \frac{1}{4} \quad as\ \epsilon \rightarrow 0. \tag{1.13}$$

For a sphere rolling without slipping, this ratio would equal one. Although the theory is not able to predict the actual velocities, it is able to determine the ratio of translation to rotation.

Only recently have studies reporting the rotation of a sphere moving parallel to a plane wall been presented in the literature. Chen & McLaughlin (1991) considered balls rolling down an inclined plane in silicone oil. The average and instantaneous rotational and translational velocities are reported for cases in which the Reynolds number ranged from 0.001 to 10 and the viscosity ranged from 20 cp to 9800 cp. The discrepancies between their results and the Goldman *et al* (1967) lubrication theory

results were attributed to surface roughness of the particles.

Chen & McLaughlin observed ratios of rotation to translation ranging from $a\Omega/\mu$ = -0.518 when δ = 76.1 Åto $a\Omega/\mu$ = -0.939 for δ = 0.98 Å. They claim their spheres had reached steady state motion and attribute instantaneous changes in velocity to changes in separation distance due to varying local surface roughnesses.

Goldman's *et al* (1967) analytical results are also in contradiction with Carty's experiments. The separation distance based on Goldman's *et al* (1967) solution found by matching Carty's data was of order 10^{-8} cm, less then the atomic radius of a single water molecule. A problem with Goldman's *et al* model then arises because a continuum of fluid between the particle and the wall can not exist across such a small gap width.

The separation distance is however, not the only inconsistency with observations. The singularity inherent in Goldman's *et al* results would mean that a particle sitting on a plane surface would require an infinite force to be pulled away. Similarly, it would take an infinite length of time for a particle approaching a wall to reach the plane surface.

1.3 Current Theories

Many possible explanations have been put forward as ways to interpret the disparities between Goldman's results and Carty's experiments.

Non-Newtonian effects have been proposed as a possible explanation for the shortcomings of the theoretical model. Near the contact point, a finite velocity difference over a separation distance which tends to zero leads to an infinite velocity gradient. Under such a scenario, it is not certain that the fluid remains perfectly Newtonian, and Non-Newtonian effects can drastically alter the theoretical behavior of the fluid.

It has been postulated that these infinite velocity gradients might lead to sphere or wall deformation. The problem of infinite velocity gradients might be resolved by not allowing the separation distance to approach zero. An infinite velocity gradient would cause pressure to tend to infinity resulting in system deformation. If the geometry of

the problem is changed, the symmetries inherent in the system no longer hold and the solution to the problem is no longer valid.

A large pressure difference might result in a change in viscosity. The theoretical model is only valid for a fluid with constant viscosity.

These three suggested explanations can not be used to resolve the disparities between the theoretical model and Carty's experimental data. They would lead to a nonlinear theoretical model, which is contrary to the experimental observations.

A fourth explanation is the possibility of fluid cavitation. Negative pressures arising from the motion of the sphere would generate cavities in the surrounding fluid. However, the singular behavior was observed by Carty independent of particle speed. It does not seem plausible to postulate the existence of fluid cavitation around an extremely slow moving particle. Also, if fluid cavitation were a contributing factor then the universal behavior of the hydrodynamic force would be dependent on fluid cavitation, and thus on particle speed. Carty did not observe this to be the case.

Sufficient experiments have been conducted to rule out each of these four explanations. Experiments could be proposed in which any one or all of these factors would affect the the hydrodynamic resistance on the particle. Enough experiments combined with real world observations preclude our discounting such discrepancies between the theoretical model and experimental data.

The theoretical model considers perfectly smooth surfaces, whereas the experiments were performed on real surfaces with roughnesses and impurities. Investigations are currently underway measuring the effects of roughness.

The experiments by Smart & Leighton (1989) show a correlation between the observed velocity of a sphere moving down an inclined plane and the roughness of the sphere surface. As the sphere rotated, the sphere's orientation shifted and the roughness near the point of contact varied. When this happened, it was argued that the hydrodynamic force changed resulting in a change of sphere velocity. As would be expected there was certain periodicity in the sphere's motion as a complete rotation sometimes resulted in the sphere's returning to its original orientation.

Małysa, Dąbroś and Van de Ven (1986) measured the force on a sphere sediment-

ing past another sphere attached to a plane wall and concluded that surface roughness was responsible for the observed deviations from symmetry. Because surface roughness was the only non-symmetric parameter in the problem, Malysa *et al* concluded that roughness must be the source of these non-symmetries. However, there was no attempt to quantify the extent of roughness present or correlate the particular roughness to the experimental results.

Carty's experiments indicate that roughness is not an important consideration. Carty's observed correlation was independent of the materials used. The experimental conditions were such that there were an enormous range of apparent roughnesses and in light of Carty's data, it does not seem possible to attribute the disparity between observation and prediction to roughness.

Carty measured velocity down an inclined plane and thus obtained averaged values for sphere velocity which in turn gave averaged values for the hydrodynamic force. Leighton & Smart focused on the instantaneous changes in velocity and correlated them to instantaneous changes in the hydrodynamic force experienced by the sphere.

One proposed explanation is that the existence of surface roughness and not the extent of roughness within certain limits is the important consideration which is omitted in the theoretical model. The experiments of Carty (1957) and Malysa *et al* (1986) would support this conclusion. However, Smart & Leighton's and Chen & McLaughlin (1991) results are at variance with this conclusion.

1.4 Slip Studies

When the gap width approaches the mean free path length of the fluid molecules, one can no longer assume the fluid adheres to surfaces near points of contact. When the Knudsen number in the vicinity of the contact point is of order 1 or higher, the basic assumptions which specify the boundary conditions of this problem are no longer valid. The remainder of this thesis examines the role of slip in the theoretical model.

As mentioned above, the ratio $a\Omega/U$ was found analytically to approach 1/4 when the sphere and the wall are in contact. There is a distinction between the observed

slipping of a sphere on a surface, and the macroscopic concept of particle slip on a surface. Nonetheless, suggesting the existence of particle slip does seem a viable possible hypothesis to explain the observed anomalous behavior.

Numerous researchers have presented solutions to sphere problems considering the slip boundary condition.

Brenner (1961) considered the case of a particle approaching a free interface in which the interface did not deform. For large separations, the wall correction factor can be approximated by,

$$\frac{F_z}{F_\infty} \simeq 1 + \frac{3}{4}\frac{a}{h} \tag{1.14}$$

This problem is hydrodynamically equivalent to the problem of a sphere approaching a plane wall with perfect slip on the wall. For this transverse case, at close separations the singularity inherent in the problem was reduced but the order of the singularity did not change. The wall correction factor for the force exerted on a sphere F_z^* scaled as $1/4\epsilon$ rather then $1/\epsilon$. Because the solution is still singular, introducing slip can not help explain the experimental observations.

Goren (1973) solved the problem of a sphere approaching a plane wall in which the partial slip boundary condition was applied on all surfaces. In this case, introducing slip significantly reduced the degree of the singularity inherent in the approach case. The author claims that the order of the singularity is reduced. However, the extent of the numerical calculations presented does not confirm this statement. In other words, all cases seemed to exhibit $\ln \epsilon$ singularity, although introducing slip seemed to reduce this term by as much as a factor of 100. Goren (1979) extended these results to include permeability on the plane wall.

Payatakes & Dassios (1987) presented the solution to a sphere approaching a plane wall utilizing stream functions in spherical bipolar coordinates. For varying degrees of slip β and permeability κ on all surfaces, the highest order singularity was removed as the separation distance went to zero. However, the change in the order of the singularity can be attributed to the permeability of the plane wall rather than the introduction of slip. The motion of a sphere towards a permeable wall with no slip

on the surfaces is not singular.

Nir(1980 and 1981) presents the solution to the problem of a sphere moving towards and away from a porous membrane. Introducing tangent sphere coordinates reduces the Stokes' equations to a fourth-order ordinary differential equation which is solved numerically using regular and singular perturbation techniques for high and low permeabilities respectively. Nir also shows a reduction in the order of the singularity for the force and torque. Again, the reduction in the order of the singularity could have been caused by allowing penetration at the wall rather then from relaxing the no-slip boundary condition. The hydrodynamic force and torque were not calculated for cases with impermeable surfaces and with the partial slip boundary condition.

O'Neill, Ranger and Brenner (1986) introduced a linear slip boundary condition to the problem of a sphere in arbitrary motion at the interface of a planar free surface bounding a semi-infinite viscous fluid. The introduction of the slightest degree of slip, represented by a large, but finite slip coefficient completely removed the highest order contact-line singularity that would have otherwise prevented the motion of a partially penetrating sphere normal to a planar free surface. Such a large slip coefficient was regarded as kinematically indistinguishable from the case of no slip represented by an infinite slip coefficient.

The results of O'Neill *et al* differed significantly from Goren's (1973) in the sense that a small amount of slip changed the order of the singularity. Goren's result showed the force varied drastically with the slip coefficient, however, the dependence on separation distance did not change with different slip coefficients. Even though changing the boundary conditions to perfect slip on all surfaces reduced by a factor of almost 100 the hydrodynamic resistance, the leading order force term was of order $\ln \epsilon$

Related Problems with Perfect Slip

The problem of a sphere moving near a plane wall with perfect slip is hydrodynamically equivalent to the problem of two spheres falling in an infinite fluid at zero

Reynolds number. The parallel case corresponds to two spheres falling side by side; and the transverse case corresponds to two balls falling one above the other. Once the spheres are given a velocity, ie once inertial terms are included, then the symmetries between the top and bottom spheres disappear and the plane midway between the two spheres is no longer shear free.

For zero Reynolds number motion, the two solutions can be taken as equivalent to the motion of a sphere near a plane wall bounding an otherwise quiescent fluid with perfect slip on the plane wall. The solution to two sphere problems are presented by Goldman, Cox and Brenner (1966) and discussed in more detail by Happel and Brenner (1965).

For a sphere translating parallel to a plane wall with the perfect sip boundary condition, the force wall correction factor in the limit when the sphere touches the wall was found to be 0.72469. The torque nondimensionalized in the usual way was found to approach the limiting value of 0.11865. For a sphere rotating above a stationary wall with the perfect slip boundary condition imposed on the wall, the force wall correction factor approached the limiting value of 0.15822. For this case, however, the hydrodynamic torque tended towards infinity as the separation distance approached zero. Based on these results, two spheres falling parallel to their line of center would not rotate. Thus, a sphere approaching a shear-free plane wall would not rotate.

Incorporating perfect slip on the sphere surface alone is hydrodynamically equivalent to the problem of the motion of a fluid bubble near a plane wall when the ratio of viscosities is appropriately set.

This problem was solved by Lee, Chadwick and Leal(1979) and Lee & Leal (1980). By appropriately setting the ratio of the viscosity of the bubble to the viscosity of the surrounding fluid, one can use these results to obtain the solution of a sphere with perfect slip moving near a plane wall in which no slip occurs.

For a sphere translating parallel to a plane, introducing complete slip removed he (force) singularity but not the (torque) singularity. The corresponding problem of a sphere rotating about an axis parallel to a nearby plane wall retained its torque

singularity for all viscosity ratios (all slip values).

Introducing slip on the sphere into the perpendicular motion case did not remove the (force) singularity. For the perpendicular rotation case, ie rotation about an axis perpendicular to a nearby plane wall, it was possible to remove the singularity in the hydrodynamic force by selecting an appropriate intermediate viscosity ratio. Both the corresponding complete slip and no-slip cases were singular.

Lee & Leal (1980) also considered the case of a bubble translating parallel to a fluid-fluid interface. Selecting the appropriate viscosity ratios enabled a hydrodynamically equivalent problem of complete slip on both the sphere and wall to be analyzed. The (force) singularity for this problem was removed in the scenario, but no evaluation of the (torque) singularity was presented.

Chapter 2

Problem Description

This thesis presents the theoretical description of a sphere moving at small Reynolds number parallel to a nearby plane wall bounding a semi-infinite viscous fluid. This chapter provides a physical description of the problem, details the coordinate systems used to specify the problem mathematically, and introduces several simplifications based on the underlying geometric symmetries of the problem.

2.1 Problem Formulation

As in Figure 2-1, consider a sphere of radius a whose center O translates with velocity U and which rotates with angular velocity Ω about an axis lying parallel to a plane wall bounding an otherwise quiescent, semi-infinite fluid ($0 < z < \infty$) of viscosity μ. The sphere center is situated at a distance h from the wall, so that the gap width δ (corresponding to the point of closest approach) is $\delta = h - a$.

The equations of low Reynolds number, incompressible fluid motion governing the velocity and pressure fields are

$$\mu \nabla^2 \underline{v} = \nabla p \tag{2.1}$$

and

$$\nabla \cdot \underline{v} = 0. \tag{2.2}$$

Semi-Infinite Region ($0 < z < \infty$)

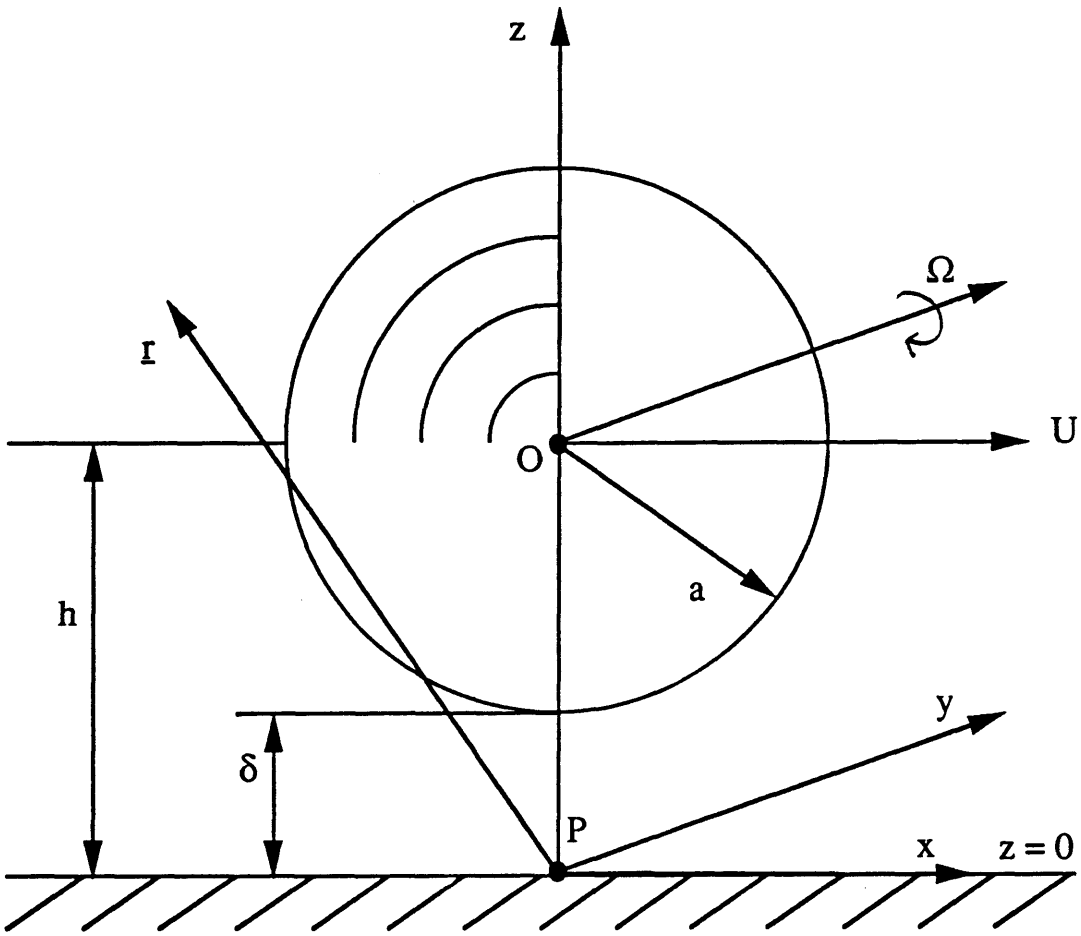

Figure 2-1: Sphere Translating and Rotating Near a Plane Wall

These are to be solved subject to the boundary conditions

$$\underline{v} = \underline{i}_x U + \underline{i}_y \Omega \times (\underline{r} - \underline{i}_z h) \quad at\ x^2 + y^2 + (z-h)^2 = a^2 \tag{2.3}$$

on the sphere, and

$$\left.\begin{array}{l} \underline{v} \to \underline{0} \\ p \to 0 \end{array}\right\} \quad as\ (|x|, |y|, z) \to \infty. \tag{2.4}$$

In the above, $\underline{r}$ is the position vector drawn from the "contact" point P on the plane wall, $(\underline{i}_x, \underline{i}_y, \underline{i}_z)$ are unit vectors collinear with the (x, y, z) axes. On the wall itself we take the boundary conditions to be

$$\underline{i}_z \cdot \underline{v} = 0 \quad at\ z = 0, \tag{2.5}$$

corresponding to the kinematical condition that the wall be impermeable to fluid, and

$$\underline{i}_z \cdot \underline{\underline{\tau}} \cdot \left\{ \begin{array}{c} \underline{i}_x \\ \underline{i}_y \end{array} \right\} = \beta' \underline{v} \cdot \left\{ \begin{array}{c} \underline{i}_x \\ \underline{i}_y \end{array} \right\} \qquad at\ z = 0, \tag{2.6}$$

corresponding to partial slip on the wall, with slip coefficient β'. Here,

$$\underline{\underline{\tau}} = \mu(\nabla \underline{v} + \nabla \underline{v}^{\dagger}) \tag{2.7}$$

is the deviatoric portion of the viscous stress tensor, with † denoting a transposition operator. The limiting case $\beta' \to \infty$ corresponds to the no-slip condition, $\underline{v} = \underline{0}$, on the wall, whereas $\beta' \to 0$ corresponds to the case of no tangential stress on the wall, $\tau_{xz}(\equiv \tau_{zx}) = \tau_{yz}(\equiv \tau_{zy}) = 0$ at $z = 0$.

2.2 Linear Superposition of Solutions

Owing to the linearity of the governing equations of motion, (2.1)-(2.5), the solution $(\underline{v}, p)$ of the system can be expressed as the sum

$$\underline{v} = \underline{v}^t + \underline{v}^r, \tag{2.8}$$

$$p = p^t + p^r, \tag{2.9}$$

where the respective translational and rotational contributions $(\underline{v}^t, p^t)$ and $(\underline{v}^r, p^r)$ to the total velocity field $(\underline{v}, p)$ satisfy Equations (2.1)-(2.2) as well as (2.4) - (2.6) and the respective boundary conditions

$$\left.\begin{aligned} \underline{v}^t &= \underline{i}_x U \\ \underline{v}^r &= \underline{i}_y \Omega \times (\underline{r} - \underline{i}_z h) \end{aligned}\right\} \quad at\ x^2 + y^2 + (z-h)^2 = a^2 \tag{2.10}$$

on the sphere.

Likewise, owing to linearity, the total hydrodynamic force $\underline{F}$ and torque $\underline{T}$ (the latter about the sphere center O) exerted by the fluid on the sphere can be expressed in the respective forms

$$\begin{aligned} \underline{F} &= \underline{F}^t + \underline{F}^r, \\ \underline{T} &= \underline{T}^t + \underline{T}^r. \end{aligned} \tag{2.11}$$

By symmetry (Goldman *et al*, 1967) one can show that

$$\underline{F} = \underline{i}_x F \tag{2.12}$$

and

$$\underline{T} = \underline{i}_y T \tag{2.13}$$

for both the t and r motions.

2.3 Bipolar Spherical Coordinates

It is useful to introduce circular cylindrical and spherical bipolar coordinate systems to describe the sphere-plane wall system geometrically. The origin P of the cylindrical polar coordinate system lies on the plane directly below the center of the sphere, as illustrated in Figure 2-2.

Transformation from Cartesian coordinates to cylindrical polar coordinates is described by:

$$\begin{aligned} x &= \rho \cos \phi \\ y &= \rho \sin \phi \\ z &= z \end{aligned} \tag{2.14}$$

Introducing spherical bipolar coordinates enables both boundaries to be parameterized by a single coordinate, with $\xi = 0$ specifying the plane wall and $\xi = \alpha$ specifying the sphere. This coordinate system has been used extensively to solve sphere-plane wall problems in fluid mechanics and other fields as well.

For a more detailed description of these coordinate systems, see Happel and Brenner (1983) and Appendix A of this text.

Bipolar coordinates formed by the ρ and z axes in the cylindrical coordinate system, as shown in Figure 2-3, are defined by the transformation,

$$z + i\rho = ic \cot \left[\frac{1}{2}(\eta + i\xi)\right], \tag{2.15}$$

from which one may obtain,

$$\begin{aligned} z &= c\frac{\sinh \xi}{\cosh \xi - \cos \eta}, \\ \rho &= c\frac{\sin \eta}{\cosh \xi - \cos \eta}. \end{aligned} \tag{2.16}$$

The constant, c, in the above equations is a constant determined from system dimensions.

One can fully describe the sphere-plane wall system by restricting the coordinates

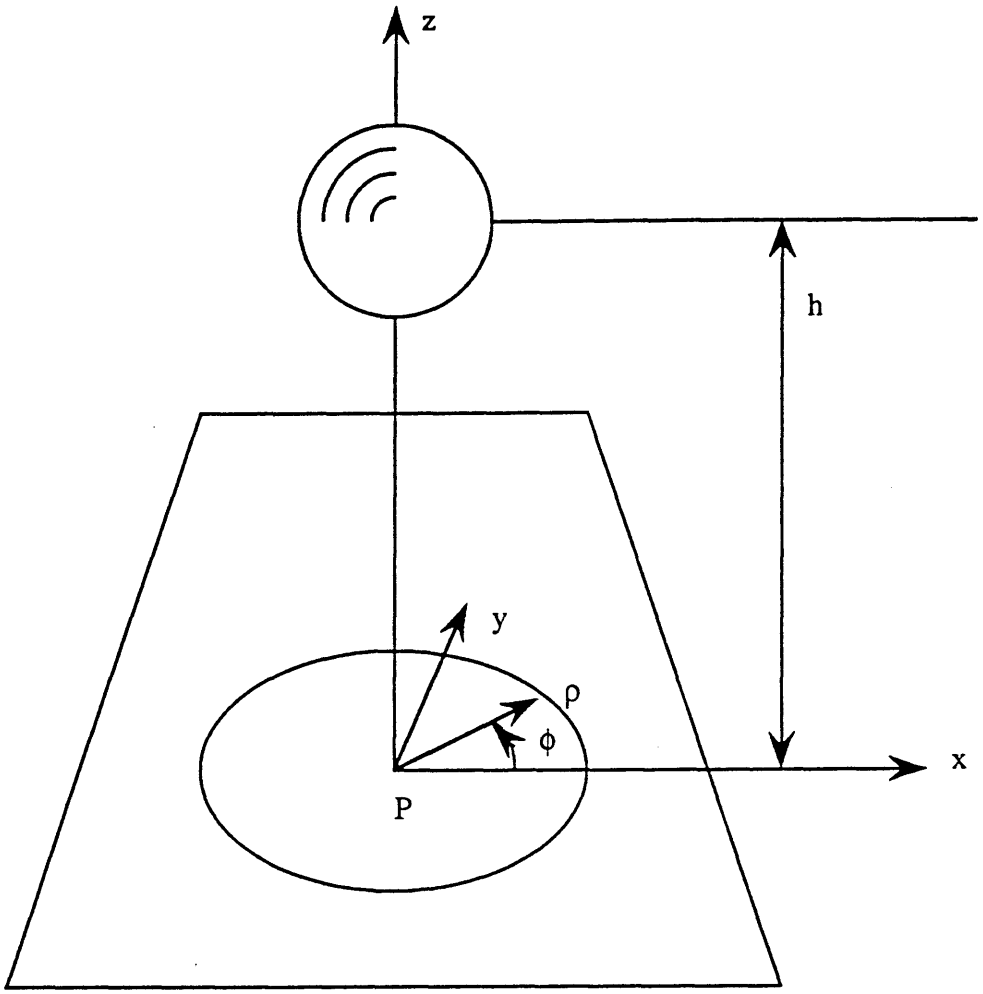

Figure 2-2: Cylindrical Polar Coordinate System

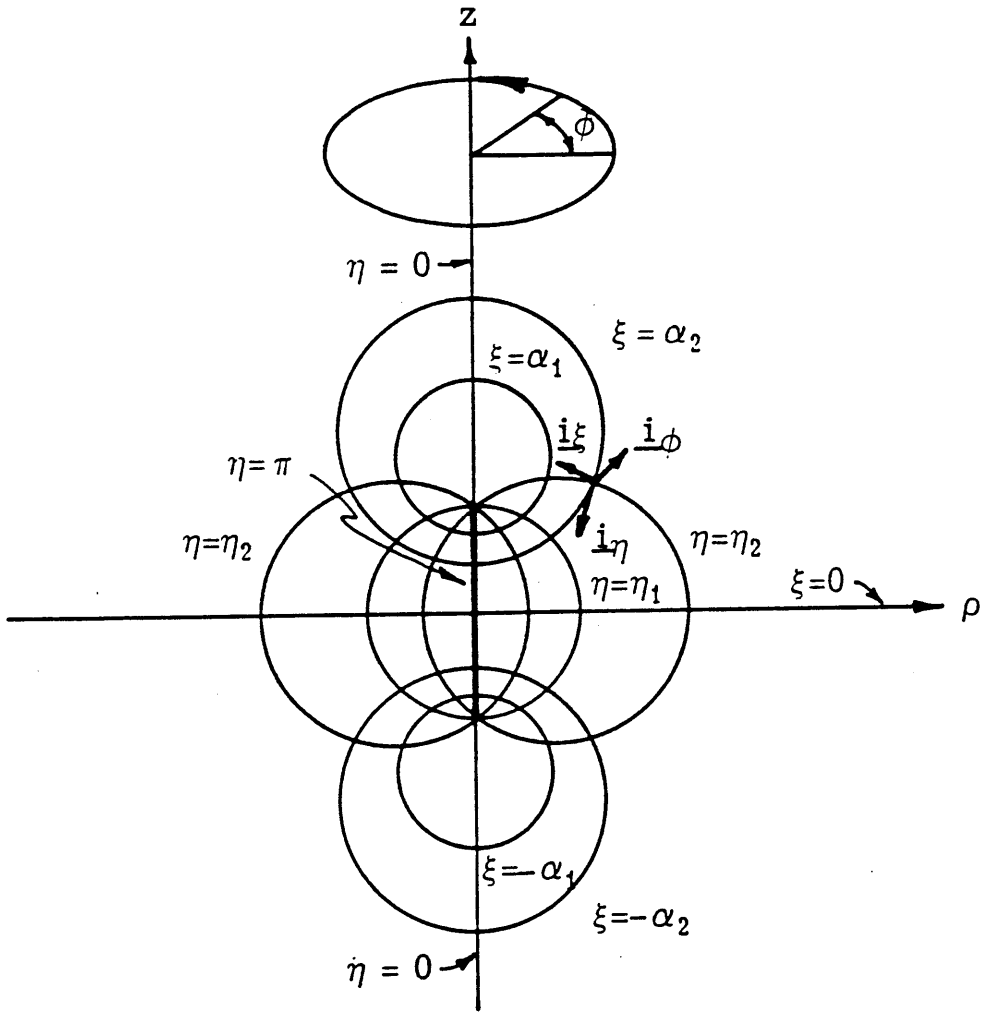

Figure 2-3: Spherical Bipolar Coordinate System

to the following ranges:

$$\begin{aligned} 0 \leq \ \eta \ &\leq \pi \\ 0 \leq \ \xi \ &\leq \infty \\ 0 \leq \ \phi \ &\leq 2\pi. \end{aligned} \tag{2.17}$$

In summary, the bipolar coordinate system is governed by the following transformations:

Cylindrical:

$$\begin{aligned} \rho &= c\frac{\sin\eta}{(\cosh\xi - \cos\eta)}, \\ \phi &= \phi, \\ z &= c\frac{\sinh\xi}{(\cosh\xi - \cos\eta)}; \end{aligned} \tag{2.18}$$

Cartesian:

$$\begin{aligned} x &= c\frac{\sin\eta\cos\phi}{(\cosh\xi - \cos\eta)}, \\ y &= c\frac{\sin\eta\sin\phi}{(\cosh\xi - \cos\eta)}, \\ z &= c\frac{\sinh\xi}{(\cosh\xi - \cos\eta)}. \end{aligned} \tag{2.19}$$

The constant, c, is derived by combining Equations (2.19), giving

$$(z - c\coth\xi)^2 + (x^2 + y^2) = (c\ \mathrm{csch}\alpha)^2. \tag{2.20}$$

For $\xi \geq 0$, Equation (2.20) describes a family of spheres $\xi = \alpha =$ constant in the semi-infinite domain $0 \leq z \leq \infty$. Appropriately selecting parameters, enables the sphere surface to be specified. Upon setting the sphere radius $r = a$ and locating the sphere center at $z = h$, Equation (2.20) furnishes the values of the parameters c and

α as

$$\begin{aligned} a &= c\,\mathrm{csch}\alpha, \\ h &= c\,\coth\alpha; \end{aligned} \tag{2.21}$$

that is

$$c = a\sinh\alpha \tag{2.22}$$

and

$$\cosh\alpha = \frac{h}{a}, \tag{2.23}$$

or, equivalently,

$$\alpha = \ln\left[\frac{h}{a} + \sqrt{\left(\frac{h}{a}\right)^2 - 1}\right]. \tag{2.24}$$

Chapter 3

Force and Torque on a Translating Sphere

The translational and rotational motions of a sphere at small Reynolds number can be decomposed into simpler constituent motions as discussed in Equations (2.8) and (2.9). This chapter considers the case of pure translation. This solution for the case where no-slip boundary conditions are imposed on all surfaces has been presented by O'Neill (1963). His solution scheme, appropriately modified to take account of slip, is followed here.

3.1 Governing Equations

The creeping flow equations (2.1) may be written in the cylindrical polar coordinate system of Figure 2-2 as (Happel & Brenner 1983)

$$\frac{1}{\mu}\frac{\partial p^t}{\partial \rho} = (\nabla^2 - \frac{1}{\rho^2})v_\rho^t - \frac{2}{\rho^2}\frac{\partial v_\phi^t}{\partial \phi} \tag{3.1}$$

$$\frac{1}{\mu}\frac{1}{\rho}\frac{\partial p^t}{\partial \phi} = (\nabla^2 - \frac{1}{\rho^2})v_\phi^t + \frac{2}{\rho^2}\frac{\partial v_\rho^t}{\partial \phi}, \tag{3.2}$$

$$\frac{1}{\mu}\frac{\partial p^t}{\partial z} = \nabla^2 v_z^t \tag{3.3}$$

where

$$\nabla^2 \equiv \frac{\partial^2}{\partial \rho^2} + \frac{1}{\rho}\frac{\partial}{\partial \rho} + \frac{1}{\rho^2}\frac{\partial^2}{\partial \phi^2} + \frac{\partial^2}{\partial z^2}. \tag{3.4}$$

Similarly, the continuity equation (2.2) is

$$\frac{1}{\rho}\frac{\partial \rho v_\rho^t}{\partial \rho} + \frac{1}{\rho}\frac{\partial v_\phi^t}{\partial \phi} + \frac{\partial v_z^t}{\partial z} = 0. \tag{3.5}$$

Upon taking advantage of the symmetries in the problem (Dean & O'Neill 1963), the pressure and velocity fields can be expressed in terms of auxiliary functions as

$$c\, p^t = \mu U W^t \cos\phi\,, \tag{3.6}$$

$$c\, v_\rho^t = \frac{1}{2} U[\rho W^t + c\,(X^t + Y^t)]\cos\phi, \tag{3.7}$$

$$c\, v_\phi^t = \frac{1}{2} U c[X^t - Y^t]\sin\phi, \tag{3.8}$$

$$c\, v_z^t = \frac{1}{2} U[z W^t + 2c\, Z^t]\cos\phi. \tag{3.9}$$

In these expressions, c is the constant (2.22). It is assumed that the auxiliary functions, W^t, X^t, Y^t and Z^t are functions only of ρ and z. While the solution scheme (3.6)-(3.9) has only been shown to hold for the non-slip case (O'Neill 1963), we assume subject to *a posteriori* verification that the same representation holds for the partial slip case.

Substituting of Equations (3.6)-(3.9) into (3.1)-(3.5) yields the following system of differential equations governing the auxiliary functions:

$$\frac{\partial^2 W^t}{\partial \rho^2} + \frac{1}{\rho}\frac{\partial W^t}{\partial \rho} - \frac{W^t}{\rho^2} + \frac{\partial^2 W^t}{\partial z^2} = 0 \tag{3.10}$$

$$\frac{\partial^2 X^t}{\partial \rho^2} + \frac{1}{\rho}\frac{\partial X^t}{\partial \rho} - \frac{4X^t}{\rho^2} + \frac{\partial^2 X^t}{\partial z^2} = 0, \tag{3.11}$$

$$\frac{\partial^2 Y^t}{\partial \rho^2} + \frac{1}{\rho}\frac{\partial Y^t}{\partial \rho} + \frac{\partial^2 Y^t}{\partial z^2} = 0, \tag{3.12}$$

$$\frac{\partial^2 Z^t}{\partial \rho^2} + \frac{1}{\rho}\frac{\partial Z^t}{\partial \rho} - \frac{Z^t}{\rho^2} + \frac{\partial^2 Z^t}{\partial z^2} = 0, \tag{3.13}$$

$$3W^t + \rho\frac{\partial W^t}{\partial \rho} + z\frac{\partial W^t}{\partial z} + c\frac{\partial Y^t}{\partial \rho} + c\frac{\partial X^t}{\partial \rho} + \frac{2c}{\rho}X^t + 2c\frac{\partial Z^t}{\partial z} = 0. \qquad (3.14)$$

3.2 Solution

The solutions of Equations (3.10)-(3.13) are most easily effected in spherical bipolar coordinates (Jeffrey 1915). The solution to these particular equations that is regular at $\eta = 0$ and π and satisfies the no-penetration boundary condition (2.5) is given by (Dean & O'Neill 1963)

$$\begin{aligned}
Z^t &= (\cosh\xi - \cos\eta)^{(1/2)} \sin\eta \\
&\quad \sum_{n=1}^{\infty} [A_n^t \sinh(n+\frac{1}{2})\xi] P'_n(\cos\eta), \qquad (3.15) \\
W^t &= (\cosh\xi - \cos\eta)^{(1/2)} \sin\eta \\
&\quad \sum_{n=1}^{\infty} [B_n^t \cosh(n+\frac{1}{2})\xi + C_n^t \sinh(n+\frac{1}{2})\xi] P'_n(\cos\eta), \qquad (3.16) \\
Y^t &= (\cosh\xi - \cos\eta)^{(1/2)} \\
&\quad \sum_{n=0}^{\infty} [D_n^t \cosh(n+\frac{1}{2})\xi + E_n^t \sinh(n+\frac{1}{2})\xi] P_n(\cos\eta), \qquad (3.17) \\
X^t &= (\cosh\xi - \cos\eta)^{(1/2)} \sin^2\eta \\
&\quad \sum_{n=2}^{\infty} [F_n^t \cosh(n+\frac{1}{2})\xi + G_n^t \sinh(n+\frac{1}{2})\xi] P''_n(\cos\eta), \qquad (3.18)
\end{aligned}$$

where $A_n^t, ..., G_n^t$ are constants to be determined. In these equations, P_n is the Legendre Polynomial of order n, and the primes denote differentiation with respect to $\cos\eta$; that is, $P'_n(\lambda) = dP'_n(\lambda)/d\lambda$ with $\lambda = \cos\eta$.

The coefficients in these series expansions are determined by satisfying the boundary conditions and continuity equations, as follows:

3.3 Boundary Conditions

On the sphere the no-slip boundary condition, as expressed by Eq. (2.10) is imposed. In cylindrical coordinates, the sphere surface velocity can be represented as:

$$\left.\begin{aligned} v_\rho^t &= U\cos\phi \\ v_\phi^t &= -U\sin\phi \\ v_z^t &= 0 \end{aligned}\right\} \quad at\ \xi = \alpha. \tag{3.19}$$

Expressed in terms of the auxiliary functions, the no-slip boundary condition on the sphere requires that

$$\left.\begin{aligned} W^t &= -\frac{2c}{z}Z^t \\ X^t &= \frac{\rho}{z}Z^t \\ Y^t &= 2+\frac{\rho}{z}Z^t \end{aligned}\right\} \quad at\ \xi = \alpha. \tag{3.20}$$

In spherical bipolar coordinates, these conditions become

$$\left.\begin{aligned} W^t &= -\frac{2(\cosh\alpha-\cos\eta)}{\sinh\alpha}Z^t \\ X^t &= \frac{\sin\eta}{\sinh\alpha}Z^t \\ Y^t &= 2+\frac{\sin\eta}{\sinh\alpha}Z^t \end{aligned}\right\} \quad at\ \xi = \alpha. \tag{3.21}$$

Our solution is required to satisfy these three conditions imposed on the auxiliary functions. Substituting the series solution to the auxiliary functions, Eqs. (3.15)-(3.18), and evaluating these expressions at $\xi = \alpha$, an infinite series expansion in η is obtained. Integrating over the range of η, $(0 \le \eta \le \pi)$, with respect to the appropriate weighting function gives the following recursion relations from the boundary conditions on the sphere:

$$C_n^t = -\coth(n+\frac{1}{2}\alpha)B_n^t - 2\coth\alpha A_n^t + \frac{2}{\sinh\alpha}\times \tag{3.22}$$
$$\left[\frac{(n+2)}{(2n+3)}\frac{\sinh(n+\frac{3}{2})\alpha}{\sinh(n+\frac{1}{2})\alpha}A_{n+1}^t + \frac{(n-1)}{(2n-1)}\frac{\sinh(n-\frac{1}{2})\alpha}{\sinh(n+\frac{1}{2})\alpha}A_{n-1}^t\right] \quad (n\geq 0),$$

$$E_n^t = \frac{2\sqrt{2}\exp\left(-(n+\frac{1}{2})\xi\right)}{\sinh(n+\frac{1}{2})\alpha)} - \coth(n+\frac{1}{2}\alpha)D_n^t + \frac{1}{\sinh\alpha}\times \tag{3.23}$$
$$\left[\frac{(n+1)(n+2)}{(2n+3)}\frac{\sinh(n+\frac{3}{2})\alpha}{\sinh(n+\frac{1}{2})\alpha}A_{n+1}^t - \frac{n(n-1)}{(2n-1)}\frac{\sinh(n-\frac{1}{2})\alpha}{\sinh(n+\frac{1}{2})\alpha}A_{n-1}^t\right] \quad (n\geq 1),$$

$$G_n^t = -\coth(n+\frac{1}{2}\alpha)F_n^t + \frac{1}{\sinh\alpha}\times \tag{3.24}$$
$$\left[-\frac{1}{(2n+3)}\frac{\sinh(n+\frac{3}{2})\alpha}{\sinh(n+\frac{1}{2})\alpha}A_{n+1}^t + \frac{1}{(2n-1)}\frac{\sinh(n-\frac{1}{2})\alpha}{\sinh(n+\frac{1}{2})\alpha}A_{n-1}^t\right] \quad (n\geq 2).$$

Appendix B presents recursion relations and integral relations for Legendre Polynomials.

On the plane, the partial slip boundary condition as expressed by Eqs. (2.5)-(2.6) is given in cylindrical coordinates as

$$\left.\begin{aligned}\beta' v_\rho^t &= \tau_{\rho z}^t \\ \beta' v_\phi^t &= \tau_{\phi z}^t \\ v_z^t &= 0\end{aligned}\right\} \quad at\ z=0. \tag{3.25}$$

The condition of no penetration on the plane wall, $v_z^t = 0$, has already been satisfied. Expressing the derivatives in cylindrical coordinates these boundary conditions become

$$\left.\begin{aligned}\frac{\partial v_z^t}{\partial\rho} + \frac{\partial v_\rho^t}{\partial z} - \frac{\beta'}{\mu}v_\rho^t &= 0 \\ \frac{\partial v_\phi^t}{\partial z} + \frac{1}{\rho}\frac{\partial v_z^t}{\partial\phi} - \frac{\beta'}{\mu}v_\phi^t &= 0\end{aligned}\right\} \quad at\ z=0. \tag{3.26}$$

Substituting Eqs. (3.6)-(3.9), the velocity and stress components can be expressed in terms of the auxiliary functions as

$$\left.\begin{aligned} \rho\frac{\partial W^t}{\partial z} - \frac{\beta' c}{\mu}\rho W^t + \frac{\partial X^t}{\partial z} + \frac{\partial Y^t}{\partial z} - \frac{\beta' c}{\mu}(X^t + Y^t) &= 0 \\ \frac{\partial X^t}{\partial z} - \frac{\partial Y^t}{\partial z} - \frac{\beta'}{\mu}(X^t - Y^t) &= 0 \end{aligned}\right\} \text{at } z = 0. \quad (3.27)$$

As an alternate method, the boundary condition on the plane, given by Eqs. (2.5)-(2.6) can be expressed in spherical bipolar coordinates as

$$\left.\begin{aligned} \beta' v_\eta^t &= \tau_{\eta\xi}^t \\ \beta' v_\phi^t &= \tau_{\phi\xi}^t \\ v_\xi^t &= 0 \end{aligned}\right\} \text{at } \xi = 0. \quad (3.28)$$

This third constraint, no penetration on the wall, $v_\xi^t = 0$, has already been satisfied. Substituting the series solution to the auxiliary functions into Eq. (3.28), the boundary condition takes the form of the following two relations:

$$\left.\begin{aligned} \frac{\beta' c}{\mu}(X^t - Y^t) &= (1 - \cos\eta)\left(\frac{\partial X^t}{\partial \xi} - \frac{\partial Y^t}{\partial \xi}\right) \\ \frac{\beta' c}{\mu}(\frac{\rho}{c}W^t + X^t + Y^t) &= (1 - \cos\eta)\left(\frac{\rho}{c}\frac{\partial W^t}{\partial \xi} + \frac{\partial X^t}{\partial \xi} + \frac{\partial Y^t}{\partial \xi}\right) \end{aligned}\right\} \text{at } \xi = 0. \quad (3.29)$$

Both forms of the boundary condition, Eqs. (3.27) and (3.29) can be expressed in terms of the coefficients $(A_n^t, B_n^t, ...G_n^t)$ by

$$\begin{aligned} &\sin^2\eta \sum_{n=1}^{\infty} C_n^t (n + \frac{1}{2}) P'_n - \frac{\beta' c}{\mu}(1 + \cos\eta) \sum_{n=1}^{\infty} B_n^t P'_n \\ &+2(1 - \cos\eta)\sin^2\eta \sum_{n=2}^{\infty} G_n^t (n + \frac{1}{2}) P''_n - 2\frac{\beta' c}{\mu}\sin^2\eta \sum_{n=2}^{\infty} F_n^t P''_n = 0, \quad (3.30) \end{aligned}$$

and

$$
\begin{aligned}
&-(1-\cos\eta)\sum_{n=0}^{\infty} E_n^t(n+\frac{1}{2})P_n + \frac{\beta' c}{\mu}\sum_{n=0}^{\infty} D_n^t P_n \\
&+(1-\cos\eta)\sin^2\eta\sum_{n=2}^{\infty} G_n^t(n+\frac{1}{2})P''_n - \frac{\beta' c}{\mu}\sin^2\eta\sum_{n=2}^{\infty} F_n^t P''_n \;=\; 0. \qquad (3.31)
\end{aligned}
$$

The principles of orthogonality used to satisfy the boundary condition on the sphere were used to obtain the following recursion relations for the boundary condition on the wall,

$$
\begin{aligned}
&-\frac{(n+2)(n+3)}{2(2n+3)}C_{n+2}^t + \frac{n(n+1)(2n+1)}{(2n-1)(2n+3)}C_n^t - \frac{(n-2)(n-1)}{2(2n-1)}C_{n-2}^t \\
&-\frac{(n+2)(n+3)(n+4)}{2(2n+3)}G_{n+2}^t + \frac{(n+2)(n+3)}{2}G_{n+1}^t \\
&-\frac{3(n-1)(n+\frac{1}{2})(n+2)}{(2n-1)(2n+3)}G_n^t \\
&-\frac{(n-1)(n-2)}{2}G_{n-1}^t + \frac{(n-1)(n-2)(n-3)}{2(2n-1)}G_{n-2}^t \qquad (3.32) \\
&-\frac{\beta' c}{\mu}\left[\frac{(n+2)}{(2n+3)}B_{n+1}^t + B_n^t + \frac{(n-1)}{(2n-1)}B_{n-1}^t\right. \\
&\left.+\frac{2(n+2)(n+3)}{(2n+3)}F_{n+1}^t - \frac{2(n-1)(n-2)}{(2n-1)}F_{n-1}^t\right] \;=\; 0,
\end{aligned}
$$

and

$$
\begin{aligned}
&-\frac{(n+2)}{2(2n+3)}E_{n+2}^t + \frac{1}{2}E_{n+1}^t + \frac{(n+\frac{1}{2})}{(2n-1)(2n+3)}E_n^t \\
&-\frac{1}{2}E_{n-1}^t + \frac{(n-1)}{2(2n-1)}E_{n-2}^t - \frac{(n+2)(n+3)(n+4)}{2(2n+3)}G_{n+2}^t \\
&+\frac{(n+2)(n+3)}{2}G_{n+1}^t - \frac{3(n-1)(n+\frac{1}{2})(n+2)}{(2n-1)(2n+3)}G_n^t \\
&-\frac{(n-1)(n-2)}{2}G_{n-1}^t + \frac{(n-1)(n-2)(n-3)}{2(2n-1)}G_{n-2}^t \qquad (3.33) \\
&-2\frac{\beta' c}{\mu}\left[\frac{1}{(2n+3)}D_{n+1} - \frac{1}{(2n-1)}D_{n-1}^t\right. \\
&\left.+\frac{(n+2)(n+3)}{(2n+3)}F_{n+1}^t - \frac{(n-1)(n-2)}{(2n-1)}F_{n-1}^t\right] \;=\; 0.
\end{aligned}
$$

3.4 Continuity

The restraints on the values of the coefficients from the continuity relations were found by substituting the series solution to the auxiliary functions given by Eqs. (3.15)-(3.18) into the continuity equation, given by Eq. (3.5). This resulted in an expression in terms of ξ and η. It is necessary to satisfy continuity at all points in the fluid thus this expression had to be satisfied at all values of ξ and η. The recursion relations found from the boundary conditions were obtained at a single value of ξ, integrating over all η.

In order to satisfy continuity at all values of (ξ,η), Eq. (3.5) was written in a form including ξ-dependence terms only of $\cosh(n+\frac{1}{2})\xi$ and $\sinh(n+\frac{1}{2})\xi$. Setting both sets of the coefficients to zero separately enabled the homogeneous equation in ξ and η to be satisfied at all values of ξ. The two sets were then integrated over the range of η and utilizing recursion and integral properties of Legendre Polynomials, two recursion relations were obtained by imposing continuity.

The terms in front of the $\cosh(n+\frac{1}{2})\xi$ term as given by Dean & O'Neill (1963) are:

$$\begin{aligned} &-(n-1)B^t_{n-1}+5B^t_n+(n+2)B^t_{n+1}-D^t_{n-1}+2D^t_n-D^t_{n+1}\\ &+(n-1)(n-2)F^t_{n-1}-2(n-1)(n+2)F^t_n+(n+2)(n+3)F^t_{n+1}\\ &-2(n-1)A^t_{n-1}+2(2n+1)A^t_n-2(n+2)A^t_{n+1}. \end{aligned} \tag{3.34}$$

The terms in front of the $\sinh(n+\frac{1}{2})\xi$ term can be found be replacing B^t_n, D^t_n and F^t_n with C^t_n, E^t_n and G^t_n, respectively and eliminating the A^t_n terms,

$$\begin{aligned} &-(n-1)C^t_{n-1}+5C^t_n+(n+2)C^t_{n+1}-E^t_{n-1}+2E^t_n-E^t_{n+1}\\ &+(n-1)(n-2)G^t_{n-1}-2(n-1)(n+2)G^t_n+(n+2)(n+3)G^t_{n+1}. \end{aligned} \tag{3.35}$$

Continuity is satisfied by setting both of these two expressions to zero for all values of n, greater then or equal to one.

Alternately, these equations could be derived by imposing continuity at any two

distinct values of ξ. The two resulting equations would be a linear combination of Eqs. (3.34)-(3.35).

3.5 Evaluation of Force and Torque

The force exerted by the fluid on the sphere is parallel to the direction of motion, and is given by (Goldman *et al*, 1967)

$$F_x^t = \pi\mu U c \int_{-1}^{1} \left(\frac{W^t}{2c}\frac{\partial \rho}{\partial \xi} - \frac{\rho}{2c}\frac{\partial W^t}{\partial \xi} - \frac{\partial Y^t}{\partial \xi}\right) d\cos\eta. \tag{3.36}$$

Substituting Eqs. (3.15)-(3.18) into Eq. (3.36), and performing the appropriate integration leads to

$$F_x^t = -\pi\mu U a\sqrt{2}\sinh\alpha \sum_{n=0}^{\infty}[D_n^t + E_n^t + n(n+1)(B_n^t + C_n^t)]. \tag{3.37}$$

It is often more convenient to consider a wall correction factor. Normalizing the force by the amount which would be exerted in the absence of the plane, one obtains

$$F_x^{t*} = \frac{F_x^t}{6\pi\mu U a} = \frac{\sqrt{2}}{6}\sinh\alpha \sum_{n=0}^{\infty}[D_n^t + E_n^t + n\,(n+1)(B_n^t + C_n^t)]. \tag{3.38}$$

The torque (about the sphere center) is parallel to the y-axis, and is given by, (Goldman *et al*, 1967)

$$T_y^t = -\pi\mu U \mathrm{csch}\alpha \int_{-1}^{1} \left[\frac{\partial \rho}{\partial \xi}\frac{\partial}{\partial \xi}\left(\frac{1}{2}zW^t + cZ^t\right) - \frac{\partial z}{\partial \xi}\frac{\partial}{\partial \xi}\left(\frac{1}{2}\rho W^t + cY^t\right)\right] d\cos\eta. \tag{3.39}$$

Substituting Eqs. (3.15)-(3.18) into Eq. (3.39), performing the appropriate integration and nondimensionalization leads to

$$
\begin{aligned}
T_y^{t*} &= \frac{T_y^t}{8\pi\mu U a^2} \\
&= -\pi\mu U \operatorname{csch}\alpha \sum_{n=0}^{\infty} \{2 + \exp[-(2n+1)\alpha]\} \\
&\quad \times [n(n+1)(2A_n^t + \coth\alpha)C_n^t - (2n+1-\coth\alpha)E_n^t] \qquad (3.40) \\
&\quad + \{2 - \exp[-(2n+1)\alpha]\} \times \\
&\quad [n(n+1)\coth\alpha B_n^t - (2n+1-\coth\alpha)D_n^t].
\end{aligned}
$$

3.6 Numerical Solution

The solution has been fully specified analytically. The coefficients appearing in the infinite series solution to the constituent equations are related by recursion relations found from the boundary conditions and continuity expression.

For each value of n ($n = 0, 1, 2, 3, ...$), there exist seven unknowns ($A_n^t, B_n^t, ...G_n^t$), and seven corresponding recursion relations, two from continuity and five from the boundary conditions. The infinite series solution is approximated by a finite series of N terms. The first $7 \times N$ set of unknowns and recursion relations correspond to a set of equations with $7 \times (N+2)$ unknowns. By assuming that higher order terms are small compared with those terms which are retained, (i.e., that $A_{N+1}^t, A_{N+2}^t ..., G_{N+2}^t \simeq 0$, approximate values for the coefficients can be obtained from simultaneous solution of the resultant linear set of equations.

The coefficients were computed numerically using a banded matrix solver. The numerical problem corresponded to a $7N \times 7N$ matrix with a band width of 49. The recursion relations involved terms ranging from A_{n-2}^t to G_{n+2}^t. The bandwidth of the matrix was set so that each row in the matrix would contain an individual recursion relation.

A CRAY X-MP computer was used for numerical computations. The determining factor in selecting a machine was the memory capacity of the computer, as our large matrix required substantial memory storage space. As a result, while the fast speeds

of the CRAY significantly reduced the time required to obtain numerical results, they did not furnish the major motivation for utilizing that supercomputer.

For a given separation distance and slip coefficient, the exact numerical solution was approximated by the technique outlined above. A number of runs were performed for each case with different values of N. In other words, the code was run by incorporating more and more 'nonzero' terms into the series until the torque and force values converged numerically to the desired significant figures. More terms were required at smaller separation distances. Calculations pertaining to complete slip or no slip converged with fewer terms then cases with partial slip. The number of terms required for convergence is not considered a significant result; however, only results for converged cases are reported.

Appendix E contains the computer output for the force and torque computations for both the translation and rotation cases. The force and torque values are given to ten significant figures for all cases. The precision of the numerical results was determined by inspection of these results. Often, the actual precision was much better then what was reported in text of the thesis.

To obtain a complete set of numerical data at a given separation distance, the number of terms required for convergence was first determined at one particular slip coefficient. An intermediate value ($\beta \equiv \beta' a/\mu = 1$) was selected as the test case as such a case required the highest number of terms for convergence at a given separation distance. The code was run with different values of β, at a fixed separation distance knowing the number of terms required for convergence. For large separation distance, namely $\epsilon = O(1)$, the use of 10 terms yielded force and torque results accurate to four decimal places; including 100 terms gave results accurate to ten decimal places. For small separations, explicitly $\epsilon = 10^{-5}$, 15,000 terms in the series gave results for the force and torque values accurate to only three decimal places. (Recall that taking 1,000 terms involved solving a set of 7,000 unknowns.)

Values of the constants $A_n^t, ..., G_n^t$ for the solution at a few sample separation distances and slip coefficients are included in Appendix D. Each such case required computing the entire set of numerical coefficients, as values did not carry from one

case to the next.

Having been able to fully describe the solution analytically and numerically, confirms *a posteriori* our *a priori* assumptions regarding the symmetry of the velocity field (in particular representing it in terms of auxiliary functions independent of ϕ).

3.7 Numerical Results

An analytic representation of the solution involving a sphere translating near, and parallel to, a plane wall bounding an otherwise semi-infinite quiescent fluid has been obtained for the case of partial slip on the wall. A tabulation of the hydrodynamic force exerted on the sphere is presented in Table 3.1 for normalized separation distances ϵ as small as 10^{-7}, and for dimensionless slip coefficients, β, given by

$$\beta \equiv \frac{\beta' a}{\mu} \tag{3.41}$$

ranging from 10^{7} to 10^{-6}.

These numerical data are more easily interpreted graphically. Figure 3-1 displays the normalized force versus separation distance for different slip coefficients on the plane. The uppermost curve represents the no-slip, $\beta = \infty$ case, which is identical to the solutions presented by Goldman *et al* (1967) and O'Neill (1964). Although our recursion relations and computer algorithms differed from those of these authors, our force and torque calculations agree exactly with theirs.

The lowest curve of Figure 3-1 corresponds to the case of perfect slip on the wall. These results are identical with those of the problem with two spheres translating perpendicular to their line of centers (Goldman *et al*, 1966), as that case is hydrodynamically equivalent to our perfect slip case. Again, the technique used to solve these two problems was quite different, whereas the numerical values obtained for the force and torque (as well as the individual coefficients) were identical.

The nature of the $\ln \epsilon$ singularity inherent in the no-slip case is apparent in this diagram. For this no-slip case the force and torque tend towards infinity as the

Table 3.1: Dimensionless Force F_x^{t*} on a Translating Sphere

Slip	Dimensionless Separation Distance, ϵ						
β	100	10	1	0.5	0.1	0.05	0.01
∞	-1.0056004	-1.053802	-1.3827524	-1.5957066	-2.2643030	-2.5989633	-3.422533
10^7	-1.0056004	-1.053802	-1.3827524	-1.5957065	-2.2643026	-2.5989623	-3.422528
10^6	-1.0056004	-1.053802	-1.3827521	-1.5957059	-2.2642983	-2.5989534	-3.422481
10^5	-1.0056004	-1.053802	-1.3827497	-1.5956997	-2.2642562	-2.5988643	-3.422010
10^4	-1.0056004	-1.053801	-1.3827257	-1.5956374	-2.2638348	-2.5979745	-3.417336
10^3	-1.0056003	-1.053796	-1.3824862	-1.5950155	-2.2596486	-2.5891883	-3.373125
10^2	-1.0055998	-1.053750	-1.3801168	-1.5889044	-2.2202939	-2.5104621	-3.069596
10^1	-1.0055948	-1.053297	-1.3585901	-1.5361509	-1.9599342	-2.0877415	-2.228138
10^0	-1.0055457	-1.049363	-1.2344126	-1.2902250	-1.3426927	-1.3474354	-1.350079
10^{-1}	-1.0051225	-1.028923	-1.0015047	-0.9668366	-0.9129275	-0.9037657	-0.895998
10^{-2}	-1.0029462	-0.992506	-0.8769637	-0.8321275	-0.7759025	-0.7671159	-0.759478
10^{-3}	-0.9990572	-0.972750	-0.8452743	-0.8009066	-0.7463368	-0.7378751	-0.730714
10^{-4}	-0.9969317	-0.967780	-0.8396166	-0.7956235	-0.7418347	-0.7336357	-0.726831
10^{-5}	-0.9963937	-0.967075	-0.8389077	-0.7949971	-0.7413420	-0.7331818	-0.726425
10^{-6}	-0.9963108	-0.967000	-0.8388343	-0.7949330	-0.7412922	-0.7331361	-0.726384
0	-0.9963008	-0.966992	-0.8388262	-0.7949259	-0.7412867	-0.7331310	-0.726379

Slip	Dimensionless Separation Distance, ϵ							
β	5×10^{-3}	1×10^{-3}	5×10^{-4}	1×10^{-4}	5×10^{-5}	5×10^{-6}	5×10^{-7}	10^{-7}
∞	-3.786730	-4.640038	-5.008972	-5.866675	-6.23626	-7.46421	-8.69224	-9.550
10^7	-3.786719	-4.639985	-5.008865	-5.866143	-6.23520	-7.45367	-8.59617	-9.188
10^6	-3.786624	-4.639507	-5.007908	-5.861376	-6.22572	-7.36814	-8.11634	-8.283
10^5	-3.785676	-4.634751	-4.998446	-5.816246	-6.14021	-6.88833	-7.07983	-7.099
10^4	-3.776305	-4.589734	-4.913054	-5.504163	-5.66053	-5.85197	-5.87422	-5.876
10^3	-3.691810	-4.278718	-4.434493	-4.601122	-4.62535	-4.64754	-4.64975	-4.650
10^2	-3.221195	-3.384137	-3.407858	-3.427171	-3.42958	-3.43175	-3.43196	-3.432
10^1	-2.248611	-2.265212	-2.267277	-2.268922	-2.26913	-2.26931	-2.26932	-2.269
10^0	-1.350302	-1.350456	-1.350473	-1.350487	-1.35049	-1.35037	-1.34941	-1.345
10^{-1}	-0.895003	-0.894194	-0.894036	-0.893917	-0.89385	-0.88935	-0.88167	-0.869
10^{-2}	-0.758583	-0.757675	-0.756820	-0.756425	-0.75601	-0.74977	-0.74624	-0.743
10^{-3}	-0.729856	-0.729074	-0.728704	-0.728539	-0.72842	-0.72736	-0.72692	-0.726
10^{-4}	-0.725974	-0.725274	-0.725154	-0.725075	-0.72505	-0.72493	-0.72489	-0.725
10^{-5}	-0.725567	-0.724878	-0.724788	-0.724718	-0.72471	-0.72469	-0.72468	-0.724
10^{-6}	-0.725526	-0.724838	-0.724751	-0.724682	-0.72467	-0.72467	-0.72466	-0.724
0	-0.725522	-0.724834	-0.724747	-0.724678	-0.72467	-0.72466	-0.72466	-0.724

Table 3.2: Limiting Value of Dimensionless Force F_x^{t*} on a Translating Sphere at $\epsilon = 0$

β	F_x^{t*}
10^5	7.1
10^4	5.88
10^3	4.65
10^2	3.43
10^1	2.27
10^0	1.35
10^{-1}	0.869
10^{-2}	0.74624
10^{-3}	0.72692
10^{-4}	0.72489
10^{-5}	0.72468
10^{-6}	0.72466
0	0.72466

separation distance approaches zero. On the other hand, the perfect slip case force converges to a finite value of $F_x^{t*} = 0.725$ as the separation distance tends towards zero.

The significant result one can see from this diagram is that cases with an intermediate values of slip converge to a *finite* value of force as the separation distance tends to zero. This indicates that the no-slip case corresponds to a singularity in the creeping flow equations when the sphere touches the wall.

To empirically determine a slip coefficient for a flow geometry, one would correlate experimentally determined separation distances and external hydrodynamic forces. If the flow geometry were such that the sphere and wall were essentially in contact, then measuring the external forces alone would enable one to correlate a slip coefficient based on limiting values of force, as from Figure 3-2 or Table 3.2.

Figure 3-2 shows two distinct trends. For small β (large amounts of slip), the force is not dependent on the slip coefficient. For large β cases (small amounts of slip), the forces varies logarithmically with slip coefficient. A best fit curve to these

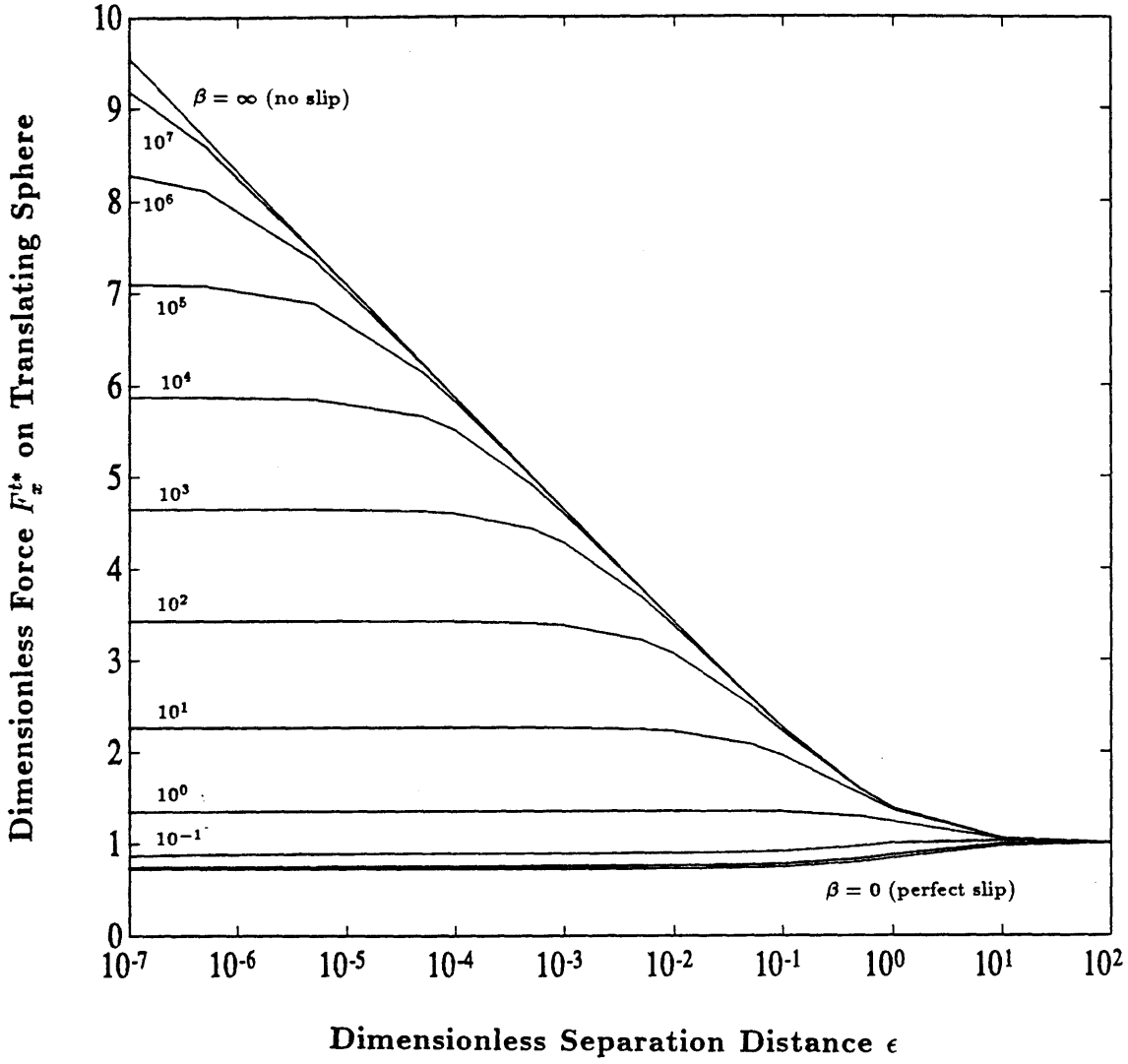

Figure 3-1: Dimensionless Force F_x^{t*} on a Translating Sphere vs Dimensionless Separation Distance ϵ at Parameters of the Dimensionless Slip Coefficient β

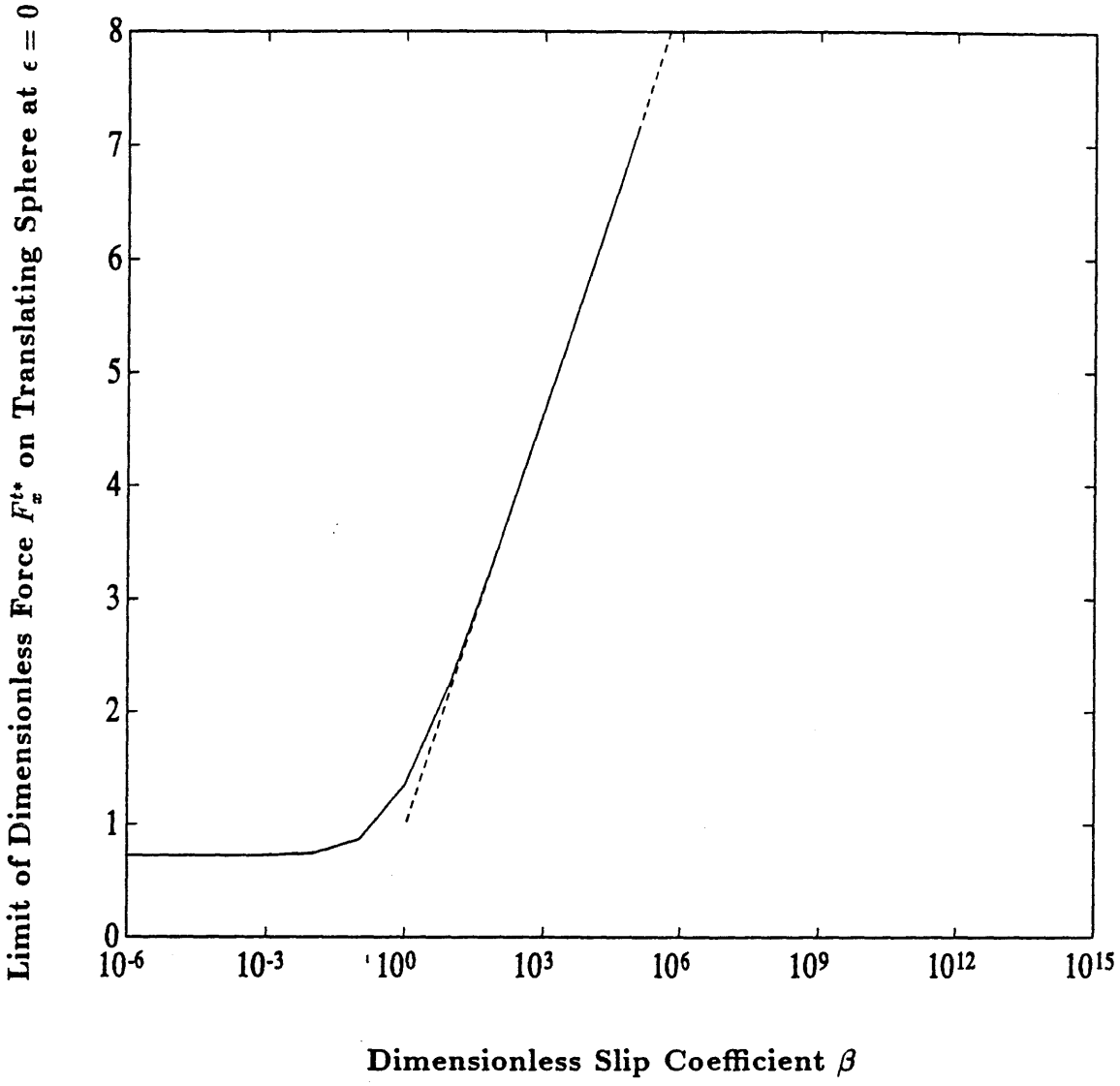

Figure 3-2: Limiting Value of Dimensionless Force F_x^{t*} on a Translating Sphere at $\epsilon = 0$ vs Dimensionless Slip Coefficient β The dashed line corresponds to a best fit curve for $\beta > 1$ given by Equation 3.42.

data gives the correlation,

$$F_x^{t*}(\epsilon = 0) = -0.981 - 1.22 \log_{10} \beta, \quad for\ \beta > 1. \tag{3.42}$$

This best fit curve is indicated by the dotted line on Figure 3-2.

Similar correlations relating the torque to the two parameters, slip and separation distance, are also presented.

Table 3.3 lists the value of non-dimensional torque for various separation distances and slip coefficients corresponding to the set of values of force computations in Table 3.1. Figure 3-3 presents this same data graphically.

The same general trends in the torque computations were observed as were seen in the force computations. The no-slip case, corresponding to the uppermost curve in Figure 3-3, displays a $\ln \epsilon$ singularity. The perfect slip case, corresponding to the lowest curve, converges to a finite value of torque, $T_y^{t*} = -0.11865$ as the separation distance tends towards zero. Cases with intermediate value of slip, corresponding to the cases between these two curves, converge to a finite value of torque as the separation distance tends to zero. This indicates that similar to the force computations, the no-slip case corresponds to a singularity in the creeping flow equations when the sphere touches the wall.

Figure 3-3 also illustrates another important concept. In this problem, there are two dimensionless length scales inherent in the problem. One is the separation distance and the other is the slip coefficient. As $\epsilon \to 0$ and $\beta \to \infty$, two length scales simultaneously approach limiting values. This effect can be seen in Figure 3-3 by noting that the value of torque does not smoothly approach a finite value as the separation distance approaches zero. Instead there is a bump in the curve. This irregularity is more noticeable at larger slip coefficients.

Table 3.4 lists the values of torque in the limit when the separation distance approaches zero. This indicates that the no-slip case corresponds to a singularity in the Navier Stokes equations when the sphere and wall are in contact.

These same limiting values are presented graphically in Figure 3-4. This plot is

Table 3.3: Dimensionless Torque T_y^{t*} on a Translating Sphere

Slip	Dimensionless Separation Distance, ϵ[†]						
β	100	10	1	0.5	0.1	0.05	0.01
∞	8.98147e-10	6.17808e-06	0.005025	0.0165740	0.088763	0.137925	0.2765
10^7	8.96801e-10	6.17808e-06	0.005025	0.0165740	0.088763	0.137925	0.276516
10^6	8.97231e-10	6.17808e-06	0.005025	0.0165740	0.088763	0.137923	0.276508
10^5	8.97263e-10	6.17806e-06	0.005025	0.0165735	0.088757	0.137910	0.276425
10^4	8.96519e-10	6.17785e-06	0.005024	0.0165691	0.088699	0.137771	0.275586
10^3	8.96553e-10	6.17579e-06	0.005015	0.0165251	0.088115	0.136371	0.266998
10^2	8.96829e-10	6.14988e-06	0.004918	0.0160643	0.082013	0.121860	0.193978
10^1	8.14944e-10	5.39551e-06	0.003608	0.0104658	0.029765	0.027447	0.000900
10^0	-6.73672e-09	-3.10547e-05	-0.010087	-0.026293	-0.080393	-0.097643	-0.118021
10^{-1}	-4.61800e-07	-5.04782e-04	-0.033453	-0.061317	-0.110973	-0.120475	-0.129094
10^{-2}	-6.22113e-06	-1.24984e-03	-0.038937	-0.065256	-0.107297	-0.114580	-0.120740
10^{-3}	-1.51414e-05	-1.46890e-03	-0.039024	-0.064588	-0.104936	-0.111844	-0.117669
10^{-4}	-1.78937e-05	-1.49552e-03	-0.038928	-0.064356	-0.104488	-0.111376	-0.117205
10^{-5}	-1.82686e-05	-1.49809e-03	-0.038912	-0.064324	-0.104437	-0.111324	-0.117155
10^{-6}	-1.83081e-05	-1.49834e-03	-0.038911	-0.064321	-0.104432	-0.111319	-0.117150
0	-1.83126e-05	-1.49837e-03	-0.038910	-0.064321	-0.104431	-0.111319	-0.117150

Slip	Dimensionless Separation Distance, ϵ							
β	5×10^{-3}	1×10^{-3}	5×10^{-4}	1×10^{-4}	5×10^{-5}	5×10^{-6}	5×10^{-7}	10^{-7}
∞	0.341946	0.499112	0.567842	0.728250	0.797486	1.0277	1.2579	1.4189
10^7	0.341944	0.499102	0.567822	0.728150	0.797286	1.0257	1.2374	1.3298
10^6	0.341927	0.499013	0.567643	0.727247	0.795473	1.0071	1.1115	1.0989
10^5	0.341754	0.498119	0.565840	0.718030	0.776979	0.8813	0.8599	0.8472
10^4	0.340015	0.488987	0.547440	0.639284	0.651235	0.6298	0.6145	0.6119
10^3	0.322247	0.411049	0.422558	0.409510	0.400659	0.3854	0.3823	0.3819
10^2	0.202806	0.187377	0.178203	0.165233	0.162626	0.1595	0.1591	0.1590
10^1	-0.009914	-0.024260	-0.027043	-0.029863	-0.030315	-0.0308	-0.0309	-0.0308
10^0	-0.121620	-0.125105	-0.125640	-0.126128	-0.126199	-0.1262	-0.1260	-0.1251
10^{-1}	-0.130298	-0.131322	-0.131450	-0.131560	-0.131565	-0.1308	-0.1294	-0.1273
10^{-2}	-0.121553	-0.122180	-0.122137	-0.122151	-0.122093	-0.1211	-0.1205	-0.1200
10^{-3}	-0.118426	-0.119020	-0.119050	-0.119095	-0.119086	-0.1189	-0.1189	-0.1188
10^{-4}	-0.117954	-0.118555	-0.118625	-0.118684	-0.118689	-0.1187	-0.1187	-0.1187
10^{-5}	-0.117904	-0.118506	-0.118580	-0.118641	-0.118648	-0.1187	-0.1187	-0.1187
10^{-6}	-0.117899	-0.118501	-0.118576	-0.118637	-0.118644	-0.1187	-0.1187	-0.1187
0	-0.117898	-0.118500	-0.118576	-0.118636	-0.118644	-0.1187	-0.1187	-0.1186

[†] Here, and in the remaining tables the e-notation means, for example, that 5e-04 = 5×10^{-4}.

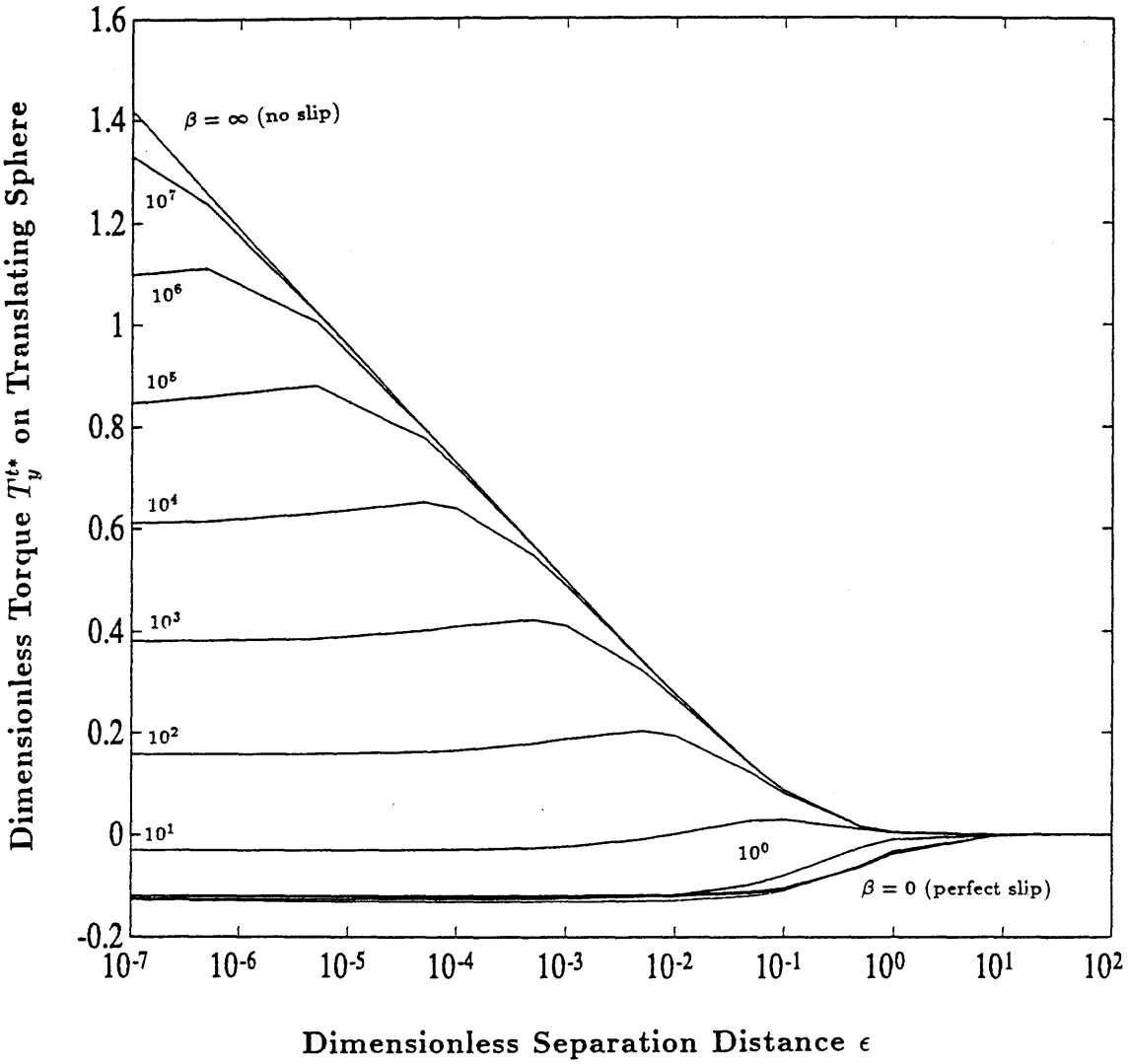

Figure 3-3: Dimensionless Torque T_y^{t*} on a Translating Sphere vs Dimensionless separation Distance ϵ at Parameters of the Dimensionless Slip Coefficient β

Table 3.4: Limiting Value of Dimensionless Torque T_y^{t*} on a Translating Sphere at $\epsilon = 0$

β	T_y^{t*}
10^6	1.10
10^5	0.85
10^4	0.61
10^3	0.382
10^2	0.159
10^1	-0.0308
10^0	-0.125
10^{-1}	-0.127
10^{-2}	-0.120
10^{-3}	-0.1189
10^{-4}	-0.11866
10^{-5}	-0.11865
10^{-6}	-0.11865
0	-0.11865

similar to the limiting force plot. For small β, the torque is not dependent on the slip coefficient. For large β, the torque varies logarithmically with slip coefficient. A best fit curve to this data gives the correlation,

$$T_y^{t*} = -0.305 + 0.230 \log_{10} \beta, \quad for\ \beta > 1. \tag{3.43}$$

This best curve is indicated by the dotted line on Figure 3-4.

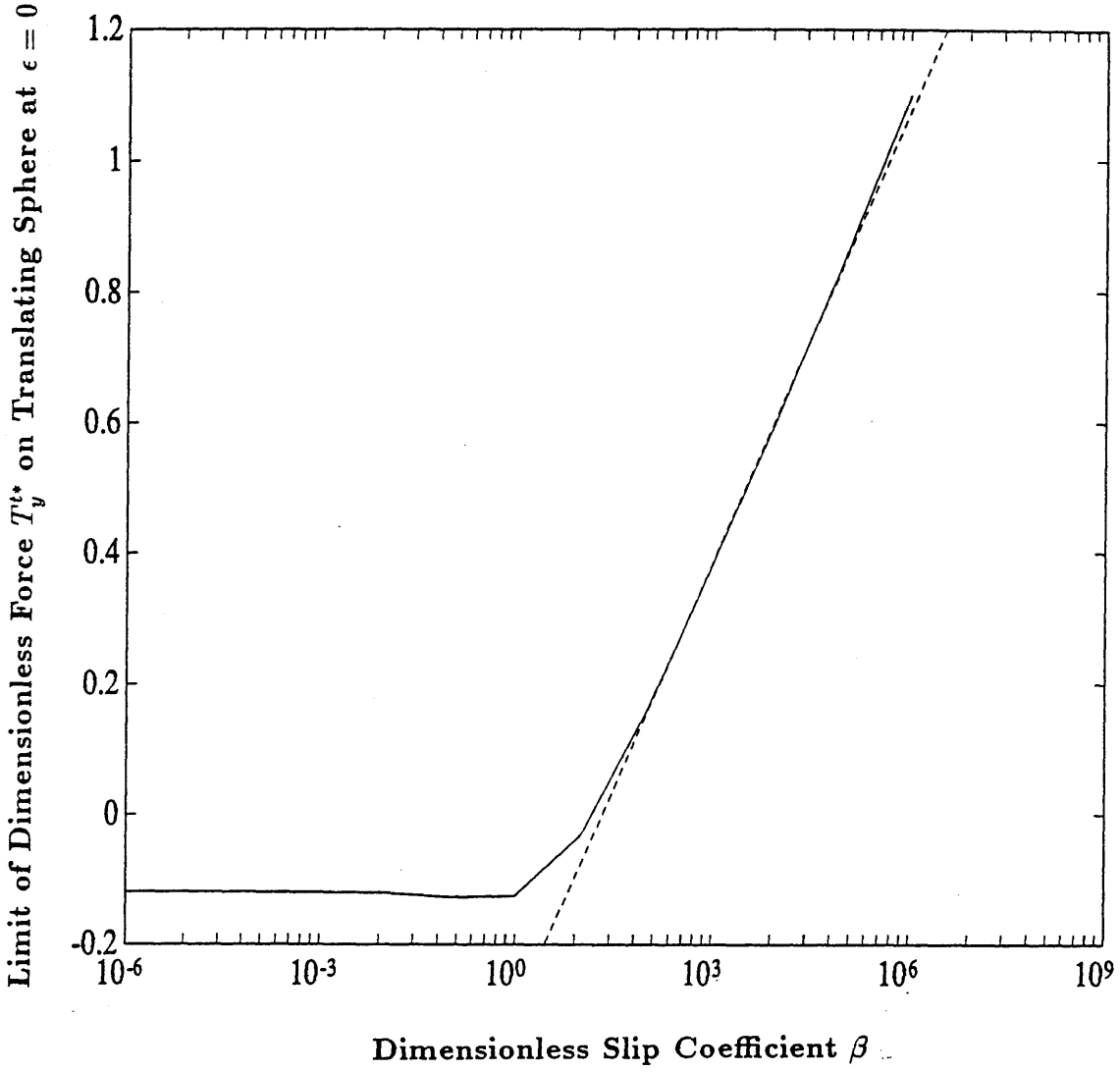

Figure 3-4: Limiting Value of Dimensionless Torque T_y^{t*} on a Translating Sphere at $\epsilon = 0$ vs Dimensionless Slip Coefficient β The dashed line corresponds to a best fit curve for $\beta > 1$ given by Equation 3.43.

Chapter 4

Force and Torque on a Rotating Sphere

This chapter considers the constituent motion of a neutrally buoyant sphere rotating at small Reynolds number above a stationary plane-wall bounding an otherwise quiescent, semi-infinite fluid. The solution for the case where no-slip boundary conditions are imposed on all surfaces has been presented by Dean & O'Neill (1964). Their solution scheme, appropriately modified to take account of slip, is followed here.

4.1 Governing Equations

The creeping flow and continuity equations are identical to those given for the translation case, with the exception of the superscript. The superscript r, for rotation, should be substituted for the superscript t, for translation, in Eqs. (3.1)-(3.5). The pressure and velocity fields can be expressed in terms of auxiliary functions for the rotation case as

$$c\,p^r = \mu U W^r \cos\phi, \tag{4.1}$$

$$c\,v_\rho^r = \frac{1}{2}U[\rho W^r + c\,(X^r + Y^r)]\cos\phi, \tag{4.2}$$

$$c\,v_\phi^r = \frac{1}{2}Uc[X^r - Y^r]\sin\phi, \tag{4.3}$$

$$c\,v_z^r = \frac{1}{2}U[zW^r + 2c\,Z^r]\cos\phi. \tag{4.4}$$

It is assumed that the auxiliary functions, W^r, X^r, Y^r and Z^r are functions only of ρ and z. While the solution scheme (4.1)-(4.4) has only been shown to hold for the non-slip case (Dean & O'Neill, 1964), we assume subject to *a posteriori* verification that the same representation holds for the partial slip case.

4.2 Solution

The solution to the auxiliary functions, found in the same manner as for the translation case, is given by

$$Z^r = (\cosh\xi - \cos\eta)^{(1/2)}\sin\eta \sum_{n=1}^{\infty}[A_n^r \sinh(n+\frac{1}{2})\xi]P'_n(\cos\eta), \tag{4.5}$$

$$W^r = (\cosh\xi - \cos\eta)^{(1/2)}\sin\eta \sum_{n=1}^{\infty}[B_n^r \cosh(n+\frac{1}{2})\xi + C_n^r \sinh(n+\frac{1}{2})\xi]P'_n(\cos\eta), \tag{4.6}$$

$$Y^r = (\cosh\xi - \cos\eta)^{(1/2)} \sum_{n=0}^{\infty}[D_n^r \cosh(n+\frac{1}{2})\xi + E_n^r \sinh(n+\frac{1}{2})\xi]P_n(\cos\eta), \tag{4.7}$$

$$X^r = (\cosh\xi - \cos\eta)^{(1/2)}\sin^2\eta \sum_{n=2}^{\infty}[F_n^r \cosh(n+\frac{1}{2})\xi + G_n^r \sinh(n+\frac{1}{2})\xi]P''_n(\cos\eta). \tag{4.8}$$

In these equations, P_n is the Legendre Polynomial of order n, and the primes denote differentiation with respect to $\cos\eta$.

4.3 Boundary Conditions

The no-slip boundary condition is imposed on the sphere, as expressed by Eq. (2.3). In cylindrical coordinates the sphere surface velocity can be represented as

$$\left.\begin{aligned} v_\rho^r &= \Omega(z-h)\cos\phi \\ v_\phi^r &= -\Omega(z-h)\sin\phi \\ v_z^r &= -\Omega\rho\cos\phi \end{aligned}\right\} \quad at\ \xi = \alpha. \tag{4.9}$$

Expressed in terms of the auxiliary functions, the no-slip boundary condition on the sphere requires that

$$\left.\begin{aligned} W^r &= -\frac{2\rho}{z} - \frac{2c}{z}Z^r \\ X^r &= \frac{\rho}{c}\left(\frac{\rho}{z} + \frac{c}{z}Z^r\right) \\ Y^r &= \frac{2}{c}(z-h) + \frac{\rho}{c}\left(\frac{\rho}{z} + \frac{c}{z}Z^r\right) \end{aligned}\right\} \quad at\ \xi = \alpha. \tag{4.10}$$

In spherical bipolar coordinates these conditions become

$$\left.\begin{aligned} W^r &= -2\frac{\sin\eta}{\sinh\alpha} - 2\frac{\cosh\alpha - \cos\eta}{\sinh\alpha}Z^r \\ X^r &= \frac{\sin\eta}{\cosh\alpha - \cos\eta}\left(\frac{\sin\eta}{\sinh\alpha} + \frac{\cosh\alpha - \cos\eta}{\sinh\alpha}Z^r\right) \\ Y^r &= 2\left(\frac{sinh\alpha}{\cosh\alpha - \cos\eta} - \coth\alpha\right) \\ &\quad + \frac{\sin\eta}{\cosh\alpha - \cos\eta}\left(\frac{\sin\eta}{\sinh\alpha} + \frac{\cosh\alpha - \cos\eta}{\sinh\alpha}Z^r\right) \end{aligned}\right\} \quad at\ \xi = \alpha. \tag{4.11}$$

Recursion relations for the coefficients are found by substituting Eqs. (4.5)-(4.8) into these expressions. Utilizing the principles of orthogonality of Legendre polynomials, the following recursion relations were found from the appropriate integrations:

$$C_n^r = -\coth(n+\frac{1}{2}\alpha)B_n^r - 2\coth\alpha A_n^r + \frac{2}{\sinh\alpha}\times \tag{4.12}$$
$$\left[\frac{(n+2)}{(2n+3)}\frac{\sinh(n+\frac{3}{2})\alpha}{\sinh(n+\frac{1}{2})\alpha}A_{n+1}^r + \frac{(n-1)}{(2n-1)}\frac{\sinh(n-\frac{1}{2})\alpha}{\sinh(n+\frac{1}{2})\alpha}A_{n-1}^r\right] \quad (n\geq 0),$$

$$E_n^r = \frac{2\sqrt{2}\exp\left(-(n+\frac{1}{2})\xi\right)}{\sinh(n+\frac{1}{2})\alpha)}\sinh(n+\frac{1}{2})\alpha) - \coth(n+\frac{1}{2}\alpha)D_n^r + \frac{1}{\sinh\alpha}\times \tag{4.13}$$
$$\left[\frac{(n+1)(n+2)}{(2n+3)}\frac{\sinh(n+\frac{3}{2})\alpha}{\sinh(n+\frac{1}{2})\alpha}A_{n+1}^r - \frac{n(n-1)}{(2n-1)}\frac{\sinh(n-\frac{1}{2})\alpha}{\sinh(n+\frac{1}{2})\alpha}A_{n-1}^r\right] \quad (n\geq 1),$$

$$G_n^r = -\coth(n+\frac{1}{2}\alpha)F_n^r + \frac{1}{\sinh\alpha}\times \tag{4.14}$$
$$\left[-\frac{1}{(2n+3)}\frac{\sinh(n+\frac{3}{2})\alpha}{\sinh(n+\frac{1}{2})\alpha}A_{n+1}^r + \frac{1}{(2n-1)}\frac{\sinh(n-\frac{1}{2})\alpha}{\sinh(n+\frac{1}{2})\alpha}A_{n-1}^r\right] \quad (n\geq 2).$$

On the plane the partial slip boundary condition is introduced. Identical recursion relations to the translation case are found as for the rotation case. Changing the superscript in Eqs. (3.32) and (3.33) yields

$$\begin{aligned}
&-\frac{(n+2)(n+3)}{2(2n+3)}C_{n+2}^r + \frac{n(n+1)(2n+1)}{(2n-1)(2n+3)}C_n^r - \frac{(n-2)(n-1)}{2(2n-1)}C_{n-2}^r \\
&\quad -\frac{(n+2)(n+3)(n+4)}{2(2n+3)}G_{n+2}^r + \frac{(n+2)(n+3)}{2}G_{n+1}^r \\
&\quad\quad -\frac{3(n-1)(n+\frac{1}{2})(n+2)}{(2n-1)(2n+3)}G_n^r \\
&\quad -\frac{(n-1)(n-2)}{2}G_{n-1}^r + \frac{(n-1)(n-2)(n-3)}{2(2n-1)}G_{n-2}^r \\
&\quad\quad -\frac{\beta' c}{\mu}\left[\frac{(n+2)}{(2n+3)}B_{n+1}^r + B_n^r + \frac{(n-1)}{(2n-1)}B_{n-1}^r\right. \\
&\quad\quad\quad \left.\frac{(n+2)(n+3)}{(2n+3)}F_{n+1}^r - \frac{(n-1)(n-2)}{(2n-1)}F_{n-1}^r\right] = 0,
\end{aligned} \tag{4.15}$$

and

$$
\begin{aligned}
&-\frac{(n+2)}{2\,(2n+3)}E^r_{n+2}+\frac{1}{2}E^r_{n+1}+\frac{(n+\frac{1}{2})}{(2n-1)\,(2n+3)}E^r_n\\
&-\frac{1}{2}E^r_{n-1}+\frac{(n-1)}{2\,(2n-1)}E^r_{n-2}-\frac{(n+2)\,(n+3)\,(n+4)}{2\,(2n+3)}G^r_{n+2}\\
&+\frac{(n+2)\,(n+3)}{2}G^r_{n+1}-\frac{3(n-1)\,(n+\frac{1}{2})\,(n+2)}{(2n-1)\,(2n+3)}G^r_n\\
&-\frac{(n-1)\,(n-2)}{2}G^r_{n-1}+\frac{(n-1)(n-2)(n-3)}{2(2n-1)}G^r_{n-2}\\
&-2\frac{\beta'\,c}{\mu}\left[\frac{1}{(2n+3)}D^r_{n+1}-\frac{1}{(2n-1)}D^r_{n-1}\right.\\
&\left.\frac{(n+2)\,(n+3)}{(2n+3)}F^r_{n+1}-\frac{(n-1)\,(n-2)}{(2n-1)}F^r_{n-1}\right] \;=\; 0.
\end{aligned}
\tag{4.16}
$$

4.4 Continuity

The recursion relations found by imposing continuity are the same for the rotation and translation cases. Altering the superscript in Eqs. (3.34)-(3.35) yields,

$$
\begin{aligned}
&-(n-1)B^r_{n-1}+5B^r_n+(n+2)B^r_{n+1}-D^r_{n-1}+2D^r_n-D^r_{n+1}\\
&+(n-1)(n-2)F^r_{n-1}-2(n-1)(n+2)F^r_n+(n+2)(n+3)F^r_{n+1}\\
&-2(n-1)A^r_{n-1}+2(2n+1)A^r_n-2(n+2)A^r_{n+1} \;=0,
\end{aligned}
\tag{4.17}
$$

and

$$
\begin{aligned}
&-(n-1)C^r_{n-1}+5C^r_n+(n+2)C^r_{n+1}-E^r_{n-1}+2E^r_n-E^r_{n+1}\\
&+(n-1)(n-2)G^r_{n-1}-2(n-1)(n+2)G^r_n+(n+2)(n+3)G^r_{n+1} \;=0.
\end{aligned}
\tag{4.18}
$$

4.5 Evaluation of Force and Torque

The force and torque expressions for the evaluation of the appropriate integrals apply to the rotation and translation cases as well. In this case, however, the torque is normalized with respect to the torque which would be exerted on a sphere in the absence of the plane wall and the force is normalized with respect to a dimensionally

correct constant. The force and torque are given by the following expressions:

$$F_x^{r*} = \frac{F_x^r}{6\pi\mu\Omega a^2} = \frac{\sqrt{2}}{6}\sinh^2\alpha\sum_{n=0}^{\infty}[D_n^r + E_n^r + n\,(n+1)(B_n^r + C_n^r)], \tag{4.19}$$

and

$$\begin{aligned} T_y^{r*} &= \frac{T_y^r}{8\pi\mu\Omega a^3} \\ &= \frac{1}{3} - \frac{\sinh^3\alpha}{12\sqrt{2}}\sum_{n=0}^{\infty}\{2+\exp[-(2n+1)\alpha]\}\times \\ &\quad [n(n+1)(2A_n^r + C_n^r\coth\alpha) - (2n+1-\coth\alpha)E_n^r] \\ &\quad +\{2-\exp[-(2n+1)\alpha]\}\times \\ &\quad [n(n+1)(B_n^r\coth\alpha) - (2n+1-\coth\alpha)D_n^r]. \end{aligned} \tag{4.20}$$

4.6 Numerical Results

An analytic representation of the solution involving a sphere rotating at small Reynolds number above a plane wall bounding an otherwise quiescent, semi-infinite fluid has been obtained for the case of partial slip on the wall. The same numerical algorithm used to obtain numerical values for the translation case was used for the rotation case.

A tabulation of the hydrodynamic force exerted on the sphere is presented in Table 4.1 for normalized separation distances ϵ as small as 10^{-7}, and for dimensionless slip coefficients $\beta = \beta' a/\mu$ ranging from 10^7 to 10^{-6}. These are the same set of separation distances and slip coefficients which were used to obtain results for the translation case.

Having been able to fully describe the solution to the rotation problem analytically and numerically, confirms *a posteriori* our *a priori* assumptions regarding the symmetry of the velocity field (in particular utilizing the same decomposition for both the rotation and translation cases with partial slip on the wall).

These data are more easily interpreted graphically. Figure 4-1 displays the normalized force versus separation distance for different slip coefficients on the plane.

Table 4.1: Dimensionless Force F_x^{r*} on a Rotating Sphere

Slip	Dimensionless Separation Distance, ϵ						
β	ϵ : 100	10	1	0.5	0.1	0.05	0.01
∞	1.20000e-09	8.23740e-06	0.0066996	0.022099	0.11835	0.183900	0.368690
10^7	1.20000e-09	8.23740e-06	0.0066996	0.022099	0.11835	0.183900	0.368689
10^6	1.20000e-09	8.23740e-06	0.0066996	0.022099	0.11835	0.183898	0.368678
10^5	1.20000e-09	8.23740e-06	0.0066995	0.022098	0.11834	0.183880	0.368566
10^4	1.20000e-09	8.23710e-06	0.0066983	0.022092	0.11827	0.183695	0.367448
10^3	1.20000e-09	8.23440e-06	0.0066861	0.022034	0.11749	0.181829	0.355997
10^2	1.20000e-09	8.19980e-06	0.0065577	0.021419	0.10935	0.162480	0.258637
10^1	1.10000e-09	7.19400e-06	0.0048101	0.013954	0.03969	0.036596	0.001200
10^0	-9.00000e-09	-4.14062e-05	-0.013450	-0.035057	-0.107191	-0.130190	-0.157361
10^{-1}	-6.15700e-07	-6.73042e-04	-0.044604	-0.081756	-0.147963	-0.160630	-0.172128
10^{-2}	-8.29480e-06	-1.66645e-03	-0.051915	-0.087004	-0.143008	-0.152659	-0.161074
10^{-3}	-2.01885e-05	-1.95846e-03	-0.052022	-0.086094	-0.139851	-0.149049	-0.156949
10^{-4}	-2.38571e-05	-1.99400e-03	-0.051901	-0.085802	-0.139308	-0.148491	-0.156280
10^{-5}	-2.43577e-05	-1.99744e-03	-0.051883	-0.085765	-0.139248	-0.148432	-0.156208
10^{-6}	-2.44108e-05	-1.99778e-03	-0.051881	-0.085762	-0.139243	-0.148426	-0.156200
0	-2.44167e-05	-1.99782e-03	-0.051881	-0.085761	-0.139242	-0.148425	-0.156200

Slip	Dimensionless Separation Distance, ϵ							
β	5×10^{-3}	1×10^{-3}	5×10^{-4}	1×10^{-4}	5×10^{-5}	5×10^{-6}	5×10^{-7}	10^{-7}
∞	0.455928	0.665483	0.757122	0.971000	1.06332	1.37022	1.6772	1.8919
10^7	0.455925	0.665469	0.757096	0.970867	1.06305	1.36754	1.6499	1.7731
10^6	0.455902	0.665351	0.756857	0.969663	1.06063	1.34286	1.4820	1.4653
10^5	0.455672	0.664159	0.754453	0.957373	1.03597	1.17504	1.1465	1.1297
10^4	0.453354	0.651983	0.729920	0.852379	0.86831	0.83969	0.8194	0.8159
10^3	0.429662	0.548066	0.563411	0.546014	0.53421	0.51384	0.5097	0.5093
10^2	0.270408	0.249837	0.237605	0.220310	0.21683	0.21268	0.2121	0.2121
10^1	-0.013219	-0.032346	-0.036057	-0.039818	-0.04042	-0.04106	-0.0412	-0.0410
10^0	-0.162160	-0.166806	-0.167521	-0.168171	-0.16827	-0.16836	-0.1683	-0.1650
10^{-1}	-0.173730	-0.175096	-0.175278	-0.175429	-0.17545	-0.17529	-0.1740	-0.1675
10^{-2}	-0.162070	-0.162906	-0.162966	-0.163001	-0.16304	-0.16236	-0.1613	-0.1595
10^{-3}	-0.157901	-0.158693	-0.158773	-0.158835	-0.15886	-0.15870	-0.1585	-0.1583
10^{-4}	-0.157272	-0.158073	-0.158171	-0.158250	-0.15826	-0.15825	-0.1582	-0.1581
10^{-5}	-0.157205	-0.158008	-0.158108	-0.158188	-0.15820	-0.15821	-0.1582	-0.1581
10^{-6}	-0.157199	-0.158001	-0.158102	-0.158182	-0.15819	-0.15820	-0.1582	-0.1581
0	-0.157198	-0.158000	-0.158101	-0.158182	-0.15819	-0.15820	-0.1582	-0.1581

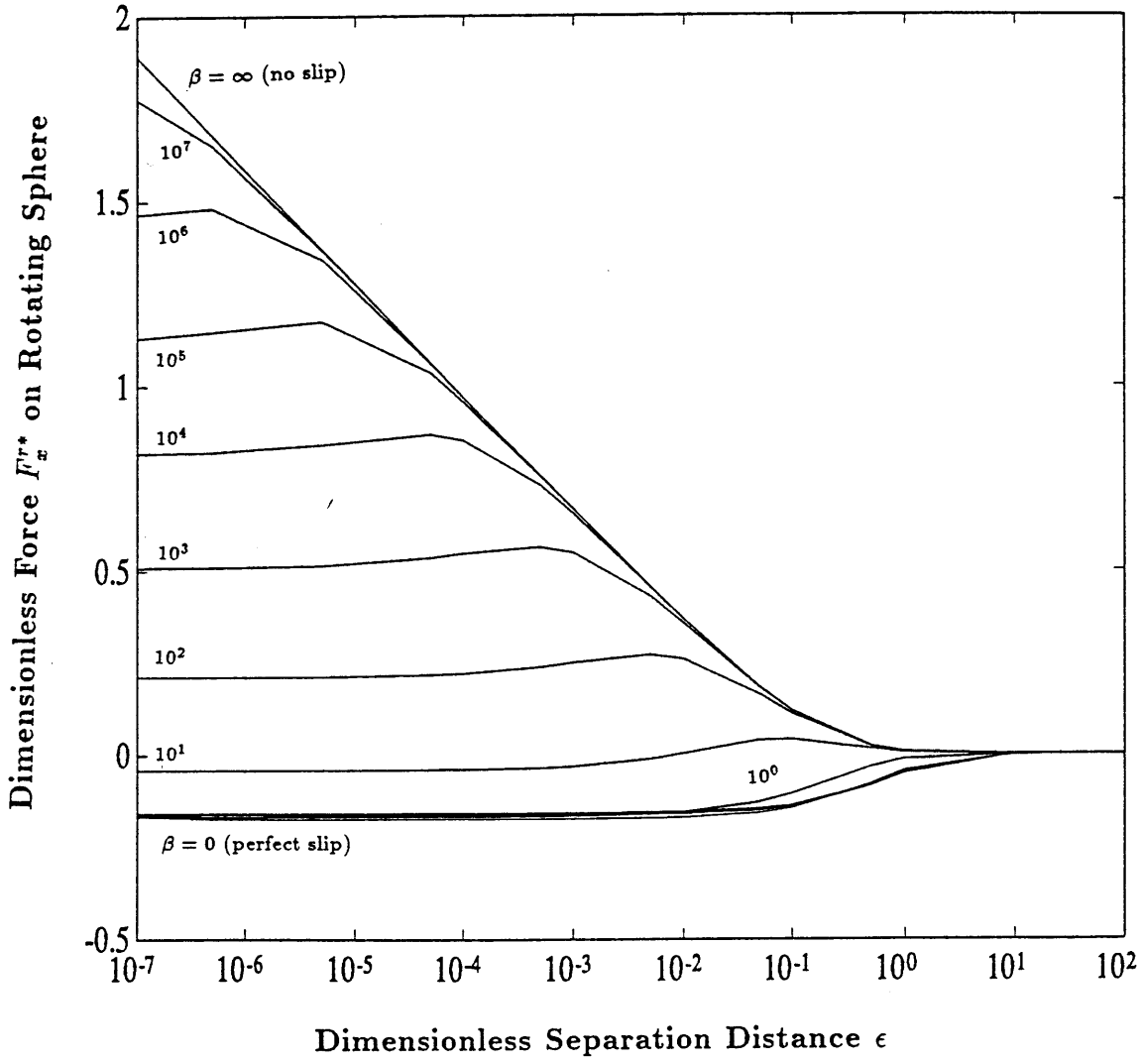

Figure 4-1: Dimensionless Force F_x^{r*} on a Rotating Sphere vs Dimensionless Separation Distance ϵ at Parameters of the Dimensionless Slip Coefficient β

The uppermost curve represents the no-slip, $\beta = \infty$ case, which is identical to the solution presented by Dean & O'Neill (1963) and Goldman *et al* (1967). The lowest curve of Figure 4-1 corresponds to the case of perfect slip on the wall. This case is identical with those of the problem of two spheres rotating without translation about axes perpendicular to their lines of center (Goldman *et al*, 1966).

The nature of the $\ln \epsilon$ singularity inherent in the no-slip case is apparent in this figure. For this no-slip case the force and torque tend towards infinity as the separation distance tends towards zero. On the other hand, the perfect slip case converges to a finite value of F_x^{r*} = -0.1582 as the separation distance tends towards zero.

The significant result one can see from this diagram is that cases with intermediate values of slip converge to a *finite* value of force as the separation distance tends to zero. This indicates that the no-slip case corresponds to a singularity in the creeping flow equations when the sphere touches the wall. Similar to the translation case, for a given slip coefficient, the value of the force approaches a constant value. This is true for all finite values of β. Thus introducing slip reduces the order of the (force) singularity inherent in the rotation case.

Figure 3-1 also illustrates another important concept. In this problem, similar to the case of torque on a translating sphere, there are two dimensionless length scales in competition. As the separation distance, ϵ approaches zero and the slip coefficient, β, approaches infinity, two length scales are approaching limiting values simultaneously. This effect can be seen in Figure 3-1 by noting that the value of force does not smoothly approach a finite value as the separation distance approaches zero. Instead there is a bump in the curve. This irregularity is more noticeable at large slip coefficients.

The degree to which the singularity is removed has yet to be determined. By plotting the limiting values of force as the separation distance tends towards zero versus slip coefficient, we are able to determine the order of the singularity with respect to β. This data is presented in Table 4.2 and plotted in Figure 4-2.

From Figure 4-2 one can see two distinct trends. For small β, cases near the perfect slip case, the force is independent on the slip coefficient. For large slip coefficients,

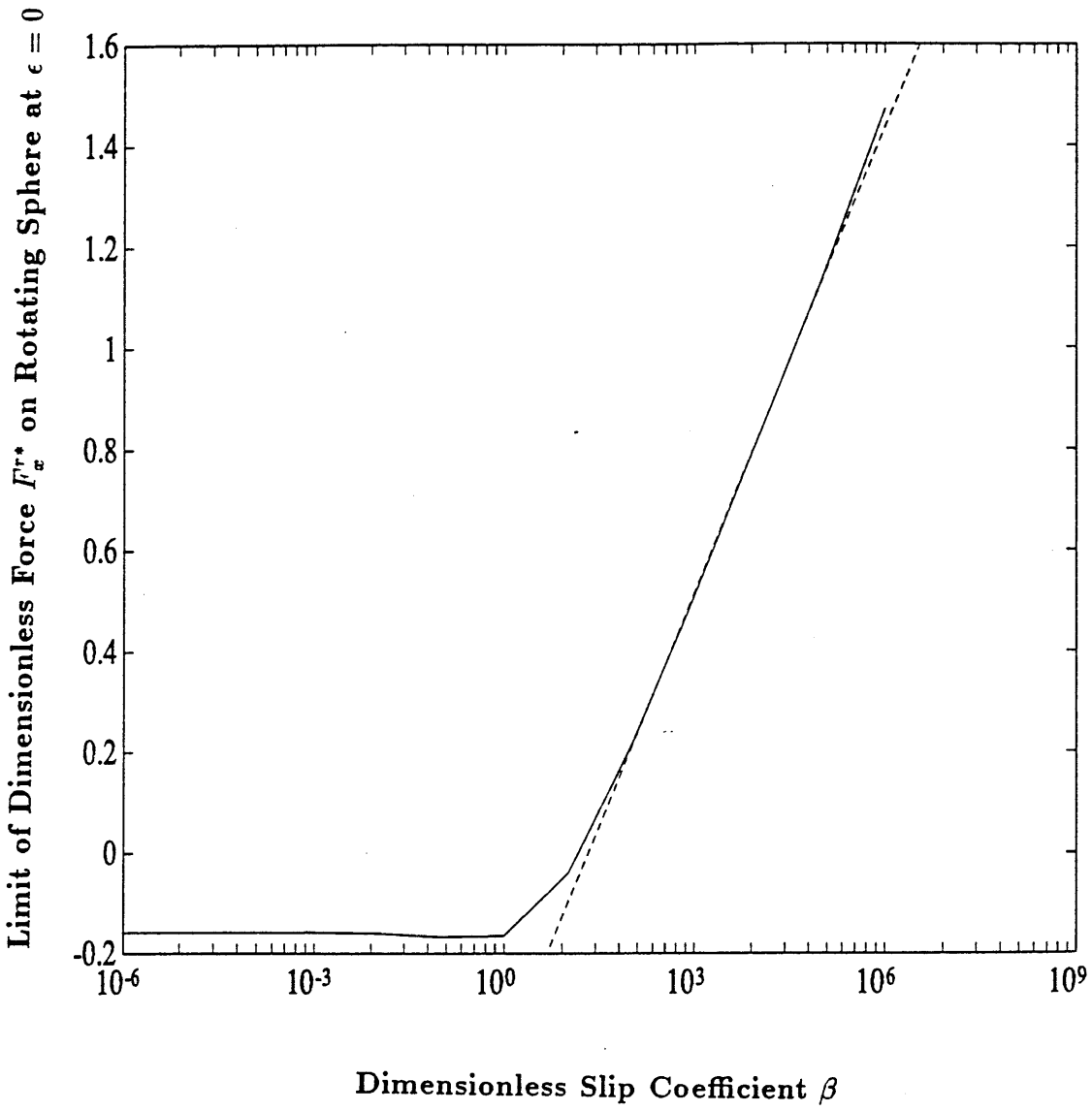

Figure 4-2: Limiting Value of Dimensionless Force F_x^{r*} on a Rotating Sphere at ϵ vs Dimensionless Slip Coefficient β The dashed line corresponds to a best fit curve for $\beta > 1$ given by Equation 4.21.

Table 4.2: Limiting Value of Dimensionless Force F_x^{r*} on a Rotating Sphere at ϵ

β	F_x^{r*}
10^6	1.47
10^5	1.13
10^4	0.82
10^3	0.509
10^2	0.212
10^1	-0.041
10^0	-0.165
10^{-1}	-0.167
10^{-2}	-0.160
10^{-3}	-0.158
10^{-4}	-0.15825
10^{-5}	-0.15820
10^{-6}	-0.15820
0	-0.15820

the force varies exponentially with respect to the slip coefficient. A best fit curve to this data gives the correlation,

$$F_x^{r*}(\epsilon = 0) = -0.405 + 0.306 \log_{10} \beta, \quad for\ \beta > 1. \tag{4.21}$$

This best fit curve is indicated by the dotted line on Figure 4-2.

Similar correlations relating the torque to the two parameters, slip and separation distance, are also presented. Table 4.3 lists the values of dimensionless torque at different separation distances and with different slip coefficients. The set of values of separation distance and slip coefficient match those used for the force computations.

Figure 4-3 displays the normalized torque versus separation distance for different slip coefficients. The uppermost curve represents the no-slip, $\beta = \infty$ case. The lowest curve represents the perfect slip case. Both of these two cases display the $\ln \epsilon$ singularity. The torque tends towards infinity as the separation distance approaches zero. Cases of intermediate slip, corresponding to curves between the no-slip and perfect slip case display similar behavior as the two cases. The actual value of the torque at a given separation distance is a function of the slip coefficient. However,

the torque dependence on separation distance does not appear to be a function of slip.

For the rotation case, this diagram indicates that introducing slip on the plane wall does not reduce the order of the (torque) singularity inherent in the problem. For the range of numerical values computed, relaxing the traditional no-slip boundary condition does not alter the order of the singularity inherent in the problem. The value of the torque does not approach a fixed value as the separation distance approaches zero.

Table 4.3: Dimensionless Torque T_y^{r*} on a Rotating Sphere

Slip	Dimensionless Separation Distance, ϵ						
β	100	10	1	0.5	0.1	0.05	0.01
∞	1.000000303	1.000235	1.041784	1.110495	1.454851	1.667461	2.240798
10^7	1.000000303	1.000235	1.041784	1.110495	1.454851	1.667460	2.240794
10^6	1.000000303	1.000235	1.041783	1.110495	1.454848	1.667454	2.240760
10^5	1.000000303	1.000235	1.041783	1.110493	1.454823	1.667396	2.240421
10^4	1.000000303	1.000235	1.041777	1.110469	1.454567	1.666809	2.237057
10^3	1.000000303	1.000235	1.041716	1.110229	1.452037	1.661058	2.206031
10^2	1.000000303	1.000235	1.041125	1.107904	1.429102	1.612368	2.019904
10^1	1.000000302	1.000229	1.036138	1.089882	1.305605	1.408595	1.638009
10^0	1.000000295	1.000186	1.016469	1.035479	1.130099	1.197908	1.399035
10^{-1}	1.000000236	1.00006	0.999684	1.002745	1.075149	1.141242	1.342392
10^{-2}	1.000000067	0.99997	0.996238	0.997129	1.066915	1.132736	1.333786
10^{-3}	0.999999961	0.99996	0.995821	0.996419	1.065715	1.131463	1.332446
10^{-4}	0.999999942	0.99996	0.995773	0.996331	1.065564	1.131306	1.332271
10^{-5}	0.999999940	0.99996	0.995768	0.996322	1.065548	1.131290	1.332253
10^{-5}	0.999999940	0.99996	0.995768	0.996322	1.065548	1.131290	1.332253
10^{-6}	0.999999940	0.99996	0.995768	0.996321	1.065546	1.131288	1.332251
0	0.999999940	0.99996	0.995769	0.996321	1.065546	1.131288	1.332251

Slip	Dimensionless Separation Distance, ϵ							
β	5×10^{-3}	1×10^{-3}	5×10^{-4}	1×10^{-4}	5×10^{-5}	5×10^{-6}	5×10^{-7}	10^{-7}
∞	2.505941	3.137984	3.413431	4.055549	4.332566	5.253356	6.174360	6.81807
10^7	2.505934	3.137944	3.413351	4.055150	4.331768	5.245489	6.105157	6.57715
10^6	2.505864	3.137588	3.412636	4.051587	4.324703	5.184158	5.809159	6.08897
10^5	2.505169	3.134052	3.405601	4.018593	4.263412	4.888206	5.274919	5.51707
10^4	2.498335	3.101324	3.344604	3.815060	3.967819	4.354344	4.700364	4.94148
10^3	2.439299	2.900254	3.051614	3.330072	3.436746	3.782603	4.127678	4.36897
10^2	2.162585	2.433080	2.538600	2.779633	2.883302	3.228237	3.573545	3.81489
10^1	1.736856	1.971652	2.074392	2.314593	2.418376	2.763565	3.108927	3.35026
10^0	1.496085	1.730847	1.833801	2.074291	2.178129	2.523381	2.868738	3.10937
10^{-1}	1.439660	1.674712	1.777721	2.018264	2.122111	2.467341	2.812493	3.05273
10^{-2}	1.431042	1.666100	1.769103	2.009642	2.113494	2.458642	2.803838	3.04492
10^{-3}	1.429701	1.664758	1.767766	2.008311	2.112160	2.457395	2.802742	3.04407
10^{-4}	1.429533	1.664592	1.767603	2.008151	2.111998	2.457257	2.802627	3.04398
10^{-5}	1.429516	1.664575	1.767586	2.008134	2.111981	2.457244	2.802616	3.04397
10^{-6}	1.429514	1.664573	1.767584	2.008133	2.111979	2.457242	2.802615	3.04397
0	1.429514	1.664573	1.767584	2.008133	2.111980	2.457242	2.802615	3.04397

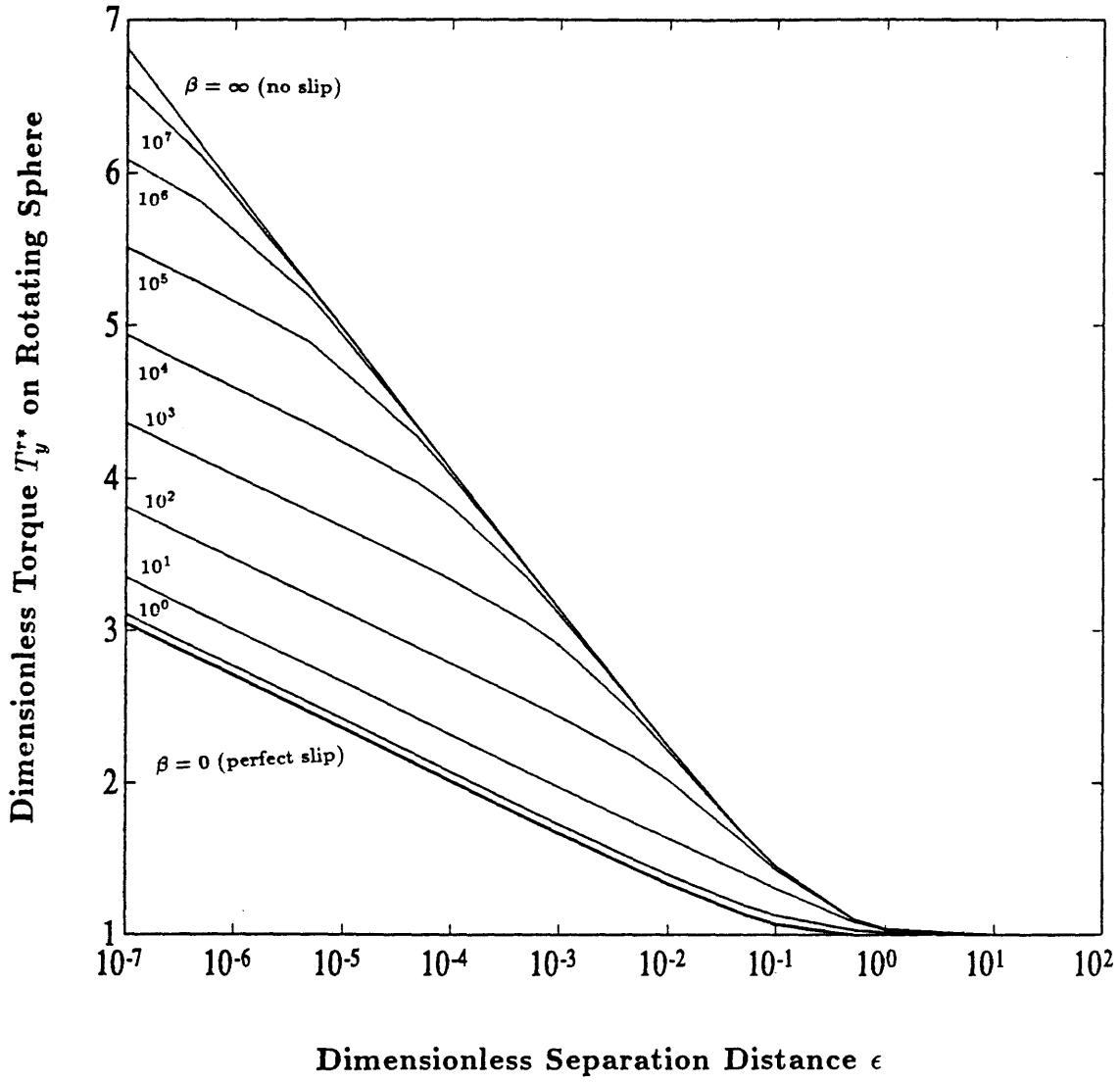

Figure 4-3: Dimensionless Torque T_y^{r*} on a Rotating Sphere vs Dimensionless Separation Distance ϵ at Parameters of the Dimensionless Slip Coefficient β

Chapter 5

Translational and Rotational Motions of a Sphere "Rolling" Down a Plane Wall Under the Influence of Gravity

This chapter considers the gravity-driven motion of a sphere moving at small Reynolds number near a stationary plane wall bounding an otherwise quiescent, semi-infinite fluid. The previous two chapters have considered the constituent motions of pure translation and pure rotation of a neutrally buoyant sphere. It is the aim of this chapter to consider the combined translational and rotational motions of a sphere, analyzing experimental data to empirically estimate a slip coefficient, for the case when the sphere touches the wall.

Solving for the general motion of a sphere requires balancing the net force and torque exerted on the sphere. This includes the hydrodynamic force and torque as well as external forces and torques.

Carty's (1957) experimental data is used here to calculate the slip coefficient. The flow geometry consisted of a sphere, immersed in a fluid, rolling down an inclined plane, in which gravity was the only external force exerted on the sphere. A torque

balance on the sphere,

$$T_y^{t*}(8\pi\mu_l U a^2) + T_y^{r*}(8\pi\mu_l \Omega a^3) = 0, \tag{5.1}$$

gives the ratio of rotation to translation as

$$\frac{a\,\Omega}{U} = \frac{-T_y^{t*}}{T_y^{r*}}. \tag{5.2}$$

The results from the previous chapters show that in the limit when the sphere touches the wall, T_y^{r*} tends to infinity while, T_y^{t*} approaches a finite value, for finite values of β. Therefore, $a\,\Omega/U = 0$, when β is finite. This means that a sphere would translate without rotating when the sphere was in contact with the wall.

Although Carty did not measure the rotational velocity of the spheres rolling down an inclined plane in his experiments, he did indicate that he did not observe pure translational motion. For now, we will consider the pure translational motion of a sphere above a plane wall.

A general force balance on the particle gives

$$F_x^{t*}(6\pi\mu_l U a) + F_x^{r*}(6\pi\mu_l \Omega a^2) + F_g = 0, \tag{5.3}$$

where F_g is the component of the net gravity force acting parallel to the plane.

For the pure translation problem the angular velocity is zero, $\Omega = 0$. Carty correlated his experimental data via a drag coefficient versus Reynolds number plot. The linear, low Reynolds number portion, of a log-log plot yielded the empirical wall-correction factor

$$F_x^{t*} = 8.96. \tag{5.4}$$

Matching this value to the numerically evaluated wall correction factor given by Eq. 3.42, gives the following relation for the slip coefficient,

$$0.981 + 1.22\log_{10}\beta = 8.96. \tag{5.5}$$

Table 5.1: Dimensional Slip Coefficients β' from Carty's (1957) Experiments

Fluid	Dimensional Slip Coefficient β' kg/(m^2 s)	
	Max Value	Min Value
Oil	1.03×10^8	2.27×10^7
Water	3.13×10^6	2.05×10^5
Air	272	

Solving for the dimensionless slip coefficient, we find $\beta^{-1} = 2.88 \times 10^{-7}$. This small slip coefficient is hardly distinguishable from the classical no slip case, $\beta^{-1} = 0$. The introduction of slip means a spherical particle moving near a plane wall would translate without rotating, with a dimensionless slip coefficient of $\beta^{-1} = 2.88 \times 10^{-7}$ when the sphere was in 'contact' with the plane wall.

Table 5.1 gives the range on dimensional slip coefficients β' found empirically from Carty's experiments in oil, water and air. Carty only performed a few experiments in air; therefore, only a single value for the dimensional slip coefficient is given. For the air experiments, it was not certain if essentially zero Reynolds number flow conditions were met the creeping flow equations were valid. The range in values for a particular fluid are due to different size spheres and also fluctuations of operating conditions, such as fluid temperature.

Introduction of the slip boundary condition has eliminated the (force) singularity inherent in the problem, enabling the velocity of a particle translating under a finite force to be evaluated. The partial slip model presents a better interpretation then the classical no-slip model of what is happening physically at points of contact between solid surfaces. However, introducing slip on the plane wall would indicate that a sphere in 'contact' with a plane wall would not be able to rotate. This conclusion, contrary to experiments and what would be expected intuitively, must be resolved. Three hypotheses for these results in light of the analytical solution in this thesis are presented.

First, it is possible that Carty's spheres did not reach steady state conditions. The analytical solution is obtained for the steady state creeping flow equations and do not

apply to transient behavior. Carty reported that steady conditions had been met in his experiments; however, his spheres only moved a few diameters from their original position before measurements were taken. This argument would explain Carty's data, but it is not consistent with what would be expected intuitively–that a sphere would roll down an inclined plane. This explanation implies that a sphere would roll down a wall until it reaches steady state conditions, at which time, it would just slide down the incline. This model is insufficient.

Second, the conclusion that a sphere in contact with a wall cannot rotate might be explained by the observation that a sphere rolling down a plane wall might not remain in 'contact' with the plane wall. Chen & McLaughlin (1991) measured the translational and rotational velocities of a sphere rolling down an inclined plane. From the velocity measurements, the separation distance was calculated. Fluctuations in velocity measurements were attributed to fluctuations in the separation distance which ranged form 3×10^{-4} to 3×10^{-3}, after the sphere was determined to have reached steady state conditions.

Chen & McLaughlin's varying separation distance could be a result of a lift force exerted on the particle which is a function of separation distance. The analytical results in this thesis are valid at all separation distances, however the singular nature of the hydrodynamic resistance only presents itself as a problem when the sphere is in 'contact' with the wall. For this scenario it is reasonable to suggest for example that a sphere moving parallel to a plane wall might spend 25 % of its time touching the plane wall. During that time the particle would translate without rotating. During the remaining 75 % of the time, the particle would be a finite distance away from the wall during which rotation and translation would both be possible. The instantaneous changes in separation distance would result in the sphere to appear to roll with slip. This is reasonable to assume in light of Chen & McLaughlin's (1991) experiments in which the ratio of translation to rotation, $a\Omega/U$, was found to range from -0.471 to 0.939 for spheres moving at close separations ($\delta < 100$ Å).

If one allows different solutions for different separation distances, it might be reasonable to ask how introducing slip has improved the model. In the no-slip scenario,

neither translation nor rotation are allowed. Once a particle touches a plane wall it is unable to move. In the slip scenario, translation is allowed, and it is possible that the sphere might move to a position where rotation would be possible.

Third, it should also be noted that the slip boundary condition has only been applied on the plane surface. There is no reason that if hydrodynamic slip occurs, it should only exist on the plane wall and not also on the sphere surface. Although not confirmed at this point, it is reasonable to suggest that introducing slip on the sphere surface might remove the (torque) singularity in the rotation case.

Introducing slip appears to present a better interpretation then the classical no-slip scenario of what is happening physically between solid surfaces in contact.

Chapter 6

Conclusions

Relaxing the traditional no-slip boundary condition in the course of solving Stokes' equations for a sphere moving in very close proximity to a wall is presented as a way to model experimentally observed non-continuum behavior. In particular the analytical solution is presented to the problem of a neutrally buoyant spherical particle translating and/or rotating parallel to a plane wall bounding an otherwise quiescent semi-infinite viscous fluid for the case where a linear slip boundary condition is applied (uniformly) on the wall. These calculations show that the singularity one observes in the classical no slip scenario for the pure translation case is removed entirely when the slightest degree of slip is permitted. Introducing slip into the rotation case however does not alter the order of the (torque) singularity inherent in the problem.

These results indicate that a spherical particle "rolling" down an inclined plane under the influence of gravity would translate without rotating. The experimental observations of Carty (1957) are evaluated in order to estimate an empirically determined slip coefficient. The dimensionless slip coefficient is found to be $\beta^{-1} = 2.88 \times 10^{-7}$, which is hardly distinguishable from the classical no slip case, $\beta^{-1} = 0$. Based on the dimensional parameters in Carty's experiments, in particular the sphere sizes, fluid viscosity and experimental conditions, the dimensional slip coefficient β' was calculated to range from 2.27×10^7 to 1.03×10^8 kg/(m^2 s) for experiments in oil, from 2.05×10^5 to 3.13×10^6 kg/(m^2 s) for experiments in water and to be 272 kg/(m^2 s) for the experiment in air. It is not certain that the runs performed in air were

conducted at essentially zero Reynolds number.

It is postulated that a spherical particle rolling down a wall might spend only a fraction of its time in 'contact' with the wall. During this time, translation without rotation would be possible. When the sphere and wall are not in contact, rotation and translation are both possible. The experiments of Chen & McLaughlin indicate such an assumption might be reasonable as a sphere moving parallel to a plane wall does not maintain a uniform separation distance.

It is also noted that the partial slip boundary condition has not been applied to the sphere surface. There is no reason to think that is hydrodynamic slip were to occur, it would not occur uniformly on all surfaces near points of contact. Although not confirmed, it is suggested that introducing slip on the sphere might remove the (torque) singularity for the rotation case.

Appendix A

Coordinate Transformations

The solutions to the equations of motion and continuity have been presented in spherical bipolar coordinates. To solve these equations and boundary conditions vectors and operations were transformed between the Cartesian, cylindrical and bipolar coordinate systems. This appendix summarizes the basic transformations used throughout this thesis. These expressions are based on the techniques described by Happel and Brenner (1965). It should be noted that the coordinate system used here is different then the one used by Happel and Brenner, in particular the right-handed coordinate system in bipolar coordinates used here, (η, ξ, ϕ) is called (ξ, η, ϕ). The only difference here is the label of the coordinate axes. This alternate naming convention was selected in order to remain consistent with other work in this field.

The use of spherical bipolar coordinates has become a standard coordinate system. Hence, much of the transformations are available in many texts and mathematical handbooks. Presented here are those transformations used frequently throughout this text.

A.1 Metrical Coefficients

In general, transformations between coordinate systems are expressed in terms of metrical coefficients which are defined by,

$$\frac{1}{h_k^2} = (\frac{\partial x}{\partial q_k})^2 + (\frac{\partial y}{\partial q_k})^2 + (\frac{\partial z}{\partial q_k})^2. \tag{A.1}$$

The following partial derivatives have been evaluated in order to evaluate the metrical coefficients.

$$\frac{\partial x}{\partial \eta} = \frac{c\cos\phi(\mu\cosh\xi - 1)}{\cosh\xi - \mu)^2} \tag{A.2}$$

$$\frac{\partial y}{\partial \eta} = \frac{c\ \sin\phi(\mu\cosh\xi - 1)}{(\cosh\xi - \mu)^2} \tag{A.3}$$

$$\frac{\partial z}{\partial \eta} = -\frac{c\ \sin\eta\sinh\xi}{\cosh\xi - \mu)^2} \tag{A.4}$$

$$\frac{\partial x}{\partial \xi} = -\frac{c\ \cos\phi\ \sin\eta\ \sinh\xi}{(\cosh\xi - \mu)^2} \tag{A.5}$$

$$\frac{\partial y}{\partial \xi} = -\frac{c\ \sin\phi\sin\eta\ \sinh\xi}{(\cosh\xi - \mu)^2} \tag{A.6}$$

$$\frac{\partial z}{\partial \xi} = -\frac{c\ (\mu\cosh\xi - 1)}{(\cosh\xi - \mu)^2} \tag{A.7}$$

$$\frac{\partial x}{\partial \phi} = -\frac{c\ \sin\phi\sin\eta}{(\cosh\xi - \mu)} \tag{A.8}$$

$$\frac{\partial y}{\partial \phi} = -\frac{c\ \cos\phi\ \sin\eta}{(\cosh\xi - \mu)} \tag{A.9}$$

$$\frac{\partial z}{\partial \phi} = 0 \tag{A.10}$$

Substituting these expressions into Eq. (A.1) one obtains the following values for the metrical coefficients:

$$h_\eta = \frac{\cosh\xi - \cos\eta}{c}, \tag{A.11}$$

$$h_\xi = \frac{\cosh\xi - \cos\eta}{c}, \tag{A.12}$$

$$h_\phi = \frac{\cosh\xi - \cos\eta}{c\,\sin\eta}. \tag{A.13}$$

A.2 Velocity Vector

In order to transform the velocity in cylindrical coordinates to spherical bipolar coordinates, the following partial derivatives were first evaluated:

$$\frac{\partial\xi}{\partial z} = \frac{1 - \cos\eta\ \cosh\xi}{c}, \tag{A.14}$$

$$\frac{\partial\xi}{\partial\rho} = \frac{-\sinh\xi\ \sin\eta}{c}, \tag{A.15}$$

and

$$\frac{\partial\eta}{\partial z} = \frac{-\sinh\xi\ \sin\eta}{c}, \tag{A.16}$$

$$\frac{\partial\eta}{\partial\rho} = \frac{\cosh\xi\ \cos\eta\ -1}{c}. \tag{A.17}$$

In terms of these partial derivatives, the following transformations related the velocity components between spherical bipolar and cylindrical polar coordinates:

$$v_\eta = \frac{(\cos\eta\ \cosh\xi - 1)}{(\cosh\xi - \cos\eta)}v_\rho - \frac{\sin\eta\ \sinh\xi}{(\cosh\xi - \cos\eta)}v_z, \tag{A.18}$$

$$v_\xi = -\frac{\sin\eta\ \sinh\xi}{(\cosh\xi - \cos\eta)}v_\rho - \frac{(\cos\eta\ \cosh\xi - 1)}{(\cosh\xi - \cos\eta)}v_z, \tag{A.19}$$

$$v_\phi = v_\phi. \tag{A.20}$$

A.3 Gradient

The nabla operator in bipolar coordinates is given by

$$\nabla = \underline{i}_\eta \frac{\cosh\xi - \cos\eta}{c}\frac{\partial}{\partial\eta} + \underline{i}_\xi \frac{\cosh\xi - \cos\eta}{c}\frac{\partial}{\partial\xi} + \underline{i}_\phi \frac{\cosh\xi - \cos\eta}{c\sin\eta}\frac{\partial}{\partial\phi}. \tag{A.21}$$

A.4 Deviatoric Stress

The stress tensor in spherical bipolar coordinates is obtained from the gradient and velocity vectors in the same coordinate system. The components of the stress tensor used in the slip boundary condition are expressed in terms of the velocity components as

$$\tau_{\xi\eta} = \frac{\mu}{2\,c}\left[(\cosh\xi - \cos\eta)\left(\frac{\partial v_\xi}{\partial\eta} + \frac{\partial v_\eta}{\partial\xi}\right) + \sin\eta\, v_\xi + \sinh\xi\, v_\eta\right], \tag{A.22}$$

$$\tau_{\xi\phi} = \frac{\mu}{2\,c}\left[(\cosh\xi - \cos\eta)\left(\frac{\partial v_\phi}{\partial\xi} + \frac{1}{\sin\eta}\frac{\partial v_\xi}{\partial\phi}\right) + \sin\eta\,\sinh\xi\, v_\phi\right]. \tag{A.23}$$

Appendix B

Integrals Involving Legendre Transformations

The equations of motion have been solved using series solutions including expansions of Legendre Polynomials.

B.1 Recursion Relations

The following recursion relations involving Legendre polynomials were used to evaluate integral expressions. (Hildebrand, 1976)

$$\mu P_m = \frac{m+1}{2m+1} P_{m+1} + \frac{m}{2m+1} P_{m-1} \tag{B.1}$$

$$\sin^2 \eta P'_m = \frac{m(m+1)}{2m+1} (P_{m-1} - P_{m+1}) \tag{B.2}$$

$$\mu P'_m = \frac{m+1}{2m+1} P'_{m-1} + \frac{m}{2m+1} P'_{m+1} \tag{B.3}$$

$$P_m = \frac{1}{2m+1} (P'_{m+1} - P'_{m-1}) \tag{B.4}$$

$$sin^2 \eta P''_m = 2\mu P'_m - m(m+1) P_m) \tag{B.5}$$

$$sin^2 \eta P''_m = \frac{(m+1)(m+2)}{(2m+1)} P'_{m-1} - \frac{m(m-1)}{(2m+1)} P'_{m+1} \tag{B.6}$$

Eqs. (B.1)-(B.6) can be combined to give these expressions involving P_m. These are the forms used to develop recursion relations.

$$\begin{aligned} sin^2\eta P_m = & \frac{m(m-1)}{(2m-3)(2m-1)(2m+1)} P'_{m-3} \\ & - \frac{(3m^2+m-6)}{(2m-3)(2m+1)(2m+3)} P'_{m-1} \\ & + \frac{(3m^2+5m-4)}{(2m-1)(2m+1)(2m+5)} P'_{m+1} \\ & - \frac{(m+1)(m+2)}{(2m+1)(2m+3)(2m+5)} P'_{m+3} \end{aligned} \tag{B.7}$$

$$\begin{aligned} \cos\eta \ \sin^2\eta \ P_m = & \frac{m(m-1)(m-2)}{(2m-5)(2m-3)(2m-1)(2m+1)} P'_{m-4} \\ & - \frac{m(2m^2-m-7)}{(2m-5)(2m-1)(2m+1)(2m+3)} P'_{m-2} \\ & + \frac{(m-2)(m-3)}{(2m-3)(2m-1)(2m+3)(2m+5)} P'_{m} \\ & + \frac{(m+1)(2m^2+5m-4)}{(2m-1)(2m+1)(2m+3)(2m+7)} P'_{m+2} \\ & - \frac{(m+1)(m+2)(m+3)}{(2m+1)(2m+3)(2m+5)(2m+7)} P'_{m+4} \end{aligned} \tag{B.8}$$

Eqs. (B.1)-(B.6) can be combined to give these expressions involving P'_m. These are the forms used to develop recursion relations.

$$\begin{aligned} \sin^2\eta \ P'_m = & - \frac{m(m+1)}{(2m-1)(2m+1)} P'_{m-2} + \frac{2m(m+1)}{(2m-1)(2m+3)} P'_{m} \\ & - \frac{m(m+1)}{(2m+1)(2m+3)} P'_{m+2} \end{aligned} \tag{B.9}$$

$$\cos\eta \ \sin^2\eta P'_m = - \frac{(m-1)m(m+1)}{(2m-3)(2m-1)(2m+1)} P'_{m-3}$$

$$
\begin{aligned}
&+ \frac{m^2(m+1)}{(2m-3)(2m+1)(2m+3)} P'_{m-1} \\
&+ \frac{m(m+1)^2}{(2m-1)(2m+1)(2m+5)} P'_{m+1} \\
&- \frac{m(m+1)(m+2)}{(2m+1)(2m+3)(2m+5)} P'_{m+3}
\end{aligned} \tag{B.10}
$$

$$
\begin{aligned}
\cos^2\eta \ \sin^2\eta P'_m = &- \frac{(m-2)(m-1)m(m+1)}{(2m-5)(2m-3)(2m-1)(2m+1)} P'_{m-4} \\
&+ \frac{3m(m+1)}{(2m-5)(2m-1)(2m+1)(2m+3)} P'_{m-2} \\
&+ \frac{2m(m+1)(n^2+n-3)}{(2m-3)(2m-1)(2m+1)(2m+3)} P'_m \\
&+ \frac{3m(m+1)}{(2m-1)(2m+1)(2m+3)(2m+7)} P'_{m+2} \\
&- \frac{m(m+1)(m+2)(m+3)}{(2m+1)(2m+3)(2m+5)(2m+7)} P'_{m+4}
\end{aligned} \tag{B.11}
$$

Eqs. (B.1)-(B.6) can be combined to give these expressions involving P''_m. These are the forms used to develop recursion relations.

$$
\begin{aligned}
\cos\eta \ \sin^2\eta \ P''_m = &\quad \frac{m(m+1)(m+2)}{(2m-1)(2m+1)} P'_{m-2} \\
&+ \frac{3(m-1)(m+2)}{(2m-1)(2m+3)} P'_m \\
&- \frac{(m-1)m(m+1)}{(2m+1)(2m+3)} P'_{m+2}
\end{aligned} \tag{B.12}
$$

$$
\begin{aligned}
\cos^2\eta \ \sin^2\eta \ P''_m = &\quad \frac{(m-1)m(m+1)(m+2)}{(2m-3)(2m-1)(2m+1)} P'_{m-3} \\
&+ \frac{(m+1)(m+2)(m^2+3m-9)}{(2m-3)(2m+1)(2m+3)} P'_{m-1} \\
&- \frac{m(m-1)(m^2-m-11)}{(2m-1)(2m+1)(2m+5)} P'_{m+1}
\end{aligned} \tag{B.13}
$$

$$- \frac{(m-1)m(m+1)(m+2)}{(2m+1)(2m+3)(2m+5)} P'_{m+3}$$

B.2 Integral Relations

Integrals of Legendre Polynomials and their derivatives as well as terms involving $(\cosh\xi - \cos\eta)^{-m/2}$ have been evaluated in order to determine recursion relations, and also to evaluate the hydrodynamic force and torque exerted on a particular boundary. The following identity,

$$(\cosh\xi - \cos\eta)^{-1/2} = \sum_{m=0}^{\infty} g_m P_m \tag{B.14}$$

where

$$g_m = \sqrt{2}\exp\left[-\left(m+\frac{1}{2}\right)\xi\right], \tag{B.15}$$

was used to represent the integral of $(\cosh\xi - \cos\eta)^{-1/2}$ in a form consistent with obtaining recursion relations. It was thus possible to simply represent non-homogeneous terms in the boundary condition expressions.

The orthogonality relations used to derive recursion relations from the boundary conditions are

$$\int_{-1}^{1} P_n P_m d\mu = \frac{2}{2n+1}\delta_{n,m}, \tag{B.16}$$

and

$$\int_{-1}^{1} P'_n P'_m d\mu = \frac{2n(n+1)}{2n+1}\delta_{n,m}. \tag{B.17}$$

Here, the Kronecker delta function, $\delta_{n,m}$ is defined as

$$\delta_{n,m} = \begin{cases} 1 \text{ for } n = m, \\ 0 \text{ for } n \neq m. \end{cases} \tag{B.18}$$

Appendix C

Source Code

The fortran codes presented in the Appendix were used to obtain the numerical results cited in this thesis. Minor variations of these codes were made for special cases and for use on different machines. The versions are compatible with the CRAY X-MP.

This program solves the case of a sphere translating past a plane wall.

```
      program trans
c
c     This program numerically solves the coefficients to the
c     analytic expression describing a sphere translating
c     past a plane surface.
c
c                                 constraints
c     BC:   no slip on sphere          (3)
c           uniform slip on plane      (2)
c     Continuity                     (2)                                    10
c
      dimension rhsar(70000,1),bar(73,70000),car(1,70000),
     &     dar(70000,1),ear(1,1)
      character*12 fname

      write(6,*)' INPUT THE VALUE OF ALPHA '
      read(5,*)alpha
      write(6,*)' INPUT THE FIRST VALUE OF THE SLIP COEFFICIENT, BETA '
      read(5,*)betap
      write(6,*)' Input the decrement factor for betap'                     20
      read(5,*)factbp
      write(6,*)' INPUT THE FIRST VALUE OF BET'
      read(5,*)bet
      write(6,*)' Input the decrement factor for beta'
      read(5,*)factb
      write(6,*)' Input the number of runs to be made'
```

```
      read(5,*)nrun
      write(6,*)' ENTER THE NUMBER OF TERMS (max 10,000, min 2)'
      read(5,*)num
c                                                                      30
c     This program uses a banded matrix solver to solve a 7n x 7n
c     matrix corresponding to the system of equations for the
c     7n unknowns.  These are a linear set of equations which can
c     be solved simultaneously.
c
      zero  = 0.0
      one   = 1.0
      two   = 2.0
      three = 3.0
      four  = 4.0                                                      40
      five  = 5.0
      half  = ONE/TWO
      sqtwo = SQRT(TWO)
c
      aval  =  one
      alpha =  alpha*one
      cval  =  aval*sinh(alpha)
      cotal =  one/tanh(alpha)

      do 500, k=1,nrun                                                 50
        betap=betap/factbp
        bet = bet/factb
        cb  = -cval*betap

        do 75, kk = 1,(7*num+21)
          do 74, kl = 1,73
            bar(kl,kk)=zero
 74         continue
          rhsar(kk,1)=zero
 75     continue                                                        60
c
c     filling in the equations corresponding to Xn, n=0
c
      bar(25,1)  = one
      rhsar(1,1) = zero

      bar(25,2)  = one
      rhsar(2,1) = zero

      bar(25,3)  = one                                                 70
      rhsar(3,1) = zero
c
c     set ft(1) = 0
c
      bar(34,4) = one
      rhsar(4,1) = zero

      bar(25,5) = -one
      bar(24,5)= -one/tanh(alpha/two)
      bar(28,5) = two/three*(cotal+one/tanh(alpha/two))                80
```

```
      rhsar(5,1) = -two*sqtwo*exp(-alpha/two)
     &     /sinh(alpha/two)

      bar(25,6)  = one
      rhsar(6,1) = zero

      bar(25,7) = one
      rhsar(7,1) = zero

      do 40, n = 1,num-1                                                  90
        rn = n*one
        cotnh = one/tanh((rn+half)*alpha)
c
c     ** equation 1 **
c       continuity C,E,G
c
        ieq = 7*n + 1
        bar(20,ieq) = -(rn-one)/two
        bar(22,ieq) = - half
        bar(24,ieq) = (rn-two)*(rn-one)/two                               100
        bar(27,ieq) = five/two
        bar(29,ieq) = one
        bar(31,ieq) = -(rn-one)*(rn+two)
        bar(34,ieq) = (rn+two)/two
        bar(36,ieq) = -half
        bar(38,ieq) = (rn+two)*(rn+three)/two
        rhsar(ieq,1) = zero
c
c     ** equation 2 **
c       continuity A,B,D,F                                                110
c
        ieq = 7*n + 2
        bar(17,ieq) = -(rn-one)
        bar(18,ieq) = -(rn-one)/two
        bar(20,ieq) = -half
        bar(22,ieq) = (rn-two)*(rn-one)/two
        bar(24,ieq) = two*rn+one
        bar(25,ieq) = five/two
        bar(27,ieq) = one
        bar(29,ieq) = -(rn-one)*(rn+two)                                  120
        bar(31,ieq) = -(rn+two)
        bar(32,ieq) = (rn+two)/two
        bar(34,ieq) = -half
        bar(36,ieq) = (rn+two)*(rn+three)/two
        rhsar(ieq,1) = zero
c
c     ** equation 3 **
c         Cn Sphere - no slip
c
        ieq = 7*n + 3                                                     130
        bar(25,ieq) = -one
        bar(16,ieq) = two*(rn-one)/(two*rn-one)*(cotal-cotnh)
        bar(23,ieq) = -2*cotal
        bar(24,ieq) = -cotnh
```

```
      bar(30,ieq) = two*(rn+two)/(two*rn+three)*(cotal+cotnh)
      rhsar(ieq,1) = zero
c
c     ** equation 4 **
c        Bn,Cn,Fn,Gn plane - uniform, beta slip
c          eta equation                                                  140
c
      ieq = 7*n + 4
      bar(30,ieq) = -cb*(rn+two)/(two*rn+three)
      bar(23,ieq) = -cb
      bar(16,ieq) = -cb*(rn-one)/(two*rn-one)

      bar(32,ieq) =  cb*two/(two*rn+three)
      bar(18,ieq) = -cb*two/(two*rn-one)

      bar(38,ieq) =  (rn+two)*(rn+three)*bet/(two*rn+three)/two             150
      bar(24,ieq) = -rn*(rn+one)*(two*rn+one)*bet
     &                /(two*rn-one) /(two*rn+three)
      bar(10,ieq) =  (rn-one)*(rn-two)*bet/(two*rn-one)/two

      bar(40,ieq) = -(rn+two)*bet/(two*rn+three)
      bar(33,ieq) =  bet
      bar(26,ieq) = (two*rn+one)/(two*rn-one)/(two*rn+three)
     &                *bet
      bar(19,ieq) = -bet
      bar(12,ieq) =  (rn-one)*bet/(two*rn-one)                          160

      rhsar(ieq,1) = zero
c
c     ** equation 5 **
c        En Sphere - no slip
c
      ieq = 7*n + 5
      bar(25,ieq) = -one
      bar(14,ieq) = -rn*(rn-one)/(two*rn-one)*
     &     (cotal-cotnh)                                                170
      bar(24,ieq) = -cotnh
      bar(28,ieq) = (rn+one)*(rn+two)/(two*rn+three)*
     &     (cotal+cotnh)
      rhsar(ieq,1) = -two*sqtwo*exp(-(rn+half)*alpha)
     &     /sinh((rn+half)*alpha)
c
c     ** equation 6 **
c        Dn,En,Fn,Gn plane - uniform, beta slip on plane
c          phi equation
c                                                                        180
      ieq = 7*n + 6
      bar(12,ieq) =  (rn-one)*(rn-two)*(rn-three)
     &     /two/(two*rn-one)*bet
      bar(19,ieq) = -(rn-one)*(rn-two)/two*bet
      bar(26,ieq) = -(rn+half)*three*(rn-one)*(rn+two)
     &     /(two*rn-one)/(two*rn+three)*bet
      bar(33,ieq) =  (rn+two)*(rn+three)/two*bet
      bar(40,ieq) = -(rn+two)*(rn+three)*(rn+four)
```

```
     &       /two/(two*rn+three)*bet
                                                                        190
        bar(32,ieq) =  cb*(rn+two)*(rn+three)/(two*rn+three)
        bar(18,ieq) = -cb*(rn-one)*(rn-two)/(two*rn-one)

        bar(10,ieq) =  (rn-one)/two/(two*rn-one)*bet
        bar(17,ieq) = -half*bet
        bar(24,ieq) =  (rn+half)/(two*rn-one)/(two*rn+three)*bet
        bar(31,ieq) =  half*bet
        bar(38,ieq) = -(rn+two)/two/(two*rn+three)*bet

        bar(30,ieq) =  cb/(two*rn+three)                                200
        bar(16,ieq) = -cb/(two*rn-one)
        rhsar(ieq,1) = zero
c
c     ** equation 7 **
c          Gn Sphere - no slip

        ieq = 7*n + 7
        bar(25,ieq) = -one
        bar(12,ieq) = (cotal-cotnh)/(two*rn-one)
        bar(24,ieq) = -cotnh                                            210
        bar(26,ieq) = -(cotal+cotnh)/(two*rn+three)
        rhsar(ieq,1) = zero

 40   continue
c
c     set gt(1) = 0
c
     bar(25,14)  = one
     bar(12,14)  = zero
     bar(24,14)  = zero                                                 220
     bar(26,14)  = zero
     rhsar(14,1) = zero
c
     tau = .5
     jn = 70000
     iband = 49
     lbd = 73
     ja = 1
     jna = 70000
     nrhs = 1                                                           230
     nod = 7*num
     iarrow = 0
     lrhs = 1

     call arrow(rhsar,bar,car,dar,ear,detlog,isign,tau,jn,iband,lbd,
    &     ja,jna,nrhs,nod,iarrow,lrhs)
c
c     The solution vector must be decomposed into the seven separate
c     vectors corresponding to the coefficients in the general
c     functions W,X,Y and Z.  As the original vector is decomposed,     240
c     the individual values are manipulated and used to determine
c     the force and torque.
```

```
c
      fsum = 0.0
      tsum = 0.0
      do 80,n=0,num
        nn = n*7
        at = rhsar(nn+1,1)
        bt = rhsar(nn+2,1)
        ct = rhsar(nn+3,1)                                          250
        dt = rhsar(nn+4,1)
        et = rhsar(nn+5,1)
        ft = rhsar(nn+6,1)
        gt = rhsar(nn+7,1)
        rn = n*one
        fsum = fsum + DT+ET + RN*(RN+ONE)*(BT+CT)
        pr1  = exp(-1.0*(TWO*RN+ONE)*ALPHA)
        val  = rn*(rn+one)*(two*AT+CT*cotal)
     &       - (TWO*RN + ONE - COTAL)*ET
        val2 = RN*(RN+one)*BT*COTAL                                 260
     &       - (TWO*RN+ONE-COTAL)*DT
        tsum = tsum + (TWO+PR1)*val + (two-pr1)*val2
 80     continue
c
      force = -sqtwo/6.0*sinh(alpha)*fsum
      torque = sinh(Alpha)*sinh(alpha)/(12.0*Sqtwo)*tsum
      write(6,1030)alpha,num,force,torque,betap,bet
 500  continue
      STOP
 1030 FORMAT(/F11.6,2X,I5,f20.10,E20.10,4X,E11.3,4X,E11.3)          270
      END
```

This program solves the case of a sphere rotating above a plane wall.

```
      program rotation
c
c     This program numerically solves the coefficients to the
c     analytic expression describing a sphere translating
c     across a plane surface.
c
c                                  constraints
c     BC:   no slip on sphere            (3)
c           uniform slip on plane        (2)
c     Continuity                       (2)                          10
c
      dimension rhsar(70000,1),bar(73,70000),car(1,70000),
     &     dar(700000,1),ear(1,1)

      write(6,*)' INPUT THE VALUE OF ALPHA '
      read(5,*)alpha
      write(6,*)' INPUT THE FIRST VALUE OF THE SLIP COEFFICIENT, BETA '
      read(5,*)betap
      write(6,*)' Input the decrement factor for betap'
      read(5,*)factbp                                               20
```

```
      write(6,*)' INPUT THE FIRST VALUE OF BET'
      read(5,*)bet
      write(6,*)' Input the decrement factor for beta'
      read(5,*)factb
      write(6,*)' Input the number of runs to be made'
      read(5,*)nrun
      write(6,*)' ENTER THE NUMBER OF TERMS (max 10,000, min 2)'
      read(5,*)num
c
c     This program uses a banded matrix solver to solve a 7n x 7n
c     matrix corresponding to the system of equations for the
c     7n unknowns.  These are a linear set of equations which can
c     be solved simultaneously.
c
      zero  = 0.0
      one   = 1.0
      two   = 2.0
      three = 3.0
      four  = 4.0
      five  = 5.0
      half  = ONE/TWO
      sqtwo = SQRT(TWO)
c
      aval  =  one
      alpha =  alpha*one
      cval  =  aval*sinh(alpha)
      cotal =  one/tanh(alpha)

      do 500, k=1,nrun
        betap=betap/factbp
        bet = bet/factb
        cb  = -cval*betap

        do 75, kk = 1,(7*num+21)
          do 74, kl = 1,73
            bar(kl,kk)=zero
 74         continue
          rhsar(kk,1)=zero
 75     continue
c
c     filling in the equations corresponding to Xn, n=0
c
      bar(25,1)  = one
      rhsar(1,1) = zero

      bar(25,2)  = one
      rhsar(2,1) = zero

      bar(25,3)  = one
      rhsar(3,1) = zero
c
c     set fr(1) = 0
c
      bar(34,4) = one
```

```
      rhsar(4,1) = zero

      bar(25,5) = -one
      bar(24,5)= -one/tanh(alpha/two)
      bar(28,5) = two/three*(cotal+one/tanh(alpha/two))
      taun = (exp(alpha/two)+exp(-alpha*three/two)/three)/sqtwo                    80
      rhsar(5,1) = -(sqtwo*exp(-alpha/two)-taun/sinh(alpha))
     &     /sinh(alpha/two)

      bar(25,6)  = one
      rhsar(6,1) = zero

      bar(25,7) = one
      rhsar(7,1) = zero

      do 40, n = 1,num-1                                                           90
        rn = n*one
        cotnh = one/tanh((rn+half)*alpha)
        rkn   = (rn+half)/tanh((rn+half)*alpha) - cotal
        taun = -(exp(-alpha*(rn-half))/(two*rn-one)-
     &       exp(-alpha*(rn+three/two))/(two*rn+three))/sqtwo
c
c     ** equation 1 **
c       continuity C,E,G
c
        ieq = 7*n + 1                                                             100
        bar(20,ieq) = -(rn-one)/two
        bar(22,ieq) = - half
        bar(24,ieq) = (rn-two)*(rn-one)/two
        bar(27,ieq) = five/two
        bar(29,ieq) = one
        bar(31,ieq) = -(rn-one)*(rn+two)
        bar(34,ieq) = (rn+two)/two
        bar(36,ieq) = -half
        bar(38,ieq) = (rn+two)*(rn+three)/two
        rhsar(ieq,1) = zero                                                       110
c
c     ** equation 2 **
c       continuity A,B,D,F
c
        ieq = 7*n + 2
        bar(17,ieq) = -(rn-one)
        bar(18,ieq) = -(rn-one)/two
        bar(20,ieq) = -half
        bar(22,ieq) = (rn-two)*(rn-one)/two
        bar(24,ieq) = two*rn+one                                                  120
        bar(25,ieq) = five/two
        bar(27,ieq) = one
        bar(29,ieq) = -(rn-one)*(rn+two)
        bar(31,ieq) = -(rn+two)
        bar(32,ieq) = (rn+two)/two
        bar(34,ieq) = -half
        bar(36,ieq) = (rn+two)*(rn+three)/two
        rhsar(ieq,1) = zero
```

```
c
c     ** equation 3 **                                                    130
c          Cn Sphere - no slip
c
          ieq = 7*n + 3
          bar(25,ieq) = -one
          bar(16,ieq) = two*(rn-one)/(two*rn-one)*(cotal-cotnh)
          bar(23,ieq) = -2*cotal
          bar(24,ieq) = -cotnh
          bar(30,ieq) = two*(rn+two)/(two*rn+three)*(cotal+cotnh)
c         bar(16,ieq) = -two*rkn*(rn-one)/(two*rn-one)
c         bar(23,ieq) = two*rkn                                           140
c         bar(30,ieq) = -two*rkn*(rn+two)/(two*rn+three)
          rhvar=-four*taun/sinh(alpha)/sinh((rn+half)*alpha)
          rhsar(ieq,1) = rhvar
c
c     ** equation 4 **
c          Bn,Cn,Fn,Gn plane - uniform, beta slip
c            eta equation
c
          ieq = 7*n + 4
          bar(30,ieq) = -cb*(rn+two)/(two*rn+three)                       150
          bar(23,ieq) = -cb
          bar(16,ieq) = -cb*(rn-one)/(two*rn-one)

          bar(32,ieq) =  cb*two/(two*rn+three)
          bar(18,ieq) = -cb*two/(two*rn-one)

          bar(38,ieq) =  (rn+two)*(rn+three)*bet/(two*rn+three)/two
          bar(24,ieq) = -rn*(rn+one)*(two*rn+one)*bet
     &                    /(two*rn-one) /(two*rn+three)
          bar(10,ieq) =  (rn-one)*(rn-two)*bet/(two*rn-one)/two           160

          bar(40,ieq) = -(rn+two)*bet/(two*rn+three)
          bar(33,ieq) =  bet
          bar(26,ieq) = (two*rn+one)/(two*rn-one)/(two*rn+three)
     &                       *bet
          bar(19,ieq) = -bet
          bar(12,ieq) =  (rn-one)*bet/(two*rn-one)

          rhsar(ieq,1) = zero
c                                                                         170
c     ** equation 5 **
c          En Sphere - no slip
c
          ieq = 7*n + 5
          bar(25,ieq) = -one
          bar(14,ieq) = -rn*(rn-one)/(two*rn-one)*
     &         (cotal-cotnh)
          bar(24,ieq) = -cotnh
          bar(28,ieq) = (rn+one)*(rn+two)/(two*rn+three)*
     &         (cotal+cotnh)                                              180

c         bar(14,ieq) = rkn*rn*(rn-one)/(two*rn-one)
```

```
c       bar(28,ieq) = -rkn*(rn+one)*(rn+two)/(two*rn+three)
        rhsar(ieq,1) = -(sqtwo*(two*rn+one)*exp(-(rn+half)*alpha)
     &       -taun/sinh(alpha))/sinh((rn+half)*alpha)
c
c     ** equation 6 **
c        Dn,En,Fn,Gn plane - uniform, beta slip on plane
c          phi equation
c                                                                    190
        ieq = 7*n + 6
        bar(12,ieq) =  (rn-one)*(rn-two)*(rn-three)
     &       /two/(two*rn-one)*bet
        bar(19,ieq) = -(rn-one)*(rn-two)/two*bet
        bar(26,ieq) = -(rn+half)*three*(rn-one)*(rn+two)
     &       /(two*rn-one)/(two*rn+three)*bet
        bar(33,ieq) =  (rn+two)*(rn+three)/two*bet
        bar(40,ieq) = -(rn+two)*(rn+three)*(rn+four)
     &       /two/(two*rn+three)*bet
                                                                    200
        bar(32,ieq) =  cb*(rn+two)*(rn+three)/(two*rn+three)
        bar(18,ieq) = -cb*(rn-one)*(rn-two)/(two*rn-one)

        bar(10,ieq) =  (rn-one)/two/(two*rn-one)*bet
        bar(17,ieq) = -half*bet
        bar(24,ieq) =  (rn+half)/(two*rn-one)/(two*rn+three)*bet
        bar(31,ieq) =  half*bet
        bar(38,ieq) = -(rn+two)/two/(two*rn+three)*bet

        bar(30,ieq) =  cb/(two*rn+three)                            210
        bar(16,ieq) = -cb/(two*rn-one)
        rhsar(ieq,1) = zero
c
c     ** equation 7 **
c        Gn Sphere - no slip

        ieq = 7*n + 7
        bar(25,ieq) = -one
        bar(12,ieq) = (cotal-cotnh)/(two*rn-one)
        bar(24,ieq) = -cotnh                                        220
        bar(26,ieq) = -(cotal+cotnh)/(two*rn+three)
        rhsar(ieq,1)= -rhvar

 40   continue
c
c     set gr(1) = 0
c
      bar(25,14)  = one
      bar(12,14)  = zero
      bar(24,14)  = zero                                            230
      bar(26,14)  = zero
      rhsar(14,1) = zero

      tau = .5
      jn = 17500
      iband = 49
```

```
      lbd = 73
      ja = 1
      jna = 17500
      nrhs = 1                                                          240
      nod = 7*num
      iarrow = 0
      lrhs = 1

      call arrow(rhsar,bar,car,dar,ear,detlog,isign,tau,jn,iband,lbd,
     &     ja,jna,nrhs,nod,iarrow,lrhs)

c     write(20,*)' detlog,isign  = ', detlog,isign
c
c     The solution vector must be decomposed into the seven separate    250
c     vectors corresponding to the coefficients in the general
c     functions W,X,Y and Z.  As the original vector is decomposed,
c     the individual values are manipulated and used to determine
c     the force and torque.
c
c     write(20,1000)alpha,num
c     write(20,1002)betap,bet,cval
c     write(20,1005)
c
      fsum = 0.0                                                        260
      tsum = 0.0
      do 80,n=0,num
        nn = n*7
        ar = rhsar(nn+1,1)
        br = rhsar(nn+2,1)
        cr = rhsar(nn+3,1)
        dr = rhsar(nn+4,1)
        er = rhsar(nn+5,1)
        fr = rhsar(nn+6,1)
        gr = rhsar(nn+7,1)                                              270
        rn = n*one
        fsum = fsum + dr+er + RN*(RN+ONE)*(br+cr)
        pr1  = exp(-1.0*(TWO*RN+ONE)*ALPHA)
        val  = rn*(rn+one)*(two*ar+cr*cotal)
     &       - (TWO*RN + ONE - COTAL)*er
        val2 = RN*(RN+one)*br*COTAL
     &       - (TWO*RN+ONE-COTAL)*dr
        tsum = tsum + (TWO+PR1)*val + (two-pr1)*val2
 80     continue
c                                                                       280
      FORCE = -SQTWO/6.0*fsum*(SINH(ALPHA))**2
      TORQUE = one/three-((SINH(ALPHA))**3)/12.0/SQTWO*TSUM
      write(6,1030)alpha,num,force,torque,betap,bet
 500  continue
      STOP
 1030 FORMAT(/F11.6,2X,I5,E20.10,E20.10,4X,E11.3,4X,E11.3)
      END
```

This banded matrix solver subroutine was used by both the above two codes to

solve the linear set of simultaneous equations.

```
c     written by:                paul thomas
c                          mit 66-256
c                          77 massachusetts avenue
c                          cambridge, ma  02139
c
c     this subroutine solves the matrix equation:
c                                    A * x = f
c
c     where A is an arrow matrix and f,x are vectors.  An arrow
c     matrix has nonzero elements only in a narrow band centered                10
c     on the main diagonal and in the last few columns and rows:
c
c                              b b      c c
c                              b b b    c c
c                               b b b   c c
c                        A =      b b b c c
c                                  b b c c
c                              d d d d d e e
c                              d d d d d e e
c                                                                               20
c     The matrix A is reduced using gaussian elimination with
c     threshold row pivoting.  The column in the band matrix is
c     searched for the maximum element.  If the diagonal element
c     is less than a fraction(tau) of the maximum element, then
c     the rows are exchanged.
c
c     tau = 1.0          partial pivoting
c     tau = 0.2-0.3        recommended range
c     tau = 0.0          no pivoting
c     tau = -1.0          solves l u x = b.  input is matrix previously          30
c                        factored with tau = 0.0
c
c     The program will return the correct L U decomposition if it
c     has not pivoted, which is indicated when npiv=0.  this can
c     be forced by setting tau=0.0, suppressing pivoting.  the
c     matrix equation is solved for multiple f vectors.  the
c     magnitude and sign of the determinant are also calculated.
c     note:  extra storage is required for the band matrix.
c
      subroutine arrow(rhs,b,c,d,e,detlog,isign,tau,                           40
     $           jn,iband,lbd,ja,jna,nrhs,nod,iarrow,lrhs)
      dimension b(lbd,jn),c(ja,jn),d(jn,ja),e(ja,ja)
      dimension rhs(jna,lrhs)
c
c     jn,lbd,ja,
c     jna,lrhs -       sizes of arrays b,c,d,e,rhs used in the
c                      dimension statements
c     nod -            dimension of the banded matrix and of the
c                      columns and rows of the arrow
c     iband -          band width of matrix b, must be odd                      50
```

```
c     iarrow -        width of the columns and rows in the arrow
c     nrhs -          number of r.h.s. vectors f
c
c     tau -           minimum ratio of diagonal to maximum element
c                     for no pivoting and  L U, set tau=0.0
c                     for full pivoting, set tau=1.0
c                     for solving  L U x = b, set tau=-1.0
c     detlog -        log 10 of the determinant
c     isign -         sign of the determinant
c     npiv -          number of times rows have been pivoted                  60
c
c     rhs(nod+iarrow,nrhs) -  holds f vectors.  the solution
c                           vector x is returned in this vector
c     e(iarrow,iarrow) -      holds the elements in the square
c                           section of the arrow matrix
c     d(nod,iarrow) -         holds the elements of the rows
c                           of the arrow matrix
c     c(iarrow, nod) -        holds the elements of the columns
c                           of the arrow matrix
c     b( 3*iband-1 , nod) -   banded part of A.  note that the                70
c       ----------                    dimensions are 50% greater than
c         2                   the bandwidth.
c
      mid=(iband+1)/2
      mex=0
      nex=0
      detlog=0.0
      isign=1
      npiv=0
c                                                                             80
c     b(mid,i)      contains the diagonal elements of matrix a
c     mex             keeps track of the maximum row exchange
c                 in the matrix b
c     nex             keeps track of the last non-zero element
c                 in the row in matrix b
c
c     clean out matrix b outside the band width
c
      do 10 i=1,nod
        do 10 j=iband+1,iband+mid-1                                           90
          b(j,i)=0.0
10    continue
c
c     gaussian elimination of matrix b.  check the column
c     for the maximum element.  if the diagonal is less than a
c     fraction, tau, of the maximum element then switch rows.
c     if tau = 0.0 then no pivoting will take place and the  l u
c     decomposition will be returned.  if tau=1.0 then full row
c     pivoting will be used.  if tau = -1.0 then the  l u  matrix
c     will be front-substituted, and then back-substituted.                   100
c

      if (tau.lt.0.0) goto 20
      do 30 i=1,nod-1
```

```
      l=i
      big=abs(b(mid,i))
      do 40 j=i+1,min(l+mid-1,nod)
        if(abs(b(mid+i-j,j)).lt.big) goto 40
        big=abs(b(mid+i-j,j))
        l=j                                                    110
40      continue
      if (abs(b(mid,i)).ge.tau*big) goto 50
c
c     exchange row i with row l of the matrices b, c, rhs.
c     the determinant of the matrix changes sign.
c
      mex=max(mex,l-i)
      nex=max(nex,l-i)
      k1=min(iband+nex,nod-i+mid)
      do 60 j=mid,k1                                           120
        trans=b(j,i)
        b(j,i)=b(j+i-l,l)
        b(j+i-l,l)=trans
60      continue
      do 70 j=1,iarrow
        trans=c(j,i)
        c(j,i)=c(j,l)
        c(j,l)=trans
70      continue
      do 80 n=1,nrhs                                           130
        trans=rhs(i,n)
        rhs(i,n)=rhs(l,n)
        rhs(l,n)=trans
80      continue
      isign=-isign
      npiv=npiv+1
c
c     the lower band matrix is eliminated and replaced with the
c     pivots for the l u decomposition.  the rhs vector and the
c     array c is updated.                                      140
c
50      diag=b(mid,i)
      nex=max(l-i,nex-1)
      j1=max(1,i+mid-nod)
      j2=max(1-nex,i+mid-nod)
      do 30 j=mid-1,j1,-1
        i1=mid+i-j
        b(j,i1)=b(j,i1)/diag
        piv=-b(j,i1)
        mmcnt=mid-j                                            150
        do 90 n=1,nrhs
          rhs(i1,n)=rhs(i1,n)+piv*rhs(i,n)
90        continue
        do 100 m=1,iarrow
          c(m,i1)=c(m,i1)+piv*c(m,i)
100       continue
        do 30 k=j+1,j+mid-j2
          b(k,i1)=b(k,i1)+piv*b(mmcnt+k,i)
```

```
30      continue
c                                                                      160
c     the array d is eliminated except for the last column and
c     replaced with the pivot for the l u decomposition.  the rhs
c     vector and the array e are updated.
c
      do 110 i=1,nod-1
        diag=b(mid,i)
        j1=min(i+mid-1+mex,nod)
        do 110 j=1,iarrow
          d(i,j)=d(i,j)/diag
          piv=-d(i,j)                                                  170
          do 120 n=1,nrhs
            rhs(nod+j,n)=rhs(nod+j,n)+piv*rhs(i,n)
120         continue
          do 130 k=i+1,j1
            d(k,j)=d(k,j)+piv*b(mid+k-i,i)
130         continue
          do 110 l=1,iarrow
            e(l,j)=e(l,j)+piv*c(l,i)
110     continue
c                                                                      180
c     the final element of the banded matrix b is checked to see
c     if it is large enough.  if it is too small, it is pivoted
c     with an element from the last column of the array d.
c
      big=abs(b(mid,nod))
      do 140 j=1,iarrow
        if(abs(d(nod,j)).lt.big) goto 140
        big=abs(d(nod,j))
        l=j
140     continue                                                       190
      if(abs(b(mid,nod)).ge.tau*big) goto 150
      do 160 n=1,nrhs
        trans=rhs(nod,n)
        rhs(nod,n)=rhs(nod+l,n)
        rhs(nod+l,n)=trans
160     continue
      do 170 j=1,iarrow
        trans=c(j,nod)
        c(j,nod)=e(j,l)
        e(j,l)=trans                                                   200
170     continue
      trans=b(mid,nod)
      b(mid,nod)=d(nod,l)
      d(nod,l)=trans
      isign=-isign
      npiv=npiv+1
c
c     the last column of the array d is eliminated.  the rhs
c     vector and the array e are updated.
c                                                                      210
150     diag=b(mid,nod)
      do 180 i=1,iarrow
```

```
        d(nod,i)=d(nod,i)/diag
        piv=-d(nod,i)
        do 190 n=1,nrhs
          rhs(nod+i,n)=rhs(nod+i,n)+piv*rhs(nod,n)
190       continue
        do 180 j=1,iarrow
          e(j,i)=e(j,i)+piv*c(j,nod)
180     continue                                                    220
c
c     the array e is eliminated using threshold row pivoting.
c     if the diagonal element is less than a fraction, tau, of the
c     maximum column element, then the rows are exchanged.  as the
c     column is eliminated, the rhs vector and the array e are
c     updated.
c
      do 200 i=1,iarrow-1
        big=abs(e(i,i))
        do 210 j=i+1,iarrow                                         230
          if(abs(e(i,j)).lt.big) goto 210
          big=abs(e(i,j))
          l=j
210       continue
        if (abs(e(i,i)).ge.tau*big) goto 220
        do 230 n=1,nrhs
          trans=rhs(nod+i,n)
          rhs(nod+i,n)=rhs(nod+l,n)
          rhs(nod+l,n)=trans
230       continue                                                  240
        do 240 j=1,iarrow
          trans=e(j,i)
          e(j,i)=e(j,l)
          e(j,l)=trans
240       continue
        isign=-isign
        npiv=npiv+1
220       diag=e(i,i)
        do 200 j=i+1,iarrow
          e(i,j)=e(i,j)/diag                                        250
          piv=-e(i,j)
          do 250 n=1,nrhs
            rhs(nod+j,n)=rhs(nod+j,n)+piv*rhs(nod+i,n)
250         continue
          do 200 k=i+1,iarrow
            e(k,j)=e(k,j)+piv*e(k,i)
200     continue
      goto 260
c
c     if tau < 0 the matrix is not decomposed, and the previous     260
c     l u  matrix is used.  the lower matrix  l  is forward
c     substituted.
c
20      do 270 i=1,nod
        i1=min(i+mid-1,nod)
        do 270 n=1,nrhs
```

```
          piv=-rhs(i,n)
          do 280 j=i+1,i1
            rhs(j,n)=rhs(j,n)+piv*b(i+mid-j,j)
280         continue                                                    270
          do 270 j=1,iarrow
            rhs(nod+j,n)=rhs(nod+j,n)+piv*d(i,j)
270       continue
        do 290 i=1,iarrow
          do 290 n=1,nrhs
            piv=-rhs(nod+i,n)
            do 290 j=i+1,iarrow
              rhs(nod+j,n)=rhs(nod+j,n)+piv*e(i,j)
290       continue
c                                                                       280
c       the upper matrix u containing the arrow is back-substituted
c       for the solution vectors x.  the magnitude and sign of the
c       matrix are calculated.
c
260       do 300 i=iarrow,1,-1
          diag=e(i,i)
          detlog=detlog+log10(abs(diag))
          if(diag.lt.0.0) isign=-isign
          do 300 n=1,nrhs
            rhs(nod+i,n)=rhs(nod+i,n)/diag                              290
            piv=-rhs(nod+i,n)
            do 310 j=i-1,1,-1
              rhs(nod+j,n)=rhs(nod+j,n)+piv*e(i,j)
310           continue
            do 300 k=nod,1,-1
              rhs(k,n)=rhs(k,n)+piv*c(i,k)
300       continue
c
c       the upper matrix u containing the banded matrix b is back-
c       substituted for the solution vectors x.  the magnitude and      300
c       sign of the determinant are calculated.
c
        do 320 i=nod,1,-1
          diag=b(mid,i)
          detlog=detlog+log10(abs(diag))
          if(diag.lt.0.0) isign=-isign
          j1=max(1,i-mid-1-mex)
          do 320 n=1,nrhs
            rhs(i,n)=rhs(i,n)/diag
            piv=-rhs(i,n)                                               310
            do 320 j=i-1,j1,-1
              rhs(j,n)=rhs(j,n)+b(mid+i-j,j)*piv
320       continue
        return
        end
```

Appendix D

Integration Constants

Solutions giving the velocity field are expressed in terms of the coefficients, $A_n^t, ..., G_n^t$. These coefficients were determined analytically from the boundary conditions and continuity expression. Their approximate values were determined numerically by simultaneous solution of a linear set of equations. The values of the coefficients were used to determine the hydrodynamic force and torque in the problem. Their actual values thus were not a significant result, but they are included in this Appendix for a number of cases corresponding to different separation distances and slip coefficients. Table D.1 lists the translation cases whose values are included.

The coefficients for the rotation case are also included in this Appendix. Table D.2 lists the rotation cases whose values are included.

Table D.1: Coefficients for Translation Cases

Dimensionless Separation Distance		Slip Coefficient	Number of Terms
ϵ	α	β	N
10	3.089	∞	10
10	3.089	0.1	10
10	3.089	0	10
1	1.317	∞	60
1	1.317	0.1	60
1	1.317	0	30

Table D.2: Coefficients for Rotation Cases

Dimensionless Separation Distance		Slip Coefficient	Number of Terms
ϵ	α	β	N
1	1.317	∞	30
1	1.317	1	30
1	1.317	0	30
0.5	0.9624	∞	30
0.5	0.9624	1	30
0.5	0.9624	0	30

Translation Coefficients

α = 3.08896990484

ϵ = 10.0

$\beta = \infty$

n	A_n^t	B_n^t	C_n^t	D_n^t	E_n^t	F_n^t	G_n^t
0				-0.507e-01	0.255e+0		
1	-0.507e-01	0.152e+00	-0.502e-01	-0.490e-03	0.632e-03		
2	-0.163e-03	-0.499e-01	0.501e-01	0.507e-01	-0.506e-01	-0.254e-01	0.253e-01
3	-0.479e-06	-0.324e-03	0.324e-03	0.490e-03	-0.490e-03	-0.817e-04	0.816e-04
4	-0.128e-08	-0.142e-05	0.143e-05	0.287e-05	-0.287e-05	-0.239e-06	0.239e-06
5	-0.326e-11	-0.509e-08	0.509e-08	0.128e-07	-0.128e-07	-0.641e-09	0.640e-09
6	-0.799e-14	-0.162e-10	0.162e-10	0.488e-10	-0.488e-10	-0.163e-11	0.163e-11
7	-0.191e-16	-0.477e-13	0.477e-13	0.168e-12	-0.168e-12	-0.400e-14	0.399e-14
8	-0.450e-19	-0.133e-15	0.133e-15	0.536e-15	-0.536e-15	-0.957e-17	0.957e-17
9	-0.104e-21	-0.356e-18	0.356e-18	0.164e-17	-0.164e-17	-0.227e-19	0.227e-19
10	-0.234e-24	-0.383e-20	0.383e-20	0.220e-19	-0.220e-19	-0.213e-21	0.213e-21

FORCE = -1.0538015671

TORQUE = 0.0000061781

Translation Coefficients

$\alpha = 3.08896990484$

$\epsilon = 10.0$

$\beta = 0.1$

n	A_n^t	B_n^t	C_n^t	D_n^t	E_n^t	F_n^t	G_n^t
0				0.176e-01	0.181e+0		
1	-0.495e-01	0.105e+00	-0.576e-02	-0.400e-01	0.401e-01		
2	-0.165e-03	-0.992e-02	0.101e-01	0.238e-02	-0.225e-02	-0.818e-02	0.811e-02
3	-0.482e-06	-0.337e-02	0.338e-02	0.451e-02	-0.451e-02	-0.176e-02	0.176e-02
4	-0.129e-08	-0.144e-02	0.144e-02	0.421e-02	-0.421e-02	-0.587e-03	0.587e-03
5	-0.326e-11	-0.639e-03	0.639e-03	0.344e-02	-0.344e-02	-0.241e-03	0.241e-03
6	-0.800e-14	-0.387e-03	0.387e-03	0.277e-02	-0.277e-02	-0.112e-03	0.112e-03
7	-0.196e-16	-0.170e-03	0.170e-03	0.212e-02	-0.212e-02	-0.551e-04	0.551e-04
8	0.295e-18	-0.161e-03	0.161e-03	0.161e-02	-0.161e-02	-0.277e-04	0.277e-04
9	-0.828e-19	-0.558e-04	0.558e-04	0.105e-02	-0.105e-02	-0.131e-04	0.131e-04
10	0.149e-19	-0.104e-03	0.104e-03	0.518e-03	-0.518e-03	-0.449e-05	0.449e-05

FORCE = -1.0288820709

TORQUE = -0.0005042410

Translation Coefficients

$\alpha = 3.08896990484$

$\epsilon = 10.0$

$\beta = 0$

n	A_n^t	B_n^t	C_n^t	D_n^t	E_n^t	F_n^t	G_n^t
0				0.187e+00	0.0e+00		
1	-0.465e-01	0.930e-01	0.0e+00	0.148e-03	0.0e+00		
2	-0.161e-03	0.193e-03	0.0e+00	0.128e-03	0.0e+00	-0.644e-04	0.0e+00
3	-0.475e-06	0.416e-06	0.0e+00	0.799e-06	0.0e+00	-0.134e-06	0.0e+00
4	-0.128e-08	0.862e-09	0.0e+00	0.337e-08	0.0e+00	-0.282e-09	0.0e+00
5	-0.325e-11	0.179e-11	0.0e+00	0.117e-10	0.0e+00	-0.588e-12	0.0e+00
6	-0.798e-14	0.370e-14	0.0e+00	0.367e-13	0.0e+00	-0.122e-14	0.0e+00
7	-0.191e-16	0.768e-17	0.0e+00	0.107e-15	0.0e+00	-0.255e-17	0.0e+00
8	-0.450e-19	0.159e-19	0.0e+00	0.296e-18	0.0e+00	-0.529e-20	0.0e+00
9	-0.104e-21	0.331e-22	0.0e+00	0.790e-21	0.0e+00	-0.110e-22	0.0e+00
10	-0.233e-24	0.575e-25	0.0e+00	0.206e-23	0.0e+00	-0.228e-25	0.0e+00

FORCE = -0.9669920593

TORQUE = -0.0014983668

Translation Coefficients

$\alpha = 1.31695789692$

$\epsilon = 1.0$

$\beta = \infty$

n	A_n^t	B_n^t	C_n^t	D_n^t	E_n^t	F_n^t	G_n^t
0				-0.385e+0	0.200e+1		
1	-0.385e+0	0.107e+1	-0.298e+0	-0.835e-1	0.124e+0		
2	-0.278e-01	-0.257e+0	0.276e+0	0.368e+0	-0.333e+0	-0.191e+0	0.173e+0
3	-0.274e-02	-0.377e-01	0.400e-01	0.809e-01	-0.764e-01	-0.138e-01	0.130e-01
4	-0.259e-03	-0.604e-02	0.622e-02	0.161e-01	-0.155e-01	-0.136e-02	0.130e-02
5	-0.231e-04	-0.795e-03	0.808e-03	0.255e-02	-0.247e-02	-0.128e-03	0.124e-03
6	-0.198e-05	-0.910e-04	0.919e-04	0.341e-03	-0.333e-03	-0.114e-04	0.111e-04
7	-0.165e-06	-0.951e-05	0.957e-05	0.410e-04	-0.401e-04	-0.981e-06	0.959e-06
8	-0.135e-07	-0.935e-06	0.940e-06	0.456e-05	-0.448e-05	-0.818e-07	0.802e-07
9	-0.108e-08	-0.880e-07	0.884e-07	0.480e-06	-0.472e-06	-0.668e-08	0.657e-08
10	-0.861e-10	-0.802e-08	0.804e-08	0.483e-07	-0.476e-07	-0.538e-09	0.530e-09
11	-0.678e-11	-0.712e-09	0.714e-09	0.469e-08	-0.463e-08	-0.428e-10	0.422e-10
12	-0.530e-12	-0.619e-10	0.620e-10	0.444e-09	-0.438e-09	-0.337e-11	0.333e-11
13	-0.411e-13	-0.529e-11	0.530e-11	0.410e-10	-0.405e-10	-0.263e-12	0.260e-12
14	-0.317e-14	-0.446e-12	0.447e-12	0.371e-11	-0.367e-11	-0.204e-13	0.202e-13
15	-0.244e-15	-0.372e-13	0.372e-13	0.331e-12	-0.327e-12	-0.158e-14	0.156e-14
16	-0.186e-16	-0.307e-14	0.308e-14	0.290e-13	-0.288e-13	-0.121e-15	0.120e-15
17	-0.142e-17	-0.243e-15	0.244e-15	0.251e-14	-0.249e-14	-0.918e-17	0.910e-17
18	-0.108e-18	-0.270e-16	0.271e-16	0.213e-15	-0.212e-15	-0.682e-18	0.676e-18
19	-0.816e-20	0.468e-17	-0.468e-17	0.160e-16	-0.159e-16	0.404e-20	-0.446e-20
20	-0.616e-21	-0.606e-17	0.606e-17	-0.838e-18	0.849e-18	0.132e-19	-0.132e-19
21	-0.464e-22	0.557e-17	-0.557e-17	-0.236e-17	0.237e-17	0.426e-19	-0.426e-19
22	-0.349e-23	-0.525e-17	0.525e-17	-0.260e-17	0.260e-17	0.130e-19	-0.130e-19
23	-0.261e-24	0.495e-17	-0.495e-17	-0.272e-17	0.272e-17	0.329e-19	-0.329e-19
24	-0.196e-25	-0.467e-17	0.467e-17	-0.284e-17	0.284e-17	0.101e-19	-0.101e-19
25	-0.146e-26	0.440e-17	-0.440e-17	-0.296e-17	0.296e-17	0.257e-19	-0.257e-19
26	-0.109e-27	-0.416e-17	0.416e-17	-0.307e-17	0.307e-17	0.795e-20	-0.795e-20
27	-0.814e-29	0.393e-17	-0.393e-17	-0.319e-17	0.319e-17	0.205e-19	-0.205e-19
28	-0.607e-30	-0.371e-17	0.371e-17	-0.330e-17	0.330e-17	0.639e-20	-0.639e-20
29	-0.530e-31	0.350e-17	-0.350e-17	-0.342e-17	0.342e-17	0.166e-19	-0.166e-19
30	-0.387e-32	-0.331e-17	0.331e-17	-0.354e-17	0.354e-17	0.521e-20	-0.521e-20

n	A_n^t	B_n^t	C_n^t	D_n^t	E_n^t	F_n^t	G_n^t
31	0.139e-32	0.313e-17	-0.313e-17	-0.365e-17	0.365e-17	0.136e-19	-0.136e-19
32	-0.727e-32	-0.295e-17	0.295e-17	-0.377e-17	0.377e-17	0.431e-20	-0.431e-20
33	0.306e-32	0.278e-17	-0.278e-17	-0.388e-17	0.388e-17	0.113e-19	-0.113e-19
34	-0.284e-32	-0.262e-17	0.262e-17	-0.400e-17	0.400e-17	0.360e-20	-0.360e-20
35	0.129e-32	0.247e-17	-0.247e-17	-0.412e-17	0.412e-17	0.951e-20	-0.951e-20
36	-0.613e-32	-0.232e-17	0.232e-17	-0.423e-17	0.423e-17	0.304e-20	-0.304e-20
37	0.128e-32	0.218e-17	-0.218e-17	-0.435e-17	0.435e-17	0.806e-20	-0.806e-20
38	-0.248e-32	-0.204e-17	0.204e-17	-0.446e-17	0.446e-17	0.259e-20	-0.259e-20
39	-0.493e-33	0.191e-17	-0.191e-17	-0.458e-17	0.458e-17	0.690e-20	-0.690e-20
40	-0.997e-33	-0.179e-17	0.179e-17	-0.470e-17	0.470e-17	0.222e-20	-0.222e-20
41	-0.177e-32	0.166e-17	-0.166e-17	-0.481e-17	0.481e-17	0.595e-20	-0.595e-20
42	-0.731e-34	-0.154e-17	0.154e-17	-0.493e-17	0.493e-17	0.192e-20	-0.192e-20
43	-0.121e-32	0.143e-17	-0.143e-17	-0.504e-17	0.504e-17	0.516e-20	-0.516e-20
44	-0.314e-32	-0.132e-17	0.132e-17	-0.516e-17	0.516e-17	0.168e-20	-0.168e-20
45	-0.167e-32	0.121e-17	-0.121e-17	-0.528e-17	0.528e-17	0.451e-20	-0.451e-20
46	-0.207e-32	-0.110e-17	0.110e-17	-0.539e-17	0.539e-17	0.147e-20	-0.147e-20
47	0.134e-33	0.999e-18	-0.999e-18	-0.551e-17	0.551e-17	0.396e-20	-0.396e-20
48	0.301e-33	-0.898e-18	0.898e-18	-0.562e-17	0.562e-17	0.129e-20	-0.129e-20
49	-0.254e-32	0.800e-18	-0.800e-18	-0.574e-17	0.574e-17	0.350e-20	-0.350e-20
50	-0.124e-32	-0.704e-18	0.704e-18	-0.586e-17	0.586e-17	0.115e-20	-0.115e-20
51	-0.271e-33	0.611e-18	-0.611e-18	-0.597e-17	0.597e-17	0.311e-20	-0.311e-20
52	-0.118e-32	-0.519e-18	0.519e-18	-0.609e-17	0.609e-17	0.102e-20	-0.102e-20
53	-0.232e-32	0.429e-18	-0.429e-18	-0.620e-17	0.620e-17	0.277e-20	-0.277e-20
54	-0.170e-32	-0.342e-18	0.342e-18	-0.632e-17	0.632e-17	0.912e-21	-0.912e-21
55	-0.114e-32	0.255e-18	-0.255e-18	-0.644e-17	0.644e-17	0.248e-20	-0.248e-20
56	-0.642e-33	-0.171e-18	0.171e-18	-0.655e-17	0.655e-17	0.818e-21	-0.818e-21
57	-0.394e-33	0.880e-19	-0.880e-19	-0.667e-17	0.667e-17	0.223e-20	-0.223e-20
58	-0.114e-32	-0.648e-20	0.648e-20	-0.678e-17	0.678e-17	0.737e-21	-0.737e-21
59	-0.263e-33	-0.737e-19	0.737e-19	-0.690e-17	0.690e-17	0.202e-20	-0.202e-20
60	0.219e-34	0.152e-18	-0.152e-18	-0.702e-17	0.702e-17	0.667e-21	-0.667e-21

FORCE = -1.3827523824

TORQUE = 0.0050247112

Translation Coefficients

$\alpha = 1.3169589692$

$\epsilon = 1.0$

$\beta = 0.1$

n	A_n^t	B_n^t	C_n^t	D_n^t	E_n^t	F_n^t	G_n^t
0				0.578e+0	0.573e+0		
1	-0.258e+0	0.503e+0	-0.609e-03	-0.237e+0	0.284e+0		
2	-0.278e-01	0.208e-01	0.102e-01	-0.127e+0	0.150e+0	-0.228e-01	0.107e-01
3	-0.289e-02	-0.376e-02	0.635e-02	-0.865e-01	0.910e-01	-0.492e-02	0.413e-02
4	-0.272e-03	-0.347e-02	0.366e-02	-0.588e-01	0.595e-01	-0.204e-02	0.198e-02
5	-0.240e-04	-0.223e-02	0.224e-02	-0.404e-01	0.404e-01	-0.110e-02	0.110e-02
6	-0.204e-05	-0.145e-02	0.145e-02	-0.281e-01	0.281e-01	-0.676e-03	0.676e-03
7	-0.169e-06	-0.100e-02	0.100e-02	-0.197e-01	0.197e-01	-0.444e-03	0.444e-03
8	-0.137e-07	-0.706e-03	0.706e-03	-0.138e-01	0.138e-01	-0.306e-03	0.306e-03
9	-0.110e-08	-0.528e-03	0.528e-03	-0.960e-02	0.960e-02	-0.219e-03	0.219e-03
10	-0.873e-10	-0.390e-03	0.390e-03	-0.656e-02	0.656e-02	-0.161e-03	0.161e-03
11	-0.686e-11	-0.308e-03	0.308e-03	-0.432e-02	0.432e-02	-0.121e-03	0.121e-03
12	-0.535e-12	-0.233e-03	0.233e-03	-0.266e-02	0.266e-02	-0.931e-04	0.931e-04
13	-0.414e-13	-0.194e-03	0.194e-03	-0.141e-02	0.141e-02	-0.727e-04	0.727e-04
14	-0.319e-14	-0.148e-03	0.148e-03	-0.488e-03	0.488e-03	-0.576e-04	0.576e-04
15	-0.245e-15	-0.129e-03	0.129e-03	0.214e-03	-0.214e-03	-0.461e-04	0.461e-04
16	-0.182e-16	-0.974e-04	0.974e-04	0.732e-03	-0.732e-03	-0.374e-04	0.374e-04
17	-0.754e-18	-0.893e-04	0.893e-04	0.112e-02	-0.112e-02	-0.306e-04	0.306e-04
18	0.378e-18	-0.662e-04	0.662e-04	0.141e-02	-0.141e-02	-0.252e-04	0.252e-04
19	-0.287e-18	-0.643e-04	0.643e-04	0.162e-02	-0.162e-02	-0.210e-04	0.210e-04
20	0.570e-18	-0.460e-04	0.460e-04	0.176e-02	-0.176e-02	-0.175e-04	0.175e-04
21	-0.813e-19	-0.478e-04	0.478e-04	0.186e-02	-0.186e-02	-0.148e-04	0.148e-04
22	0.147e-16	-0.324e-04	0.324e-04	0.192e-02	-0.192e-02	-0.125e-04	0.125e-04
23	-0.249e-16	-0.366e-04	0.366e-04	0.196e-02	-0.196e-02	-0.107e-04	0.107e-04
24	0.145e-18	-0.231e-04	0.231e-04	0.196e-02	-0.196e-02	-0.911e-05	0.911e-05
25	0.129e-16	-0.287e-04	0.287e-04	0.196e-02	-0.196e-02	-0.783e-05	0.783e-05
26	-0.153e-16	-0.164e-04	0.164e-04	0.194e-02	-0.194e-02	-0.675e-05	0.675e-05
27	0.876e-17	-0.231e-04	0.231e-04	0.191e-02	-0.191e-02	-0.584e-05	0.584e-05
28	-0.839e-18	-0.116e-04	0.116e-04	0.187e-02	-0.187e-02	-0.507e-05	0.507e-05
29	-0.142e-16	-0.190e-04	0.190e-04	0.183e-02	-0.183e-02	-0.442e-05	0.442e-05
30	0.285e-17	-0.813e-05	0.813e-05	0.178e-02	-0.178e-02	-0.386e-05	0.386e-05

n	A_n^t	B_n^t	C_n^t	D_n^t	E_n^t	F_n^t	G_n^t
31	0.159e-16	-0.160e-04	0.160e-04	0.173e-02	-0.173e-02	-0.338e-05	0.338e-05
32	-0.171e-16	-0.550e-05	0.550e-05	0.167e-02	-0.167e-02	-0.297e-05	0.297e-05
33	0.232e-16	-0.137e-04	0.137e-04	0.162e-02	-0.162e-02	-0.261e-05	0.261e-05
34	-0.902e-17	-0.352e-05	0.352e-05	0.156e-02	-0.156e-02	-0.230e-05	0.230e-05
35	-0.458e-17	-0.120e-04	0.120e-04	0.150e-02	-0.150e-02	-0.203e-05	0.203e-05
36	0.850e-17	-0.200e-05	0.200e-05	0.144e-02	-0.144e-02	-0.179e-05	0.179e-05
37	-0.132e-18	-0.106e-04	0.106e-04	0.138e-02	-0.138e-02	-0.158e-05	0.158e-05
38	-0.972e-17	-0.834e-06	0.834e-06	0.132e-02	-0.132e-02	-0.140e-05	0.140e-05
39	0.101e-16	-0.959e-05	0.959e-05	0.126e-02	-0.126e-02	-0.124e-05	0.124e-05
40	-0.277e-17	0.751e-07	-0.751e-07	0.120e-02	-0.120e-02	-0.110e-05	0.110e-05
41	-0.462e-17	-0.879e-05	0.879e-05	0.115e-02	-0.115e-02	-0.974e-06	0.974e-06
42	-0.112e-16	0.786e-06	-0.786e-06	0.108e-02	-0.108e-02	-0.861e-06	0.861e-06
43	0.134e-16	-0.816e-05	0.816e-05	0.103e-02	-0.103e-02	-0.761e-06	0.761e-06
44	-0.388e-17	0.135e-05	-0.135e-05	0.962e-03	-0.962e-03	-0.672e-06	0.672e-06
45	0.779e-17	-0.766e-05	0.766e-05	0.907e-03	-0.907e-03	-0.592e-06	0.592e-06
46	-0.429e-17	0.179e-05	-0.179e-05	0.842e-03	-0.842e-03	-0.519e-06	0.519e-06
47	-0.908e-17	-0.727e-05	0.727e-05	0.785e-03	-0.785e-03	-0.454e-06	0.454e-06
48	0.313e-17	0.213e-05	-0.213e-05	0.719e-03	-0.719e-03	-0.395e-06	0.395e-06
49	0.608e-17	-0.696e-05	0.696e-05	0.662e-03	-0.662e-03	-0.342e-06	0.342e-06
50	-0.560e-18	0.241e-05	-0.241e-05	0.594e-03	-0.594e-03	-0.293e-06	0.293e-06
51	-0.176e-17	-0.672e-05	0.672e-05	0.535e-03	-0.535e-03	-0.248e-06	0.248e-06
52	0.363e-18	0.262e-05	-0.262e-05	0.465e-03	-0.465e-03	-0.208e-06	0.208e-06
53	0.388e-17	-0.653e-05	0.653e-05	0.404e-03	-0.404e-03	-0.170e-06	0.170e-06
54	-0.424e-17	0.279e-05	-0.279e-05	0.331e-03	-0.331e-03	-0.135e-06	0.135e-06
55	-0.377e-18	-0.639e-05	0.639e-05	0.267e-03	-0.267e-03	-0.103e-06	0.103e-06
56	0.137e-18	0.291e-05	-0.291e-05	0.191e-03	-0.191e-03	-0.737e-07	0.737e-07
57	0.108e-17	-0.628e-05	0.628e-05	0.123e-03	-0.123e-03	-0.460e-07	0.460e-07
58	-0.153e-18	0.301e-05	-0.301e-05	0.432e-04	-0.432e-04	-0.201e-07	0.201e-07
59	-0.195e-19	-0.620e-05	0.620e-05	-0.292e-04	0.292e-04	0.417e-08	-0.417e-8
60	0.464e-21	0.308e-05	-0.308e-05	-0.113e-03	0.113e-03	0.271e-07	-0.271e-7

FORCE = -1.0014903445

TORQUE = -0.0334515322

Translation Coefficients

$\alpha = 1.3169589692$

$\epsilon = 1.0$

$\beta = 0$

n	A_n^t	B_n^t	C_n^t	D_n^t	E_n^t	F_n^t	G_n^t
0				0.959e+0	0.0e+00		
1	-0.213e+0	0.410e+0	0.0e+00	0.442e-01	0.0e+00		
2	-0.247e-01	0.289e-01	0.0e+00	0.195e-01	0.0e+00	-0.993e-02	0.0e+00
3	-0.266e-02	0.247e-02	0.0e+00	0.392e-02	0.0e+00	-0.702e-03	0.0e+00
4	-0.255e-03	0.183e-03	0.0e+00	0.611e-03	0.0e+00	-0.543e-04	0.0e+00
5	-0.229e-04	0.132e-04	0.0e+00	0.770e-04	0.0e+00	-0.406e-05	0.0e+00
6	-0.197e-05	0.943e-06	0.0e+00	0.854e-05	0.0e+00	-0.298e-06	0.0e+00
7	-0.164e-06	0.676e-07	0.0e+00	0.875e-06	0.0e+00	-0.217e-07	0.0e+00
8	-0.134e-07	0.484e-08	0.0e+00	0.848e-07	0.0e+00	-0.157e-08	0.0e+00
9	-0.108e-08	0.347e-09	0.0e+00	0.790e-08	0.0e+00	-0.113e-09	0.0e+00
10	-0.859e-10	0.249e-10	0.0e+00	0.713e-09	0.0e+00	-0.816e-11	0.0e+00
11	-0.677e-11	0.179e-11	0.0e+00	0.629e-10	0.0e+00	-0.587e-12	0.0e+00
12	-0.529e-12	0.128e-12	0.0e+00	0.544e-11	0.0e+00	-0.423e-13	0.0e+00
13	-0.411e-13	0.921e-14	0.0e+00	0.463e-12	0.0e+00	-0.304e-14	0.0e+00
14	-0.317e-14	0.661e-15	0.0e+00	0.389e-13	0.0e+00	-0.218e-15	0.0e+00
15	-0.243e-15	0.474e-16	0.0e+00	0.323e-14	0.0e+00	-0.157e-16	0.0e+00
16	-0.186e-16	0.341e-17	0.0e+00	0.266e-15	0.0e+00	-0.113e-17	0.0e+00
17	-0.142e-17	0.244e-18	0.0e+00	0.216e-16	0.0e+00	-0.810e-19	0.0e+00
18	-0.108e-18	0.175e-19	0.0e+00	0.175e-17	0.0e+00	-0.582e-20	0.0e+00
19	-0.815e-20	0.126e-20	0.0e+00	0.141e-18	0.0e+00	-0.418e-21	0.0e+00
20	-0.616e-21	0.904e-22	0.0e+00	0.112e-19	0.0e+00	-0.300e-22	0.0e+00
21	-0.464e-22	0.649e-23	0.0e+00	0.893e-21	0.0e+00	-0.216e-23	0.0e+00
22	-0.348e-23	0.466e-24	0.0e+00	0.706e-22	0.0e+00	-0.155e-24	0.0e+00
23	-0.261e-24	0.335e-25	0.0e+00	0.555e-23	0.0e+00	-0.111e-25	0.0e+00
24	-0.196e-25	0.240e-26	0.0e+00	0.435e-24	0.0e+00	-0.798e-27	0.0e+00
25	-0.146e-26	0.172e-27	0.0e+00	0.340e-25	0.0e+00	-0.573e-28	0.0e+00
26	-0.109e-27	0.124e-28	0.0e+00	0.265e-26	0.0e+00	-0.412e-29	0.0e+00
27	-0.813e-29	0.889e-30	0.0e+00	0.205e-27	0.0e+00	-0.296e-30	0.0e+00
28	-0.605e-30	0.638e-31	0.0e+00	0.159e-28	0.0e+00	-0.212e-31	0.0e+00
29	-0.450e-31	0.458e-32	0.0e+00	0.122e-29	0.0e+00	-0.152e-32	0.0e+00
30	-0.334e-32	0.330e-33	0.0e+00	0.943e-31	0.0e+00	-0.109e-33	0.0e+00

FORCE = -0.838826157

TORQUE = -0.0389104282

Rotation Coefficients

$\alpha = 1.31695789692$

$\epsilon = 1.0$

$\beta = \infty$

n	A_n^r	B_n^r	C_n^r	D_n^r	E_n^r	F_n^r	G_n^r
0				-0.12e+0	-0.130e+0		
1	-0.120e+0	0.343e+0	-0.330e+0	-0.174e-1	0.228e+0		
2	-0.580e-02	-0.927e-01	0.877e-01	0.117e+0	-0.863e-01	-0.598e-01	0.595e-01
3	-0.432e-03	-0.875e-02	0.872e-02	0.171e-01	-0.141e-01	-0.288e-02	0.295e-02
4	-0.328e-04	-0.102e-02	0.102e-02	0.255e-02	-0.227e-02	-0.215e-03	0.217e-03
5	-0.245e-05	-0.106e-03	0.106e-03	0.324e-03	-0.298e-03	-0.163e-04	0.164e-04
6	-0.181e-06	-0.100e-04	0.100e-04	0.364e-04	-0.341e-04	-0.122e-05	0.123e-05
7	-0.132e-07	-0.895e-06	0.896e-06	0.376e-05	-0.357e-05	-0.900e-07	0.903e-07
8	-0.965e-09	-0.770e-07	0.770e-07	0.368e-06	-0.352e-06	-0.659e-08	0.660e-08
9	-0.701e-10	-0.645e-08	0.645e-08	0.345e-07	-0.332e-07	-0.480e-09	0.481e-09
10	-0.508e-11	-0.529e-09	0.529e-09	0.313e-08	-0.303e-08	-0.349e-10	0.349e-10
11	-0.367e-12	-0.427e-10	0.427e-10	0.277e-09	-0.269e-09	-0.253e-11	0.253e-11
12	-0.265e-13	-0.340e-11	0.340e-11	0.241e-10	-0.234e-10	-0.183e-12	0.183e-12
13	-0.192e-14	-0.269e-12	0.269e-12	0.206e-11	-0.200e-11	-0.132e-13	0.132e-13
14	-0.138e-15	-0.211e-13	0.211e-13	0.173e-12	-0.169e-12	-0.953e-15	0.954e-15
15	-0.996e-17	-0.164e-14	0.164e-14	0.144e-13	-0.141e-13	-0.687e-16	0.687e-16
16	-0.718e-18	-0.128e-15	0.128e-15	0.118e-14	-0.116e-14	-0.494e-17	0.494e-17
17	-0.517e-19	-0.833e-17	0.833e-17	0.944e-16	-0.927e-16	-0.332e-18	0.332e-18
18	-0.372e-20	-0.199e-17	0.199e-17	0.521e-17	-0.507e-17	-0.172e-19	0.172e-19
19	-0.268e-21	0.103e-17	-0.103e-17	-0.216e-17	0.217e-17	0.162e-19	-0.162e-19
20	-0.193e-22	-0.939e-18	0.939e-18	-0.288e-17	0.288e-17	0.613e-20	-0.613e-20
21	-0.139e-23	0.795e-18	-0.795e-18	-0.307e-17	0.307e-17	0.135e-19	-0.135e-19
22	-0.997e-25	-0.664e-18	0.664e-18	-0.322e-17	0.322e-17	0.473e-20	-0.473e-20
23	-0.717e-26	0.540e-18	-0.540e-18	-0.336e-17	0.336e-17	0.103e-19	-0.103e-19
24	-0.515e-27	-0.422e-18	0.422e-18	-0.351e-17	0.351e-17	0.366e-20	-0.366e-20
25	-0.371e-28	0.309e-18	-0.309e-18	-0.365e-17	0.365e-17	0.806e-20	-0.806e-20
26	-0.266e-29	-0.201e-18	0.201e-18	-0.379e-17	0.379e-17	0.289e-20	-0.289e-20
27	-0.192e-30	0.977e-19	-0.977e-19	-0.394e-17	0.394e-17	0.642e-20	-0.642e-20
28	-0.136e-31	0.196e-20	-0.196e-20	-0.408e-17	0.408e-17	0.232e-20	-0.232e-20
29	-0.847e-33	-0.982e-19	0.982e-19	-0.422e-17	0.422e-17	0.520e-20	-0.520e-20
30	-0.194e-34	0.191e-18	-0.191e-18	-0.436e-17	0.436e-17	0.190e-20	-0.190e-20

FORCE = 0.0066996150

TORQUE = 1.0417835548

Rotation Coefficients

$\alpha = 1.31695789692$

$\epsilon = 1.0$

$\beta = 1$

n	A_n^r	B_n^r	C_n^r	D_n^r	E_n^r	F_n^r	G_n^r
0				-0.143e+0	-0.862e-1		
1	-0.118e+0	0.128e+0	-0.112e+0	0.921e-01	0.113e+0		
2	-0.648e-02	-0.116e-01	0.798e-02	0.244e-01	0.674e-02	-0.197e-01	0.193e-01
3	-0.472e-03	-0.498e-02	0.495e-02	0.880e-02	-0.575e-02	-0.376e-02	0.380e-02
4	-0.348e-04	-0.207e-02	0.207e-02	0.569e-02	-0.539e-02	-0.104e-02	0.104e-02
5	-0.254e-05	-0.895e-03	0.895e-03	0.387e-02	-0.385e-02	-0.355e-03	0.355e-03
6	-0.185e-06	-0.419e-03	0.419e-03	0.263e-02	-0.262e-02	-0.142e-03	0.142e-03
7	-0.135e-07	-0.211e-03	0.211e-03	0.178e-02	-0.178e-02	-0.635e-04	0.635e-04
8	-0.975e-09	-0.112e-03	0.112e-03	0.122e-02	-0.122e-02	-0.308e-04	0.308e-04
9	-0.706e-10	-0.623e-04	0.623e-04	0.840e-03	-0.840e-03	-0.159e-04	0.159e-04
10	-0.510e-11	-0.361e-04	0.361e-04	0.586e-03	-0.586e-03	-0.861e-05	0.861e-05
11	-0.369e-12	-0.215e-04	0.215e-04	0.413e-03	-0.413e-03	-0.486e-05	0.486e-05
12	-0.266e-13	-0.132e-04	0.132e-04	0.295e-03	-0.295e-03	-0.284e-05	0.284e-05
13	-0.192e-14	-0.824e-05	0.824e-05	0.212e-03	-0.212e-03	-0.171e-05	0.171e-05
14	-0.138e-15	-0.532e-05	0.532e-05	0.154e-03	-0.154e-03	-0.105e-05	0.105e-05
15	-0.100e-16	-0.343e-05	0.343e-05	0.113e-03	-0.113e-03	-0.663e-06	0.663e-06
16	-0.686e-18	-0.232e-05	0.232e-05	0.838e-04	-0.838e-04	-0.426e-06	0.426e-06
17	-0.513e-19	-0.152e-05	0.152e-05	0.626e-04	-0.626e-04	-0.278e-06	0.278e-06
18	0.320e-19	-0.108e-05	0.108e-05	0.471e-04	-0.471e-04	-0.184e-06	0.184e-06
19	-0.518e-19	-0.702e-06	0.702e-06	0.357e-04	-0.357e-04	-0.124e-06	0.124e-06
20	0.335e-19	-0.535e-06	0.535e-06	0.273e-04	-0.273e-04	-0.841e-07	0.841e-07
21	-0.108e-19	-0.334e-06	0.334e-06	0.210e-04	-0.210e-04	-0.578e-07	0.578e-07
22	-0.262e-20	-0.283e-06	0.283e-06	0.163e-04	-0.163e-04	-0.400e-07	0.400e-07
23	0.150e-20	-0.161e-06	0.161e-06	0.126e-04	-0.126e-04	-0.279e-07	0.279e-07
24	-0.851e-21	-0.163e-06	0.163e-06	0.988e-05	-0.988e-05	-0.196e-07	0.196e-07
25	-0.201e-20	-0.765e-07	0.765e-07	0.766e-05	-0.766e-05	-0.137e-07	0.137e-07
26	0.483e-20	-0.104e-06	0.104e-06	0.593e-05	-0.593e-05	-0.948e-08	0.948e-08
27	0.221e-20	-0.353e-07	0.353e-07	0.445e-05	-0.445e-05	-0.643e-08	0.643e-08
28	-0.204e-20	-0.756e-07	0.756e-07	0.322e-05	-0.322e-05	-0.416e-08	0.416e-08
29	-0.682e-21	-0.163e-07	0.163e-07	0.206e-05	-0.206e-05	-0.242e-08	0.242e-08
30	-0.511e-22	-0.638e-07	0.638e-07	0.985e-06	-0.985e-06	-0.102e-08	0.102e-08

FORCE = -0.0134498298

TORQUE = 1.0164691259

Rotation Coefficients

$\alpha = 1.31695789692$

$\epsilon = 1.0$

$\beta = 0$

n	A_n^r	B_n^r	C_n^r	D_n^r	E_n^r	F_n^r	G_n^r
0				-0.199e+00	0.0e+00		
1	-0.123e+00	0.304e-01	0.0e+00	0.200e+00	0.0e+00		
2	-0.654e-02	-0.399e-02	0.0e+00	0.315e-01	0.0e+00	-0.641e-03	0.0e+00
3	-0.483e-03	-0.122e-04	0.0e+00	0.306e-02	0.0e+00	0.385e-04	0.0e+00
4	-0.358e-04	0.714e-06	0.0e+00	0.297e-03	0.0e+00	0.168e-05	0.0e+00
5	-0.263e-05	0.457e-07	0.0e+00	0.270e-04	0.0e+00	0.741e-07	0.0e+00
6	-0.192e-06	0.243e-08	0.0e+00	0.236e-05	0.0e+00	0.354e-08	0.0e+00
7	-0.139e-07	0.132e-09	0.0e+00	0.199e-06	0.0e+00	0.181e-09	0.0e+00
8	-0.101e-08	0.735e-11	0.0e+00	0.164e-07	0.0e+00	0.973e-11	0.0e+00
9	-0.728e-10	0.422e-12	0.0e+00	0.133e-08	0.0e+00	0.542e-12	0.0e+00
10	-0.526e-11	0.248e-13	0.0e+00	0.107e-09	0.0e+00	0.311e-13	0.0e+00
11	-0.379e-12	0.148e-14	0.0e+00	0.846e-11	0.0e+00	0.182e-14	0.0e+00
12	-0.273e-13	0.901e-16	0.0e+00	0.664e-12	0.0e+00	0.109e-15	0.0e+00
13	-0.197e-14	0.555e-17	0.0e+00	0.518e-13	0.0e+00	0.660e-17	0.0e+00
14	-0.142e-15	0.345e-18	0.0e+00	0.401e-14	0.0e+00	0.406e-18	0.0e+00
15	-0.102e-16	0.217e-19	0.0e+00	0.309e-15	0.0e+00	0.252e-19	0.0e+00
16	-0.733e-18	0.137e-20	0.0e+00	0.237e-16	0.0e+00	0.158e-20	0.0e+00
17	-0.527e-19	0.877e-22	0.0e+00	0.181e-17	0.0e+00	0.100e-21	0.0e+00
18	-0.379e-20	0.563e-23	0.0e+00	0.138e-18	0.0e+00	0.639e-23	0.0e+00
19	-0.273e-21	0.364e-24	0.0e+00	0.104e-19	0.0e+00	0.410e-24	0.0e+00
20	-0.196e-22	0.236e-25	0.0e+00	0.790e-21	0.0e+00	0.265e-25	0.0e+00
21	-0.141e-23	0.154e-26	0.0e+00	0.596e-22	0.0e+00	0.172e-26	0.0e+00
22	-0.101e-24	0.101e-27	0.0e+00	0.449e-23	0.0e+00	0.112e-27	0.0e+00
23	-0.727e-26	0.666e-29	0.0e+00	0.337e-24	0.0e+00	0.735e-29	0.0e+00
24	-0.523e-27	0.440e-30	0.0e+00	0.253e-25	0.0e+00	0.484e-30	0.0e+00
25	-0.376e-28	0.291e-31	0.0e+00	0.189e-26	0.0e+00	0.319e-31	0.0e+00
26	-0.270e-29	0.194e-32	0.0e+00	0.141e-27	0.0e+00	0.211e-32	0.0e+00
27	-0.194e-30	0.131e-33	0.0e+00	0.105e-28	0.0e+00	0.139e-33	0.0e+00
28	-0.139e-31	0.104e-34	0.0e+00	0.786e-30	0.0e+00	0.766e-35	0.0e+00
29	-0.950e-33	0.149e-35	0.0e+00	0.599e-31	0.0e+00	-0.102e-35	0.0e+00
30	-0.215e-34	-0.974e-34	0.0e+00	0.440e-32	0.0e+00	0.000e+0	0.0e+00

FORCE = -0.0518805710

TORQUE = 0.9957677096

Rotation Coefficients

$\alpha = 0.962423650119$

$\epsilon = 0.5$

$\beta = \infty$

n	A_n^r	B_n^r	C_n^r	D_n^r	E_n^r	F_n^r	G_n^r
0				-0.413e+00	-0.460e+00		
1	-0.413e+00	0.114e+01	-0.102e+1	-0.990e-01	0.704e+000		
2	-0.330e-01	-0.267e+00	0.224e+00	0.385e+00	-0.196e+00	-0.204e+00	0.198e+00
3	-0.465e-02	-0.370e-01	0.359e-01	0.919e-01	-0.581e-01	-0.161e-01	0.170e-01
4	-0.716e-03	-0.818e-02	0.816e-02	0.263e-01	-0.198e-01	-0.227e-02	0.237e-02
5	-0.110e-03	-0.177e-02	0.177e-02	0.680e-02	-0.559e-02	-0.349e-03	0.359e-03
6	-0.168e-04	-0.353e-03	0.354e-03	0.158e-02	-0.137e-02	-0.539e-04	0.548e-04
7	-0.253e-05	-0.662e-04	0.663e-04	0.339e-03	-0.301e-03	-0.820e-05	0.830e-05
8	-0.378e-06	-0.118e-04	0.118e-04	0.682e-04	-0.619e-04	-0.124e-05	0.125e-05
9	-0.561e-07	-0.205e-05	0.205e-05	0.131e-04	-0.121e-04	-0.185e-06	0.186e-06
10	-0.831e-08	-0.345e-06	0.345e-06	0.244e-05	-0.227e-05	-0.274e-07	0.276e-07
11	-0.123e-08	-0.572e-07	0.572e-07	0.443e-06	-0.415e-06	-0.406e-08	0.408e-08
12	-0.181e-09	-0.934e-08	0.935e-08	0.785e-07	-0.740e-07	-0.600e-09	0.602e-09
13	-0.266e-10	-0.151e-08	0.151e-08	0.137e-07	-0.130e-07	-0.884e-10	0.886e-10
14	-0.391e-11	-0.241e-09	0.241e-09	0.235e-08	-0.224e-08	-0.130e-10	0.130e-10
15	-0.573e-12	-0.383e-10	0.383e-10	0.399e-09	-0.381e-09	-0.191e-11	0.191e-11
16	-0.841e-13	-0.605e-11	0.605e-11	0.669e-10	-0.642e-10	-0.281e-12	0.281e-12
17	-0.123e-13	-0.948e-12	0.949e-12	0.111e-10	-0.107e-10	-0.411e-13	0.412e-13
18	-0.181e-14	-0.148e-12	0.148e-12	0.184e-11	-0.177e-11	-0.603e-14	0.604e-14
19	-0.265e-15	-0.230e-13	0.230e-13	0.301e-12	-0.290e-12	-0.884e-15	0.885e-15
20	-0.387e-16	-0.356e-14	0.356e-14	0.489e-13	-0.474e-13	-0.129e-15	0.130e-15
21	-0.567e-17	-0.552e-15	0.552e-15	0.792e-14	-0.768e-14	-0.189e-16	0.190e-16
22	-0.829e-18	-0.831e-16	0.831e-16	0.127e-14	-0.123e-14	-0.275e-17	0.275e-17
23	-0.121e-18	-0.144e-16	0.144e-16	0.200e-15	-0.195e-15	-0.393e-18	0.394e-18
24	-0.177e-19	-0.762e-18	0.762e-18	0.285e-16	-0.276e-16	-0.404e-19	0.404e-19
25	-0.259e-20	-0.138e-17	0.138e-17	0.856e-18	-0.723e-18	0.887e-21	-0.881e-21
26	-0.379e-21	0.895e-18	-0.895e-18	-0.368e-17	0.370e-17	0.137e-19	-0.137e-19
27	-0.553e-22	-0.817e-18	0.817e-18	-0.454e-17	0.454e-17	0.744e-20	-0.744e-20
28	-0.795e-23	0.683e-18	-0.683e-18	-0.482e-17	0.482e-17	0.120e-19	-0.120e-19
29	-0.104e-23	-0.563e-18	0.563e-18	-0.501e-17	0.501e-17	0.617e-20	-0.617e-20
30	-0.288e-25	0.446e-18	-0.446e-18	-0.518e-17	0.518e-17	0.981e-20	-0.981e-20

FORCE = 0.0220986159

TORQUE = 1.1104954933

Rotation Coefficients

$\alpha = 0.962423650119$

$\epsilon = 0.5$

$\beta = 1.0$

n	A_n^r	B_n^r	C_n^r	D_n^r	E_n^r	F_n^r	G_n^r
0				-0.494e+0	-0.222e+0		
1	-0.389e+0	0.381e+0	-0.251e+0	0.283e+0	0.264e+0		
2	-0.374e-01	-0.314e-01	-0.342e-03	0.120e+0	0.647e-01	-0.534e-01	0.478e-01
3	-0.536e-02	-0.953e-02	0.879e-02	0.281e-01	0.711e-02	-0.114e-01	0.119e-01
4	-0.802e-03	-0.535e-02	0.533e-02	0.140e-01	-0.711e-02	-0.378e-02	0.384e-02
5	-0.120e-03	-0.281e-02	0.281e-02	0.103e-01	-0.903e-02	-0.147e-02	0.147e-02
6	-0.178e-04	-0.150e-02	0.150e-02	0.820e-02	-0.797e-02	-0.645e-03	0.645e-03
7	-0.264e-05	-0.833e-03	0.833e-03	0.648e-02	-0.644e-02	-0.313e-03	0.313e-03
8	-0.389e-06	-0.484e-03	0.484e-03	0.505e-02	-0.505e-02	-0.164e-03	0.164e-03
9	-0.574e-07	-0.292e-03	0.292e-03	0.392e-02	-0.392e-02	-0.913e-04	0.913e-04
10	-0.844e-08	-0.183e-03	0.183e-03	0.304e-02	-0.304e-02	-0.533e-04	0.533e-04
11	-0.124e-08	-0.117e-03	0.117e-03	0.236e-02	-0.236e-02	-0.323e-04	0.323e-04
12	-0.182e-09	-0.777e-04	0.777e-04	0.184e-02	-0.184e-02	-0.202e-04	0.202e-04
13	-0.268e-10	-0.518e-04	0.518e-04	0.144e-02	-0.144e-02	-0.130e-04	0.130e-04
14	-0.392e-11	-0.360e-04	0.360e-04	0.113e-02	-0.113e-02	-0.856e-05	0.856e-05
15	-0.575e-12	-0.245e-04	0.245e-04	0.899e-03	-0.899e-03	-0.575e-05	0.575e-05
16	-0.843e-13	-0.179e-04	0.179e-04	0.716e-03	-0.716e-03	-0.393e-05	0.393e-05
17	-0.123e-13	-0.123e-04	0.123e-04	0.574e-03	-0.574e-03	-0.272e-05	0.272e-05
18	-0.181e-14	-0.943e-05	0.943e-05	0.463e-03	-0.463e-03	-0.191e-05	0.191e-05
19	-0.265e-15	-0.637e-05	0.637e-05	0.375e-03	-0.375e-03	-0.136e-05	0.136e-05
20	-0.388e-16	-0.527e-05	0.527e-05	0.305e-03	-0.305e-03	-0.976e-06	0.976e-06
21	-0.555e-17	-0.340e-05	0.340e-05	0.249e-03	-0.249e-03	-0.707e-06	0.707e-06
22	-0.898e-18	-0.314e-05	0.314e-05	0.205e-03	-0.205e-03	-0.514e-06	0.514e-06
23	-0.201e-18	-0.186e-05	0.186e-05	0.168e-03	-0.168e-03	-0.376e-06	0.376e-06
24	0.234e-19	-0.201e-05	0.201e-05	0.137e-03	-0.137e-03	-0.274e-06	0.274e-06
25	-0.763e-19	-0.103e-05	0.103e-05	0.111e-03	-0.111e-03	-0.199e-06	0.199e-06
26	0.228e-19	-0.141e-05	0.141e-05	0.891e-04	-0.891e-04	-0.143e-06	0.143e-06
27	-0.514e-19	-0.591e-06	0.591e-06	0.687e-04	-0.687e-04	-0.991e-07	0.991e-07
28	0.121e-19	-0.110e-05	0.110e-05	0.503e-04	-0.503e-04	-0.651e-07	0.651e-07
29	-0.459e-20	-0.373e-06	0.373e-06	0.320e-04	-0.320e-04	-0.377e-07	0.377e-07
30	0.694e-21	-0.953e-06	0.953e-06	0.144e-04	-0.144e-04	-0.150e-07	0.150e-07

FORCE = -0.0350567909

TORQUE = 1.0354791053

Rotation Coefficients

$\alpha = 0.962423650119$

$\epsilon = 0.5$

$\beta = 0$

n	A_n^r	B_n^r	C_n^r	D_n^r	E_n^r	F_n^r	G_n^r
0				-0.604e+00	0.0e+00		
1	-0.400e+00	0.183e+00	0.0e+00	0.520e+00	0.0e+00		
2	-0.369e-01	-0.353e-01	0.0e+00	0.186e+00	0.0e+00	-0.746e-02	0.0e+00
3	-0.535e-02	-0.665e-3	0.0e+00	0.350e-01	0.0e+00	0.595e-03	0.0e+00
4	-0.812e-03	0.287e-05	0.0e+00	0.683e-02	0.0e+00	0.622e-04	0.0e+00
5	-0.123e-03	0.266e-05	0.0e+00	0.127e-02	0.0e+00	0.589e-05	0.0e+00
6	-0.183e-04	0.357e-06	0.0e+00	0.227e-03	0.0e+00	0.580e-06	0.0e+00
7	-0.272e-05	0.415e-07	0.0e+00	0.392e-04	0.0e+00	0.603e-07	0.0e+00
8	-0.403e-06	0.478e-08	0.0e+00	0.660e-05	0.0e+00	0.657e-08	0.0e+00
9	-0.594e-07	0.560e-09	0.0e+00	0.109e-05	0.0e+00	0.741e-09	0.0e+00
10	-0.874e-08	0.668e-10	0.0e+00	0.178e-06	0.0e+00	0.862e-10	0.0e+00
11	-0.128e-08	0.813e-11	0.0e+00	0.288e-07	0.0e+00	0.102e-10	0.0e+00
12	-0.188e-09	0.100e-11	0.0e+00	0.460e-08	0.0e+00	0.124e-11	0.0e+00
13	-0.276e-10	0.125e-12	0.0e+00	0.730e-09	0.0e+00	0.153e-12	0.0e+00
14	-0.405e-11	0.159e-13	0.0e+00	0.115e-09	0.0e+00	0.191e-13	0.0e+00
15	-0.593e-12	0.203e-14	0.0e+00	0.180e-10	0.0e+00	0.241e-14	0.0e+00
16	-0.868e-13	0.261e-15	0.0e+00	0.281e-11	0.0e+00	0.306e-15	0.0e+00
17	-0.127e-13	0.338e-16	0.0e+00	0.437e-12	0.0e+00	0.394e-16	0.0e+00
18	-0.186e-14	0.441e-17	0.0e+00	0.676e-13	0.0e+00	0.510e-17	0.0e+00
19	-0.272e-15	0.580e-18	0.0e+00	0.104e-13	0.0e+00	0.665e-18	0.0e+00
20	-0.397e-16	0.765e-19	0.0e+00	0.160e-14	0.0e+00	0.871e-19	0.0e+00
21	-0.580e-17	0.101e-19	0.0e+00	0.246e-15	0.0e+00	0.115e-19	0.0e+00
22	-0.848e-18	0.135e-20	0.0e+00	0.377e-16	0.0e+00	0.152e-20	0.0e+00
23	-0.124e-18	0.181e-21	0.0e+00	0.575e-17	0.0e+00	0.203e-21	0.0e+00
24	-0.181e-19	0.243e-22	0.0e+00	0.877e-18	0.0e+00	0.271e-22	0.0e+00
25	-0.264e-20	0.327e-23	0.0e+00	0.133e-18	0.0e+00	0.362e-23	0.0e+00
26	-0.386e-21	0.447e-24	0.0e+00	0.203e-19	0.0e+00	0.483e-24	0.0e+00
27	-0.563e-22	0.651e-25	0.0e+00	0.307e-20	0.0e+00	0.608e-25	0.0e+00
28	-0.809e-23	0.133e-25	0.0e+00	0.469e-21	0.0e+00	0.402e-26	0.0e+00
29	-0.106e-23	0.607e-26	0.0e+00	0.748e-22	0.0e+00	-0.35e-26	0.0e+00
30	-0.292e-25	-0.28e-24	0.0e+00	0.108e-22	0.0e+00	0.588e-28	0.0e+00

FORCE = -0.0857611042

TORQUE = 0.9963210500

Appendix E

Force and Torque Computations

This chapter includes the actual computer output for the force and torque computations for the rotation and translation cases. There are seven numbers reported for each case, alpha and eps are α and ϵ corresponding to the dimensionless separation distance, N the number of terms taken in the series, force and torque the computed force and torque results reported to ten significant figures and beta and betap corresponding to the slip coefficient. The actual value of the slip coefficient β is equal to beta / betap. In order to specify the $\beta = \infty$ case, betap was set to zero. For most of the runs, the values of beta and betap were kept in the range $[0, 1]$.

To determine the actual precision of the numerical calculations, cases were run including more nonzero terms in the series expressions. For a given separation, numerical convergence was determined at the value $\beta = 1$. These results are included before the results for each separation distance.

Translation Results: Cray X-MP

alpha	eps	n	force	torque	beta	betap
5.308243,	100.000000,	40,	-1.0055456801,	-0.6736738427E-08,	0.100E+01,	0.100E+01
5.308243,	100.000000,	100,	-1.0055456801,	-0.6736722258E-08,	0.100E+01,	0.100E+01
5.308243,	100.000000,	300,	-1.0055456801,	-0.6736738891E-08,	0.100E+01,	0.100E+01
5.308243,	100.000000,	200,	-1.0056003768,	0.8981470763E-09,	0.100E+01,	0.000E+00
5.308243,	100.000000,	100,	-1.0056003768,	0.8968009554E-09,	0.100E+01,	0.100E-06
5.308243,	100.000000,	100,	-1.0056003768,	0.8972312315E-09,	0.100E+01,	0.100E-05
5.308243,	100.000000,	200,	-1.0056003763,	0.8972634393E-09,	0.100E+01,	0.100E-04
5.308243,	100.000000,	200,	-1.0056003713,	0.8965194427E-09,	0.100E+01,	0.100E-03
5.308243,	100.000000,	200,	-1.0056003211,	0.8965534018E-09,	0.100E+01,	0.100E-02
5.308243,	100.000000,	200,	-1.0055998194,	0.8968289193E-09,	0.100E+01,	0.100E-01
5.308243,	100.000000,	200,	-1.0055948121,	0.8149438151E-09,	0.100E+01,	0.100E+00
5.308243,	100.000000,	200,	-1.0055456801,	-0.6736722266E-08,	0.100E+01,	0.100E+01
5.308243,	100.000000,	200,	-1.0051225040,	-0.4617999988E-06,	0.100E+00,	0.100E+01
5.308243,	100.000000,	200,	-1.0029462480,	-0.6221126863E-05,	0.100E-01,	0.100E+01
5.308243,	100.000000,	200,	-0.9990572381,	-0.1514143544E-04,	0.100E-02,	0.100E+01
5.308243,	100.000000,	200,	-0.9969317174,	-0.1789371450E-04,	0.100E-03,	0.100E+01
5.308243,	100.000000,	200,	-0.9963937126,	-0.1826857283E-04,	0.100E-04,	0.100E+01
5.308243,	100.000000,	200,	-0.9963108450,	-0.1830813286E-04,	0.100E-05,	0.100E+01
5.308243,	100.000000,	200,	-0.9963008034,	-0.1831255634E-04,	0.000E+00,	0.100E+01
3.088970,	10.000000,	100,	-1.0493631379,	-0.3105468474E-04,	0.100E+01,	0.100E+01
3.088970,	10.000000,	300,	-1.0493631379,	-0.3105468475E-04,	0.100E+01,	0.100E+01
3.088970,	10.000000,	100,	-1.0538015671,	0.6178077473E-05,	0.100E+01,	0.000E+00
3.088970,	10.000000,	100,	-1.0538015666,	0.6178077248E-05,	0.100E+01,	0.100E-06
3.088970,	10.000000,	100,	-1.0538015620,	0.6178075264E-05,	0.100E+01,	0.100E-05
3.088970,	10.000000,	100,	-1.0538015157,	0.6178055175E-05,	0.100E+01,	0.100E-04
3.088970,	10.000000,	100,	-1.0538010532,	0.6177854196E-05,	0.100E+01,	0.100E-03
3.088970,	10.000000,	100,	-1.0537964291,	0.6175791846E-05,	0.100E+01,	0.100E-02
3.088970,	10.000000,	100,	-1.0537502720,	0.6149880291E-05,	0.100E+01,	0.100E-01
3.088970,	10.000000,	100,	-1.0532968116,	0.5395507064E-05,	0.100E+01,	0.100E+00
3.088970,	10.000000,	100,	-1.0493631379,	-0.3105468474E-04,	0.100E+01,	0.100E+01
3.088970,	10.000000,	100,	-1.0289226621,	-0.5047815073E-03,	0.100E+00,	0.100E+01
3.088970,	10.000000,	100,	-0.9925060839,	-0.1249842584E-02,	0.100E-01,	0.100E+01
3.088970,	10.000000,	100,	-0.9727503112,	-0.1468904182E-02,	0.100E-02,	0.100E+01
3.088970,	10.000000,	100,	-0.9677802821,	-0.1495521127E-02,	0.100E-03,	0.100E+01
3.088970,	10.000000,	100,	-0.9670749093,	-0.1498085380E-02,	0.100E-04,	0.100E+01
3.088970,	10.000000,	100,	-0.9670003885,	-0.1498338737E-02,	0.100E-05,	0.100E+01
3.088970,	10.000000,	100,	-0.9669920593,	-0.1498366849E-02,	0.000E+00,	0.100E+01
1.316958,	1.000000,	500,	-1.3827523824,	0.5024711229E-02,	0.100E+01,	0.000E+00
1.316958,	1.000000,	500,	-1.3827523558,	0.5024710225E-02,	0.100E+01,	0.100E-06
1.316958,	1.000000,	500,	-1.3827521159,	0.5024701186E-02,	0.100E+01,	0.100E-05
1.316958,	1.000000,	500,	-1.3827497177,	0.5024610788E-02,	0.100E+01,	0.100E-04
1.316958,	1.000000,	500,	-1.3827257381,	0.5023706260E-02,	0.100E+01,	0.100E-03
1.316958,	1.000000,	500,	-1.3824862065,	0.5014605544E-02,	0.100E+01,	0.100E-02
1.316958,	1.000000,	500,	-1.3801168126,	0.4918309536E-02,	0.100E+01,	0.100E-01
1.316958,	1.000000,	500,	-1.3585900721,	0.3607572508E-02,	0.100E+01,	0.100E+00
1.316958,	1.000000,	500,	-1.2344126175,	-0.1008739494E-01,	0.100E+01,	0.100E+01
1.316958,	1.000000,	500,	-1.0015047339,	-0.3345291647E-01,	0.100E+00,	0.100E+01
1.316958,	1.000000,	500,	-0.8769637411,	-0.3893671871E-01,	0.100E-01,	0.100E+01
1.316958,	1.000000,	500,	-0.8452742946,	-0.3902420724E-01,	0.100E-02,	0.100E+01
1.316958,	1.000000,	500,	-0.8396165677,	-0.3892837129E-01,	0.100E-03,	0.100E+01
1.316958,	1.000000,	500,	-0.8389076808,	-0.3891233535E-01,	0.100E-04,	0.100E+01
1.316958,	1.000000,	500,	-0.8388343369,	-0.3891062014E-01,	0.100E-05,	0.100E+01
1.316958,	1.000000,	600,	-0.8388261579,	-0.3891042821E-01,	0.000E+00,	0.100E+01

Translation Results: Cray X-MP

alpha	eps	n	force	torque	beta	betap
0.962424,	0.500000,	500,	-1.2902250446,	-0.2629305574E-01,	0.100E+01,	0.100E+01
0.962424,	0.500000,	600,	-1.2902250446,	-0.2629305574E-01,	0.100E+01,	0.100E+01
0.962424,	0.500000,	500,	-1.5957066190,	0.1657396190E-01,	0.100E+01,	0.000E+00
0.962424,	0.500000,	500,	-1.5957065497,	0.1657395705E-01,	0.100E+01,	0.100E-06
0.962424,	0.500000,	500,	-1.5957059266,	0.1657391333E-01,	0.100E+01,	0.100E-05
0.962424,	0.500000,	500,	-1.5956996955,	0.1657347617E-01,	0.100E+01,	0.100E-04
0.962424,	0.500000,	500,	-1.5956373950,	0.1656910226E-01,	0.100E+01,	0.100E-03
0.962424,	0.500000,	500,	-1.5950155039,	0.1652513264E-01,	0.100E+01,	0.100E-02
0.962424,	0.500000,	500,	-1.5889043762,	0.1606429313E-01,	0.100E+01,	0.100E-01
0.962424,	0.500000,	500,	-1.5361509165,	0.1046578029E-01,	0.100E+01,	0.100E+00
0.962424,	0.500000,	500,	-1.2902250446,	-0.2629305574E-01,	0.100E+01,	0.100E+01
0.962424,	0.500000,	500,	-0.9668365598,	-0.6131716914E-01,	0.100E+00,	0.100E+01
0.962424,	0.500000,	500,	-0.8321275034,	-0.6525618545E-01,	0.100E-01,	0.100E+01
0.962424,	0.500000,	500,	-0.8009066100,	-0.6458846751E-01,	0.100E-02,	0.100E+01
0.962424,	0.500000,	500,	-0.7956235113,	-0.6435550351E-01,	0.100E-03,	0.100E+01
0.962424,	0.500000,	500,	-0.7949971181,	-0.6432441228E-01,	0.100E-04,	0.100E+01
0.962424,	0.500000,	500,	-0.7949330329,	-0.6432118781E-01,	0.100E-05,	0.100E+01
0.962424,	0.500000,	500,	-0.7949258953,	-0.6432082818E-01,	0.000E+00,	0.100E+01
0.443568,	0.100000,	500,	-1.3426927240,	-0.8039308410E-01,	0.100E+01,	0.100E+01
0.443568,	0.100000,	600,	-1.3426927240,	-0.8039308410E-01,	0.100E+01,	0.100E+01
0.443568,	0.100000,	500,	-2.2643030354,	0.8876334417E-01,	0.100E+01,	0.000E+00
0.443568,	0.100000,	500,	-2.2643029885,	0.8876333774E-01,	0.100E+01,	0.100E-07
0.443568,	0.100000,	500,	-2.2643025668,	0.8876327986E-01	0.100E+01,	0.100E-06
0.443568,	0.100000,	500,	-2.2642983495,	0.8876270102E-01,	0.100E+01,	0.100E-05
0.443568,	0.100000,	500,	-2.2642561792,	0.8875691221E-01,	0.100E+01,	0.100E-04
0.443568,	0.100000,	500,	-2.2638347595,	0.8869897988E-01,	0.100E+01,	0.100E-03
0.443568,	0.100000,	500,	-2.2596485647,	0.8811543497E-01,	0.100E+01,	0.100E-02
0.443568,	0.100000,	500,	-2.2202939060,	0.8201306372E-01,	0.100E+01,	0.100E-01
0.443568,	0.100000,	500,	-1.9599341939,	0.2976477713E-01,	0.100E+01,	0.100E+00
0.443568,	0.100000,	500,	-1.3426927240,	-0.8039308410E-01,	0.100E+01,	0.100E+01
0.443568,	0.100000,	500,	-0.9129274714,	-0.1109725312E+00,	0.100E+00,	0.100E+01
0.443568,	0.100000,	500,	-0.7759024795,	-0.1072970328E+00,	0.100E-01,	0.100E+01
0.443568,	0.100000,	500,	-0.7463367839,	-0.1049361034E+00,	0.100E-02,	0.100E+01
0.443568,	0.100000,	500,	-0.7418346846,	-0.1044877921E+00,	0.100E-03,	0.100E+01
0.443568,	0.100000,	500,	-0.7413420101,	-0.1044370633E+00,	0.100E-04,	0.100E+01
0.443568,	0.100000,	500,	-0.7412922331,	-0.1044319195E+00,	0.100E-05,	0.100E+01
0.443568,	0.100000,	500,	-0.7412866965,	-0.1044313472E+00,	0.000E+00,	0.100E+01
0.314925,	0.050000,	500,	-1.3474354445,	-0.9764270625E-01,	0.100E+01,	0.100E+01
0.314925,	0.050000,	800,	-1.3474354445,	-0.9764270625E-01,	0.100E+01,	0.100E+01
0.314925,	0.050000,	1000,	-1.3474354445,	-0.9764270625E-01,	0.100E+01,	0.100E+01
0.314925,	0.050000,	500,	-2.5989632790,	0.1379253408E+00,	0.100E+01,	0.000E+00
0.314925,	0.050000,	500,	-2.5989622890,	0.1379251871E+00,	0.100E+01,	0.100E-06
0.314925,	0.050000,	500,	-2.5989533795,	0.1379238033E+00,	0.100E+01,	0.100E-05
0.314925,	0.050000,	500,	-2.5988642954,	0.1379099641E+00,	0.100E+01,	0.100E-04
0.314925,	0.050000,	500,	-2.5979745894,	0.1377714114E+00,	0.100E+01,	0.100E-03
0.314925,	0.050000,	500,	-2.5891883446,	0.1363713571E+00,	0.100E+01,	0.100E-02
0.314925,	0.050000,	500,	-2.5104621603,	0.1218596603E+00,	0.100E+01,	0.100E-01
0.314925,	0.050000,	500,	-2.0877415373,	0.2744725350E-01,	0.100E+01,	0.100E+00
0.314925,	0.050000,	500,	-1.3474354445,	-0.9764270625E-01,	0.100E+01,	0.100E+01
0.314925,	0.050000,	500,	-0.9037656679,	-0.1204751282E+00,	0.100E+00,	0.100E+01
0.314925,	0.050000,	500,	-0.7671159273,	-0.1145795803E+00,	0.100E-01,	0.100E+01
0.314925,	0.050000,	500,	-0.7378751637,	-0.1118440079E+00,	0.100E-02,	0.100E+01
0.314925,	0.050000,	500,	-0.7336357043,	-0.1113757852E+00,	0.100E-03,	0.100E+01
0.314925,	0.050000,	500,	-0.7331818296,	-0.1113244933E+00,	0.100E-04,	0.100E+01
0.314925,	0.050000,	500,	-0.7331361008,	-0.1113193131E+00,	0.100E-05,	0.100E+01
0.314925,	0.050000,	500,	-0.7331310160,	-0.1113187370E+00,	0.000E+00,	0.100E+01

Translation Results: Cray X-MP

alpha	eps	n	force	torque	beta	betap
0.141304,	0.010000,	500,	-1.3500792213,	-0.1180205109E+00,	0.100E+01,	0.100E+01
0.141304,	0.010000,	600,	-1.3500792236,	-0.1180205114E+00,	0.100E+01,	0.100E+01
0.141304,	0.010000,	700,	-1.3500792240,	-0.1180205115E+00,	0.100E+01,	0.100E+01
0.141304,	0.010000,	1000,	-1.3500792241,	-0.1180205115E+00,	0.100E+01,	0.100E+01
0.141304,	0.010000,	700,	-3.4225329664,	0.2765174027E+00,	0.100E+01,	0.000E+00
0.141304,	0.010000,	700,	-3.4225277374,	0.2765164752E+00,	0.100E+01,	0.100E-06
0.141304,	0.010000,	700,	-3.4224806800,	0.2765081278E+00,	0.100E+01,	0.100E-05
0.141304,	0.010000,	700,	-3.4220103899,	0.2764246176E+00,	0.100E+01,	0.100E-04
0.141304,	0.010000,	700,	-3.4173356206,	0.2755860513E+00,	0.100E+01,	0.100E-03
0.141304,	0.010000,	700,	-3.3731249920,	0.2669976656E+00,	0.100E+01,	0.100E-02
0.141304,	0.010000,	700,	-3.0695958433,	0.1939773451E+00,	0.100E+01,	0.100E-01
0.141304,	0.010000,	700,	-2.2281382723,	0.8999162473E-03,	0.100E+01,	0.100E+00
0.141304,	0.010000,	700,	-1.3500792240,	-0.1180205115E+00,	0.100E+01,	0.100E+01
0.141304,	0.010000,	700,	-0.8959982376,	-0.1290940614E+00,	0.100E+00,	0.100E+01
0.141304,	0.010000,	700,	-0.7594781968,	-0.1207403570E+00,	0.100E-01,	0.100E+01
0.141304,	0.010000,	700,	-0.7307144157,	-0.1176693602E+00,	0.100E-02,	0.100E+01
0.141304,	0.010000,	700,	-0.7268314313,	-0.1172046014E+00,	0.100E-03,	0.100E+01
0.141304,	0.010000,	700,	-0.7264248174,	-0.1171552365E+00,	0.100E-04,	0.100E+01
0.141304,	0.010000,	700,	-0.7263839570,	-0.1171502685E+00,	0.100E-05,	0.100E+01
0.141304,	0.010000,	700,	-0.7263794147,	-0.1171497162E+00,	0.000E+00,	0.100E+01
0.099958,	0.005000,	800,	-1.3503019950,	-0.1216203042E+00,	0.100E+01,	0.100E+01
0.099958,	0.005000,	1000,	-1.3503019958,	-0.1216203044E+00,	0.100E+01,	0.100E+01
0.099958,	0.005000,	1200,	-1.3503019958,	-0.1216203044E+00,	0.100E+01,	0.100E+01
0.099958,	0.005000,	1000,	-3.7867298869,	0.3419456910E+00,	0.100E+01,	0.000E+00
0.099958,	0.005000,	1000,	-3.7867193366,	0.3419437752E+00,	0.100E+01,	0.100E-06
0.099958,	0.005000,	1000,	-3.7866243955,	0.3419265320E+00,	0.100E+01,	0.100E-05
0.099958,	0.005000,	1000,	-3.7856761214,	0.3417539564E+00,	0.100E+01,	0.100E-04
0.099958,	0.005000,	1000,	-3.7763045575,	0.3400153203E+00,	0.100E+01,	0.100E-03
0.099958,	0.005000,	1000,	-3.6918096508,	0.3222466129E+00,	0.100E+01,	0.100E-02
0.099958,	0.005000,	1000,	-3.2211951035,	0.2028062512E+00,	0.100E+01,	0.100E-01
0.099958,	0.005000,	1000,	-2.2486111511,	-0.9914283603E-02,	0.100E+01,	0.100E+00
0.099958,	0.005000,	1000,	-1.3503019958,	-0.1216203044E+00,	0.100E+01,	0.100E+01
0.099958,	0.005000,	1000,	-0.8950025476,	-0.1302975094E+00,	0.100E+00,	0.100E+01
0.099958,	0.005000,	1000,	-0.7585833690,	-0.1215526790E+00,	0.100E-01,	0.100E+01
0.099958,	0.005000,	1000,	-0.7298560720,	-0.1184261171E+00,	0.100E-02,	0.100E+01
0.099958,	0.005000,	1000,	-0.7259738134,	-0.1179540563E+00,	0.100E-03,	0.100E+01
0.099958,	0.005000,	1000,	-0.7255671522,	-0.1179039189E+00,	0.100E-04,	0.100E+01
0.099958,	0.005000,	1000,	-0.7255262856,	-0.1178988732E+00,	0.100E-05,	0.100E+01
0.099958,	0.005000,	1000,	-0.7255221969,	-0.1178983683E+00,	0.100E-06,	0.100E+01
0.099958,	0.005000,	1000,	-0.7255217426,	-0.1178983122E+00,	0.000E+00,	0.100E+01
0.044718,	0.001000,	1000,	-1.3504554935,	-0.1251048026E+00,	0.100E+01,	0.100E+01
0.044718,	0.001000,	1200,	-1.3504556116,	-0.1251048296E+00,	0.100E+01,	0.100E+01
0.044718,	0.001000,	1500,	-1.3504556410,	-0.1251048363E+00,	0.100E+01,	0.100E+01
0.044718,	0.001000,	2000,	-1.3504556454,	-0.1251048373E+00,	0.100E+01,	0.100E+01
0.044718,	0.001000,	2200,	-1.3504556456,	-0.1251048373E+00,	0.100E+01,	0.100E+01
0.044718,	0.001000,	2000,	-4.6400381652,	0.4991118448E+00,	0.100E+01,	0.000E+00
0.044718,	0.001000,	2200,	-4.6399849788,	0.4991019561E+00,	0.100E+01,	0.100E-06
0.044718,	0.001000,	2200,	-4.6395065890,	0.4990129223E+00,	0.100E+01,	0.100E-05
0.044718,	0.001000,	2000,	-4.6347508418,	0.4981192118E+00,	0.100E+01,	0.100E-04
0.044718,	0.001000,	2000,	-4.5897340038,	0.4889873032E+00,	0.100E+01,	0.100E-03
0.044718,	0.001000,	2000,	-4.2787176103,	0.4110492442E+00,	0.100E+01,	0.100E-02
0.044718,	0.001000,	2000,	-3.3841373404,	0.1873774158E+00,	0.100E+01,	0.100E-01
0.044718,	0.001000,	2000,	-2.2652115229,	-0.2425979721E-01,	0.100E+01,	0.100E+00
0.044718,	0.001000,	2000,	-1.3504556454,	-0.1251048373E+00,	0.100E+01,	0.100E+01

Translation Results: Cray X-MP

alpha	eps	n	force	torque	beta	betap
0.044718,	0.001000,	2000,	-0.8941937611,	-0.1313221960E+00,	0.100E+01,	0.100E+02
0.044718,	0.001000,	2000,	-0.7576751285,	-0.1221803447E+00,	0.100E-01,	0.100E+01
0.044718,	0.001000,	2000,	-0.7290739325,	-0.1190199843E+00,	0.100E-02,	0.100E+01
0.044718,	0.001000,	2000,	-0.7252740583,	-0.1185549079E+00,	0.100E-03,	0.100E+01
0.044718,	0.001000,	2000,	-0.7248777017,	-0.1185057868E+00,	0.100E-04,	0.100E+01
0.044718,	0.001000,	2000,	-0.7248378895,	-0.1185008464E+00,	0.100E-05,	0.100E+01
0.044718,	0.001000,	2000,	-0.7248334640,	-0.1185002972E+00,	0.000E+00,	0.100E+01
0.031621,	0.000500,	2000,	-1.3504730115,	-0.1256403614E+00,	0.100E+01,	0.100E+01
0.031621,	0.000500,	2200,	-1.3504730161,	-0.1256403624E+00,	0.100E+01,	0.100E+01
0.031621,	0.000500,	2490,	-1.3504730184,	-0.1256403630E+00,	0.100E+01,	0.100E+01
0.031621,	0.000500,	2200,	-5.0089716826,	0.5678415613E+00,	0.100E+01,	0.000E+00
0.031621,	0.000500,	2200,	-5.0088651844,	0.5678216833E+00,	0.100E+01,	0.100E-06
0.031621,	0.000500,	2200,	-5.0079078490,	0.5676426389E+00,	0.100E+01,	0.100E-05
0.031621,	0.000500,	2200,	-4.9984457162,	0.5658394983E+00,	0.100E+01,	0.100E-04
0.031621,	0.000500,	2200,	-4.9130543608,	0.5474401520E+00,	0.100E+01,	0.100E-03
0.031621,	0.000500,	2200,	-4.4344930411,	0.4225580767E+00,	0.100E+01,	0.100E-02
0.031621,	0.000500,	2200,	-3.4078582641,	0.1782033808E+00,	0.100E+01,	0.100E-01
0.031621,	0.000500,	2200,	-2.2672770551,	-0.2704283023E-01,	0.100E+01,	0.100E+00
0.031621,	0.000500,	2000,	-0.8940358045,	-0.1314503619E+00,	0.100E+00,	0.100E+01
0.031621,	0.000500,	2000,	-0.7568202993,	-0.1221374807E+00,	0.100E-01,	0.100E+01
0.031621,	0.000500,	2000,	-0.7287035160,	-0.1190498769E+00,	0.100E-02,	0.100E+01
0.031621,	0.000500,	2000,	-0.7251543184,	-0.1186249590E+00,	0.100E-03,	0.100E+01
0.031621,	0.000500,	2000,	-0.7247881186,	-0.1185806798E+00,	0.100E-04,	0.100E+01
0.031621,	0.000500,	2000,	-0.7247513797,	-0.1185762331E+00,	0.100E-05,	0.100E+01
0.031621,	0.000500,	2200,	-0.7247472962,	-0.1185757388E+00,	0.000E+00,	0.100E+01
0.014142,	0.000100,	3000,	-1.3504863299,	-0.1261279737E+00,	0.100E+01,	0.100E+01
0.014142,	0.000100,	4000,	-1.3504865376,	-0.1261280212E+00,	0.100E+01,	0.100E+01
0.014142,	0.000100,	5000,	-1.3504865564,	-0.1261280255E+00,	0.100E+01,	0.100E+01
0.014142,	0.000100,	7000,	-1.3504865591,	-0.1261280261E+00,	0.100E+01,	0.100E+01
0.014142,	0.000100,	4000,	-5.8666753895,	0.7282497717E+00,	0.100E+01,	0.000E+00
0.014142,	0.000100,	4000,	-5.8661425593,	0.7281498831E+00,	0.100E+01,	0.100E-06
0.014142,	0.000100,	4000,	-5.8613755239,	0.7272474883E+00,	0.100E+01,	0.100E-05
0.014142,	0.000100,	4000,	-5.8162461739,	0.7180295420E+00,	0.100E+01,	0.100E-04
0.014142,	0.000100,	4000,	-5.5041631450,	0.6392840049E+00,	0.100E+01,	0.100E-03
0.014142,	0.000100,	4000,	-4.6011223042,	0.4095104197E+00,	0.100E+01,	0.100E-02
0.014142,	0.000100,	4000,	-3.4271714260,	0.1652328195E+00,	0.100E+01,	0.100E-01
0.014142,	0.000100,	4000,	-2.2689217574;	-0.2986322656E-01,	0.100E+01,	0.100E+00
0.014142,	0.000100,	4000,	-1.3504865376,	-0.1261280212E+00,	0.100E+01,	0.100E+01
0.014142,	0.000100,	4000,	-0.8939169690,	-0.1315601829E+00,	0.100E+00,	0.100E+01
0.014142,	0.000100,	4000,	-0.7564246612,	-0.1221513502E+00,	0.100E-01,	0.100E+01
0.014142,	0.000100,	4000,	-0.7285388865,	-0.1190954141E+00,	0.100E-02,	0.100E+01
0.014142,	0.000100,	4000,	-0.7250744613,	-0.1186836427E+00,	0.100E-03,	0.100E+01
0.014142,	0.000100,	4000,	-0.7247180584,	-0.1186408915E+00,	0.100E-04,	0.100E+01
0.014142,	0.000100,	4000,	-0.7246823136,	-0.1186365999E+00,	0.100E-05,	0.100E+01
0.014142,	0.000100,	4000,	-0.7246787381,	-0.1186361706E+00,	0.100E-06,	0.100E+01
0.014142,	0.000100,	4000,	-0.7246783408,	-0.1186361229E+00,	0.000E+00,	0.100E+01
0.010000,	0.000050,	5000,	-1.3504881652,	-0.1261988743E+00,	0.100E+01,	0.100E+01
0.010000,	0.000050,	10000,	-1.3504882266,	-0.1261988883E+00,	0.100E+01,	0.100E+01
0.010000,	0.000050,	5000,	-6.2362597333,	0.7974862100E+00,	0.100E+01,	0.000E+00
0.010000,	0.000050,	5000,	-6.2351945380,	0.7972862152E+00,	0.100E+01,	0.100E-06
0.010000,	0.000050,	5000,	-6.2257201627,	0.7954734365E+00,	0.100E+01,	0.100E-05
0.010000,	0.000050,	5000,	-6.1402073018,	0.7769791675E+00,	0.100E+01,	0.100E-04
0.010000,	0.000050,	5000,	-5.6605336681,	0.6512352686E+00,	0.100E+01,	0.100E-03
0.010000,	0.000050,	5000,	-4.6253459807,	0.4006591357E+00,	0.100E+01,	0.100E-02
0.010000,	0.000050,	5000,	-3.4295842602,	0.1626260836E+00,	0.100E+01,	0.100E-01
0.010000,	0.000050,	5000,	-2.2691265795,	-0.3031505299E-01,	0.100E+01,	0.100E+00

Translation Results: Cray X-MP

alpha	eps	n	force	torque	beta	betap
0.010000,	0.000050,	5000,	-1.3504881651,	-0.1261988743E+00,	0.100E+01,	0.100E+01
0.010000,	0.000050,	5000,	-0.8938448615,	-0.1315647077E+00,	0.100E+00,	0.100E+01
0.010000,	0.000050,	5000,	-0.7560115842,	-0.1220930651E+00,	0.100E-01,	0.100E+01
0.010000,	0.000050,	5000,	-0.7284233461,	-0.1190855609E+00,	0.100E-02,	0.100E+01
0.010000,	0.000050,	5000,	-0.7250538367,	-0.1186892394E+00,	0.100E-03,	0.100E+01
0.010000,	0.000050,	5000,	-0.7247082230,	-0.1186482438E+00,	0.100E-04,	0.100E+01
0.010000,	0.000050,	5000,	-0.7246735713,	-0.1186441301E+00,	0.100E-05,	0.100E+01
0.010000,	0.000050,	5000,	-0.7246701052,	-0.1186437185E+00,	0.100E-06,	0.100E+01
0.010000,	0.000050,	5000,	-0.7246697201,	-0.1186436728E+00,	0.000E+00,	0.100E+01
0.003162,	0.000005,	5000,	-1.3503676614,	-0.1262425320E+00,	0.100E+01,	0.100E+01
0.003162,	0.000005,	10000,	-1.3504878014,	-0.1262698582E+00,	0.100E+01,	0.100E+01
0.003162,	0.000005,	5000,	-7.4642116812,	0.1027665519E+01,	0.100E+01,	0.000E+00
0.003162,	0.000005,	5000,	-7.4536704069,	0.1025651312E+01,	0.100E+01,	0.100E-06
0.003162,	0.000005,	5000,	-7.3681422004,	0.1007144350E+01,	0.100E+01,	0.100E-05
0.003162,	0.000005,	5000,	-6.8883255049,	0.8812821909E+00,	0.100E+01,	0.100E-04
0.003162,	0.000005,	5000,	-5.8519650093,	0.6297640300E+00,	0.100E+01,	0.100E-03
0.003162,	0.000005,	5000,	-4.6475377577,	0.3853796175E+00,	0.100E+01,	0.100E-02
0.003162,	0.000005,	5000,	-3.4317480350,	0.1595134371E+00,	0.100E+01,	0.100E-01
0.003162,	0.000005,	5000,	-2.2693106786,	-0.3079811296E-01,	0.100E+01,	0.100E+00
0.003162,	0.000005,	5000,	-1.3503676616,	-0.1262425318E+00,	0.100E+01,	0.100E+01
0.003162,	0.000005,	5000,	-0.8893456579,	-0.1307843495E+00,	0.100E+00,	0.100E+01
0.003162,	0.000005,	5000,	-0.7497736048,	-0.1210731430E+00,	0.100E-01,	0.100E+01
0.003162,	0.000005,	5000,	-0.7273573291,	-0.1189193805E+00,	0.100E-02,	0.100E+01
0.003162,	0.000005,	5000,	-0.7249335632,	-0.1186776592E+00,	0.100E-03,	0.100E+01
0.003162,	0.000005,	5000,	-0.7246891425,	-0.1186531903E+00,	0.100E-04,	0.100E+01
0.003162,	0.000005,	5000,	-0.7246646798,	-0.1186507404E+00,	0.100E-05,	0.100E+01
0.003162,	0.000005,	5000,	-0.7246622333,	-0.1186504954E+00,	0.100E-06,	0.100E+01
0.003162,	0.000005,	5000,	-0.7246619614,	-0.1186504681E+00,	0.000E+00,	0.100E+01
0.001000,	0.0000005,	5000,	-1.3314081465,	-0.1229315223E+00,	0.100E+01,	0.100E+01
0.001000,	0.0000005,	8000,	-1.3477299844,	-0.1256712604E+00,	0.100E+01,	0.100E+01
0.001000,	0.0000005,	10000,	-1.3494122457,	-0.1260368005E+00,	0.100E+01,	0.100E+01
0.001000,	0.0000005,	10000,	-8.6922441203,	0.1257914366E+01,	0.100E+01,	0.000E+00
0.001000,	0.0000005,	10000,	-8.5961726722,	0.1237391386E+01,	0.100E+01,	0.100E-06
0.001000,	0.0000005,	10000,	-8.1163383389,	0.1111514314E+01,	0.100E+01,	0.100E-05
0.001000,	0.0000005,	10000,	-7.0798286794,	0.8598698052E+00,	0.100E+01,	0.100E-04
0.001000,	0.0000005,	10000,	-5.8742169342,	0.6145304147E+00,	0.100E+01,	0.100E-03
0.001000,	0.0000005,	10000,	-4.6497474986,	0.3822970770E+00,	0.100E+01,	0.100E-02
0.001000,	0.0000005,	10000,	-3.4319621754,	0.1590464066E+00,	0.100E+01,	0.100E-01
0.001000,	0.0000005,	10000,	-2.2693243787,	-0.3086109358E-01,	0.100E+01,	0.100E+00
0.001000,	0.0000005,	10000,	-1.3494122539,	-0.1260368040E+00,	0.100E+01,	0.100E+01
0.001000,	0.0000005,	10000,	-0.8816706727,	-0.1294402320E+00,	0.100E+00,	0.100E+01
0.001000,	0.0000005,	10000,	-0.7462386593,	-0.1204953730E+00,	0.100E-01,	0.100E+01
0.001000,	0.0000005,	10000,	-0.7269163368,	-0.1188487763E+00,	0.100E-02,	0.100E+01
0.001000,	0.0000005,	10000,	-0.7248864447,	-0.1186710414E+00,	0.100E-03,	0.100E+01
0.001000,	0.0000005,	10000,	-0.7246824095,	-0.1186531273E+00,	0.100E-04,	0.100E+01
0.001000,	0.0000005,	10000,	-0.7246619954,	-0.1186513345E+00,	0.100E-05,	0.100E+01
0.001000,	0.0000005,	10000,	-0.7246599539,	-0.1186511552E+00,	0.100E-06,	0.100E+01
0.001000,	0.0000005,	10000,	-0.7246597268,	-0.1186511345E+00,	0.000E+00,	0.100E+01
0.000447,	0.0000001,	8000,	-1.2803319708,	-0.1162723525E+00,	0.100E+01,	0.100E+01
0.000447,	0.0000001,	10000,	-1.3203976110,	-0.1214219905E+00,	0.100E+01,	0.100E+01
0.000447,	0.0000001,	15000,	-1.3448318797,	-0.1250915645E+00,	0.100E+01,	0.100E+01

Translation Results: Cray X-MP

alpha	eps	n	force	torque	beta	betap
0.000447,	0.0000001,15000,		-9.5502788774,	0.1418865483E+01,	0.100E+01,	0.000E+00
0.000447,	0.0000001,15000,		-9.1875919343,	0.1329755251E+01,	0.100E+01,	0.100E-06
0.000447,	0.0000001,15000,		-8.2832198916,	0.1098909968E+01,	0.100E+01,	0.100E-05
0.000447,	0.0000001,15000,		-7.0992815061,	0.8472209376E+00,	0.100E+01,	0.100E-04
0.000447,	0.0000001,15000,		-5.8758511821,	0.6118905519E+00,	0.100E+01,	0.100E-03
0.000447,	0.0000001,15000,		-4.6496043537,	0.3819090506E+00,	0.100E+01,	0.100E-02
0.000447,	0.0000001,15000,		-3.4316420223,	0.1590030896E+00,	0.100E+01,	0.100E-01
0.000447,	0.0000001,15000,		-2.2688479148,	-0.3081987347E-01,	0.100E+01,	0.100E+00
0.000447,	0.0000001,15000,		-1.3448318164,	-0.1250915105E+00,	0.100E+01,	0.100E+01
0.000447,	0.0000001,15000,		-0.8687946157,	-0.1272698096E+00,	0.100E+00,	0.100E+01
0.000447,	0.0000001,15000,		-0.7425150245,	-0.1199406047E+00,	0.100E-01,	0.100E+01
0.000447,	0.0000001,15000,		-0.7262012376,	-0.1187807491E+00,	0.100E-02,	0.100E+01
0.000447,	0.0000001,15000,		-0.7245174159,	-0.1186585437E+00,	0.100E-03,	0.100E+01
0.000447,	0.0000001,15000,		-0.7243484864,	-0.1186462578E+00,	0.100E-04,	0.100E+01
0.000447,	0.0000001,15000,		-0.7243315884,	-0.1186450286E+00,	0.100E-05,	0.100E+01
0.000447,	0.0000001,15000,		-0.7243298987,	-0.1186449062E+00,	0.100E-06,	0.100E+01
0.000447,	0.0000001,15000,		-0.7243297100,	-0.1186448878E+00,	0.000E+00,	0.100E+01
0.000316,	0.0000005,12000,		-1.2937444374,	-0.1179869471E+00,	0.100E+01,	0.100E+01
0.000316,	0.0000005,14000,		-1.3191607623,	-0.1212588092E+00,	0.100E+01,	0.100E+01
0.000316,	0.0000005,15000,		-1.3268028313,	-0.1222872031E+00,	0.100E+01,	0.100E+01
0.000316,	0.0000005,15000,		-9.9140183038,	0.1488459565E+01,	0.100E+01,	0.000E+00
0.000316,	0.0000005,15000,		-9.3380999744,	0.1342059951E+01,	0.100E+01,	0.100E-06
0.000316,	0.0000005,15000,		-8.3015587353,	0.1090402103E+01,	0.100E+01,	0.100E-05
0.000316,	0.0000005,15000,		-7.0957893001,	0.8449482988E+00,	0.100E+01,	0.100E-04
0.000316,	0.0000005,15000,		-5.8701081119,	0.6117573382E+00,	0.100E+01,	0.100E-03
0.000316,	0.0000005,15000,		-4.6436090274,	0.3821487055E+00,	0.100E+01,	0.100E-02
0.000316,	0.0000005,15000,		-3.4254456671,	0.1593461481E+00,	0.100E+01,	0.100E-01
0.000316,	0.0000005,15000,		-2.2612614548,	-0.3010928195E-01,	0.100E+01,	0.100E+00
0.000316,	0.0000005,15000,		-1.3268029335,	-0.1222872581E+00,	0.100E+01,	0.100E+01
0.000316,	0.0000005,15000,		-0.8464340930,	-0.1243299843E+00,	0.100E+00,	0.100E+01
0.000316,	0.0000005,15000,		-0.7334326959,	-0.1192341603E+00,	0.100E-01,	0.100E+01
0.000316,	0.0000005,15000,		-0.7198898846,	-0.1185082078E+00,	0.100E-02,	0.100E+01
0.000316,	0.0000005,15000,		-0.7185071906,	-0.1184328157E+00,	0.100E-03,	0.100E+01
0.000316,	0.0000005,15000,		-0.7183686276,	-0.1184252476E+00,	0.100E-04,	0.100E+01
0.000316,	0.0000005,15000,		-0.7183547698,	-0.1184244904E+00,	0.100E-05,	0.100E+01
0.000316,	0.0000005,15000,		-0.7183533852,	-0.1184244153E+00,	0.100E-06,	0.100E+01
0.000316,	0.0000005,15000,		-0.7183532277,	-0.1184243998E+00,	0.000E+00,	0.100E+01
0.000141,	0.0000001,14000,		-1.0072042791,	-0.7570548161E-01,	0.100E+01,	0.100E+01
0.000141,	0.0000001,15000,		-1.0511341185,	-0.8285198331E-01,	0.100E+01,	0.100E+01
0.000141,	0.0000001,15000,		-10.6048458635,	0.1673410373E+01,	0.100E+01,	0.000E+00
0.000141,	0.0000001,15000,		-9.3325537125,	0.1354937041E+01,	0.100E+01,	0.100E-06
0.000141,	0.0000001,15000,		-8.1467551125,	0.1103758956E+01,	0.100E+01,	0.100E-05
0.000141,	0.0000001,15000,		-6.9223243684,	0.8685239911E+00,	0.100E+01,	0.100E-04
0.000141,	0.0000001,15000,		-5.6940612239,	0.6377281055E+00,	0.100E+01,	0.100E-03
0.000141,	0.0000001,15000,		-4.4651242736,	0.4090575368E+00,	0.100E+01,	0.100E-02
0.000141,	0.0000001,15000,		-3.2391900490,	0.1880375211E+00,	0.100E+01,	0.100E-01
0.000141,	0.0000001,15000,		-2.0372521617,	0.5830460244E-02,	0.100E+01,	0.100E+00
0.000141,	0.0000001,15000,		-1.0511341616,	-0.8285209789E-01,	0.100E+01,	0.100E+01
0.000141,	0.0000001,15000,		-0.6412965364,	-0.9833274304E-01,	0.100E+00,	0.100E+01
0.000141,	0.0000001,15000,		-0.5768785359,	-0.9979667882E-01,	0.100E-01,	0.100E+01
0.000141,	0.0000001,15000,		-0.5700268285,	-0.9993968221E-01,	0.100E-02,	0.100E+01
0.000141,	0.0000001,15000,		-0.5693372219,	-0.9995394582E-01,	0.100E-03,	0.100E+01
0.000141,	0.0000001,15000,		-0.5692682319,	-0.9995537040E-01,	0.100E-04,	0.100E+01
0.000141,	0.0000001,15000,		-0.5692613357,	-0.9995551848E-01,	0.100E-05,	0.100E+01
0.000141,	0.0000001,15000,		-0.5692606458,	-0.9995553267E-01,	0.100E-06,	0.100E+01
0.000141,	0.0000001,15000,		-0.5692605590,	-0.9995554162E-01,	0.000E+00,	0.100E+01

Rotation Results:CRAY X-MP

alpha	eps	n	force	torque	beta	betap
5.308243,	.100000E+03,	100,	-0.0000000090,	0.1000000295E+01,	0.100E+01,	0.100E+01
5.308243,	.100000E+03,	500,	-0.0000000090,	0.1000000295E+01,	0.100E+01,	0.100E+01
5.308243,	.100000E+03,	100,	0.0000000012,	0.1000000303E+01,	0.100E+01,	0.000E+00
5.308243,	.100000E+03,	100,	0.0000000012,	0.1000000303E+01,	0.100E+01,	0.100E-06
5.308243,	.100000E+03,	100,	0.0000000012,	0.1000000303E+01,	0.100E+01,	0.100E-05
5.308243,	.100000E+03,	100,	0.0000000012,	0.1000000303E+01,	0.100E+01,	0.100E-04
5.308243,	.100000E+03,	100,	0.0000000012,	0.1000000303E+01,	0.100E+01,	0.100E-03
5.308243,	.100000E+03,	100,	0.0000000012,	0.1000000303E+01,	0.100E+01,	0.100E-02
5.308243,	.100000E+03,	100,	0.0000000012,	0.1000000303E+01,	0.100E+01,	0.100E-01
5.308243,	.100000E+03,	100,	0.0000000011,	0.1000000302E+01,	0.100E+01,	0.100E+00
5.308243,	.100000E+03,	100,	-0.0000000090,	0.1000000295E+01,	0.100E+01,	0.100E+01
5.308243,	.100000E+03,	100,	-0.0000006157,	0.1000000236E+01,	0.100E+00,	0.100E+01
5.308243,	.100000E+03,	100,	-0.0000082948,	0.1000000067E+01,	0.100E-01,	0.100E+01
5.308243,	.100000E+03,	100,	-0.0000201885,	0.9999999614E+00,	0.100E-02,	0.100E+01
5.308243,	.100000E+03,	100,	-0.0000238571,	0.9999999422E+00,	0.100E-03,	0.100E+01
5.308243,	.100000E+03,	100,	-0.0000243577,	0.9999999400E+00,	0.100E-04,	0.100E+01
5.308243,	.100000E+03,	100,	-0.0000244108,	0.9999999398E+00,	0.100E-05,	0.100E+01
5.308243,	.100000E+03,	100,	-0.0000244167,	0.9999999398E+00,	0.000E+00,	0.100E+01
3.088970,	.100000E+02,	100,	-0.0000414062,	0.1000185763E+01,	0.100E+01,	0.100E+01
3.088970,	.100000E+02,	500,	-0.0000414062,	0.1000185763E+01,	0.100E+01,	0.100E+01
3.088970,	.100000E+02,	100,	0.0000082374,	0.1000234874E+01,	0.100E+01,	0.000E+00
3.088970,	.100000E+02,	100,	0.0000082374,	0.1000234874E+01,	0.100E+01,	0.100E-06
3.088970,	.100000E+02,	100,	0.0000082374,	0.1000234874E+01,	0.100E+01,	0.100E-05
3.088970,	.100000E+02,	100,	0.0000082374,	0.1000234874E+01,	0.100E+01,	0.100E-04
3.088970,	.100000E+02,	100,	0.0000082371,	0.1000234868E+01,	0.100E+01,	0.100E-03
3.088970,	.100000E+02,	100,	0.0000082344,	0.1000234810E+01,	0.100E+01,	0.100E-02
3.088970,	.100000E+02,	100,	0.0000081998,	0.1000234235E+01,	0.100E+01,	0.100E-01
3.088970,	.100000E+02,	100,	0.0000071940,	0.1000228667E+01,	0.100E+01,	0.100E+00
3.088970,	.100000E+02,	100,	-0.0000414062,	0.1000185763E+01,	0.100E+01,	0.100E+01
3.088970,	.100000E+02,	100,	-0.0006730418,	0.1000056767E+01,	0.100E+00,	0.100E+01
3.088970,	.100000E+02,	100,	-0.0016664505,	0.9999733797E+00,	0.100E-01,	0.100E+01
3.088970,	.100000E+02,	100,	-0.0019584585,	0.9999580692E+00,	0.100E-02,	0.100E+01
3.088970,	.100000E+02,	100,	-0.0019940041,	0.9999563659E+00,	0.100E-03,	0.100E+01
3.088970,	.100000E+02,	100,	-0.0019974441,	0.9999561932E+00,	0.100E-04,	0.100E+01
3.088970,	.100000E+02,	100,	-0.0019977843,	0.9999561759E+00,	0.100E-05,	0.100E+01
3.088970,	.100000E+02,	100,	-0.0019978225,	0.9999561739E+00,	0.000E+00,	0.100E+01
1.316958,	.100000E+01,	300,	-0.0134498599,	0.1016469128E+01,	0.100E+01,	0.100E+01
1.316958,	.100000E+01,	500,	-0.0134498599,	0.1016469128E+01,	0.100E+01,	0.100E+01
1.316958,	.100000E+01,	2500,	-0.0134498599,	0.1016469128E+01,	0.100E+01,	0.100E+01
1.316958,	.100000E+01,	300,	0.0066996150,	0.1041783555E+01,	0.100E+01,	0.000E+00
1.316958,	.100000E+01,	300,	0.0066996136,	0.1041783548E+01,	0.100E+01,	0.100E-06
1.316958,	.100000E+01,	300,	0.0066996016,	0.1041783488E+01,	0.100E+01,	0.100E-05
1.316958,	.100000E+01,	300,	0.0066994811,	0.1041782883E+01,	0.100E+01,	0.100E-04
1.316958,	.100000E+01,	300,	0.0066982750,	0.1041776836E+01,	0.100E+01,	0.100E-03
1.316958,	.100000E+01,	300,	0.0066861407,	0.1041716492E+01,	0.100E+01,	0.100E-02
1.316958,	.100000E+01,	300,	0.0065577460,	0.1041124687E+01,	0.100E+01,	0.100E-01
1.316958,	.100000E+01,	300,	0.0048100967,	0.1036138207E+01,	0.100E+01,	0.100E+00
1.316958,	.100000E+01,	300,	-0.0134498599,	0.1016469128E+01,	0.100E+01,	0.100E+01
1.316958,	.100000E+01,	300,	-0.0446038886,	0.9996843640E+00,	0.100E+00,	0.100E+01
1.316958,	.100000E+01,	300,	-0.0519148852,	0.9962381378E+00,	0.100E-01,	0.100E+01
1.316958,	.100000E+01,	300,	-0.0520222837,	0.9958214151E+00,	0.100E-02,	0.100E+01
1.316958,	.100000E+01,	300,	-0.0519009855,	0.9957733683E+00,	0.100E-03,	0.100E+01
1.316958,	.100000E+01,	300,	-0.0518827028,	0.9957682797E+00,	0.100E-04,	0.100E+01
1.316958,	.100000E+01,	300,	-0.0518807851,	0.9957677667E+00,	0.100E-05,	0.100E+01
1.316958,	.100000E+01,	300,	-0.0518805710,	0.9957677096E+00,	0.000E+00,	0.100E+01

Rotation Results:CRAY X-MP

alpha	eps	n	force	torque	beta	betap
0.962424,	.500000E+00,	300,	-0.0350574077,	0.1035479189E+01,	0.100E+01,	0.100E+01
0.962424,	.500000E+00,	500,	-0.0350574077,	0.1035479189E+01,	0.100E+01,	0.100E+01
0.962424,	.500000E+00,	300,	0.0220986159,	0.1110495493E+01,	0.100E+01,	0.000E+00
0.962424,	.500000E+00,	300,	0.0220986094,	0.1110495467E+01,	0.100E+01,	0.100E-06
0.962424,	.500000E+00,	300,	0.0220985511,	0.1110495226E+01,	0.100E+01,	0.100E-05
0.962424,	.500000E+00,	300,	0.0220979682,	0.1110492820E+01,	0.100E+01,	0.100E-04
0.962424,	.500000E+00,	300,	0.0220921363,	0.1110468766E+01,	0.100E+01,	0.100E-03
0.962424,	.500000E+00,	300,	0.0220335102,	0.1110228981E+01,	0.100E+01,	0.100E-02
0.962424,	.500000E+00,	300,	0.0214190575,	0.1107903904E+01,	0.100E+01,	0.100E-01
0.962424,	.500000E+00,	300,	0.0139543737,	0.1089881539E+01,	0.100E+01,	0.100E+00
0.962424,	.500000E+00,	300,	-0.0350574077,	0.1035479189E+01,	0.100E+01,	0.100E+01
0.962424,	.500000E+00,	300,	-0.0817562228,	0.1002745102E+01,	0.100E+00,	0.100E+01
0.962424,	.500000E+00,	300,	-0.0870039989,	0.9971294660E+00,	0.100E-01,	0.100E+01
0.962424,	.500000E+00,	300,	-0.0860936461,	0.9964186963E+00,	0.100E-02,	0.100E+01
0.962424,	.500000E+00,	300,	-0.0858015006,	0.9963313872E+00,	0.100E-03,	0.100E+01
0.962424,	.500000E+00,	300,	-0.0857652361,	0.9963220912E+00,	0.100E-04,	0.100E+01
0.962424,	.500000E+00,	300,	-0.0857615184,	0.9963211542E+00,	0.100E-05,	0.100E+01
0.962424,	.500000E+00,	300,	-0.0857611042,	0.9963210500E+00,	0.000E+00,	0.100E+01
0.443568,	.100000E+00,	300,	-0.1071907788,	0.1130098928E+01,	0.100E+01,	0.100E+01
0.443568,	.100000E+00,	500,	-0.1071907788,	0.1130098928E+01,	0.100E+01,	0.100E+01
0.443568,	.100000E+00,	300,	0.1183511256,	0.1454851210E+01,	0.100E+01,	0.000E+00
0.443568,	.100000E+00,	300,	0.1183510398,	0.1454850926E+01,	0.100E+01,	0.100E-06
0.443568,	.100000E+00,	300,	0.1183502680,	0.1454848365E+01,	0.100E+01,	0.100E-05
0.443568,	.100000E+00,	300,	0.1183425496,	0.1454822762E+01,	0.100E+01,	0.100E-04
0.443568,	.100000E+00,	300,	0.1182653065,	0.1454567004E+01,	0.100E+01,	0.100E-03
0.443568,	.100000E+00,	300,	0.1174872466,	0.1452036676E+01,	0.100E+01,	0.100E-02
0.443568,	.100000E+00,	300,	0.1093507516,	0.1429102402E+01,	0.100E+01,	0.100E-01
0.443568,	.100000E+00,	300,	0.0396863695,	0.1305604754E+01,	0.100E+01,	0.100E+00
0.443568,	.100000E+00,	300,	-0.1071907788,	0.1130098928E+01,	0.100E+01,	0.100E+01
0.443568,	.100000E+00,	300,	-0.1479627679,	0.1075149048E+01,	0.100E+00,	0.100E+01
0.443568,	.100000E+00,	300,	-0.1430076583,	0.1066914739E+01,	0.100E-01,	0.100E+01
0.443568,	.100000E+00,	300,	-0.1398508642,	0.1065715074E+01,	0.100E-02,	0.100E+01
0.443568,	.100000E+00,	300,	-0.1393076129,	0.1065563542E+01,	0.100E-03,	0.100E+01
0.443568,	.100000E+00,	300,	-0.1392484330,	0.1065547714E+01,	0.100E-04,	0.100E+01
0.443568,	.100000E+00,	300,	-0.1392424605,	0.1065546124E+01,	0.100E-05,	0.100E+01
0.443568,	.100000E+00,	300,	-0.1392417963,	0.1065545947E+01,	0.000E+00,	0.100E+01
0.314925,	.500000E-01,	300,	-0.1301902750,	0.1197907629E+01,	0.100E+01,	0.100E+01
0.314925,	.500000E-01,	500,	-0.1301902750,	0.1197907629E+01,	0.100E+01,	0.100E+01
0.314925,	.500000E-01,	300,	0.1839004544,	0.1667461009E+01,	0.100E+01,	0.000E+00
0.314925,	.500000E-01,	300,	0.1839002494,	0.1667460356E+01,	0.100E+01,	0.100E-06
0.314925,	.500000E-01,	300,	0.1838984044,	0.1667454480E+01,	0.100E+01,	0.100E-05
0.314925,	.500000E-01,	300,	0.1838799521,	0.1667395732E+01,	0.100E+01,	0.100E-04
0.314925,	.500000E-01,	300,	0.1836952152,	0.1666809404E+01,	0.100E+01,	0.100E-03
0.314925,	.500000E-01,	300,	0.1818284761,	0.1661058422E+01,	0.100E+01,	0.100E-02
0.314925,	.500000E-01,	300,	0.1624795470,	0.1612368211E+01,	0.100E+01,	0.100E-01
0.314925,	.500000E-01,	300,	0.0365963380,	0.1408594923E+01,	0.100E+01,	0.100E+00
0.314925,	.500000E-01,	300,	-0.1301902750,	0.1197907629E+01,	0.100E+01,	0.100E+01
0.314925,	.500000E-01,	300,	-0.1606303254,	0.1141241896E+01,	0.100E+00,	0.100E+01
0.314925,	.500000E-01,	300,	-0.1526594279,	0.1132736355E+01,	0.100E-01,	0.100E+01
0.314925,	.500000E-01,	300,	-0.1490486252,	0.1131462721E+01,	0.100E-02,	0.100E+01
0.314925,	.500000E-01,	300,	-0.1484909442,	0.1131306057E+01,	0.100E-03,	0.100E+01
0.314925,	.500000E-01,	300,	-0.1484316178,	0.1131289859E+01,	0.100E-04,	0.100E+01
0.314925,	.500000E-01,	300,	-0.1484256465,	0.1131288234E+01,	0.100E-05,	0.100E+01
0.314925,	.500000E-01,	300,	-0.1484249826,	0.1131288053E+01,	0.000E+00,	0.100E+01

Rotation Results:CRAY X-MP

alpha	eps	n	force	torque	beta	betap
0.141304,	.100000E-01,	300,	-0.1573606013,	0.1399035295E+01,	0.100E+01,	0.100E+01
0.141304,	.100000E-01,	500,	-0.1573606810,	0.1399035313E+01,	0.100E+01,	0.100E+01
0.141304,	.100000E-01,	700,	-0.1573606819,	0.1399035313E+01,	0.100E+01,	0.100E+01
0.141304,	.100000E-01,	1000,	-0.1573606820,	0.1399035313E+01,	0.100E+01,	0.100E+01
0.141304,	.100000E-01,	1000,	0.3686898702,	0.2240797649E+01,	0.100E+01,	0.000E+00
0.141304,	.100000E-01,	1000,	0.3686886336,	0.2240793876E+01,	0.100E+01,	0.100E-06
0.141304,	.100000E-01,	1000,	0.3686775038,	0.2240759918E+01,	0.100E+01,	0.100E-05
0.141304,	.100000E-01,	1000,	0.3685661568,	0.2240420643E+01,	0.100E+01,	0.100E-04
0.141304,	.100000E-01,	1000,	0.3674480684,	0.2237057459E+01,	0.100E+01,	0.100E-03
0.141304,	.100000E-01,	1000,	0.3559968875,	0.2206030772E+01,	0.100E+01,	0.100E-02
0.141304,	.100000E-01,	1000,	0.2586364602,	0.2019904203E+01,	0.100E+01,	0.100E-01
0.141304,	.100000E-01,	1000,	0.0011998883,	0.1638009443E+01,	0.100E+01,	0.100E+00
0.141304,	.100000E-01,	1000,	-0.1573606820,	0.1399035313E+01,	0.100E+01,	0.100E+01
0.141304,	.100000E-01,	1000,	-0.1721278330,	0.1342391961E+01,	0.100E+00,	0.100E+01
0.141304,	.100000E-01,	1000,	-0.1610741193,	0.1333785530E+01,	0.100E-01,	0.100E+01
0.141304,	.100000E-01,	1000,	-0.1569489042,	0.1332445806E+01,	0.100E-02,	0.100E+01
0.141304,	.100000E-01,	1000,	-0.1562801425,	0.1332271116E+01,	0.100E-03,	0.100E+01
0.141304,	.100000E-01,	1000,	-0.1562077365,	0.1332252765E+01,	0.100E-04,	0.100E+01
0.141304,	.100000E-01,	1000,	-0.1562004337,	0.1332250921E+01,	0.100E-05,	0.100E+01
0.141304,	.100000E-01,	1000,	-0.1561996216,	0.1332250715E+01,	0.000E+00,	0.100E+01
0.141304,	.100000E-01,	500,	-0.1721161539,	0.1342389914E+01,	0.100E+00,	0.100E+01
0.141304,	.100000E-01,	500,	-0.1608458582,	0.1333748351E+01,	0.100E-01,	0.100E+01
0.141304,	.100000E-01,	500,	-0.1568340095,	0.1332427262E+01,	0.100E-02,	0.100E+01
0.141304,	.100000E-01,	500,	-0.1562657673,	0.1332268798E+01,	0.100E-03,	0.100E+01
0.141304,	.100000E-01,	500,	-0.1562062649,	0.1332252528E+01,	0.100E-04,	0.100E+01
0.141304,	.100000E-01,	500,	-0.1562002862,	0.1332250897E+01,	0.100E-05,	0.100E+01
0.099958,	.500000E-02,	1000,	-0.1621604059,	0.1496085032E+01,	0.100E+01,	0.100E+01
0.099958,	.500000E-02,	1500,	-0.1621604059,	0.1496085032E+01,	0.100E+01,	0.100E+01
0.099958,	.500000E-02,	1000,	0.4559275880,	0.2505941376E+01,	0.110E+02,	0.000E+00
0.099958,	.500000E-02,	1000,	0.4559250336,	0.2505933639E+01,	0.100E+01,	0.100E-06
0.099958,	.500000E-02,	1000,	0.4559020426,	0.2505864012E+01,	0.100E+01,	0.100E-05
0.099958,	.500000E-02,	1000,	0.4556719418,	0.2505168948E+01,	0.100E+01,	0.100E-04
0.099958,	.500000E-02,	1000,	0.4533537605,	0.2498335327E+01,	0.100E+01,	0.100E-03
0.099958,	.500000E-02,	1000,	0.4296621505,	0.2439299404E+01,	0.100E+01,	0.100E-02
0.099958,	.500000E-02,	1000,	0.2704083349,	0.2162585188E+01,	0.100E+01,	0.100E-01
0.099958,	.500000E-02,	1000,	-0.0132190448,	0.1736855570E+01,	0.100E+01,	0.100E+00
0.099958,	.500000E-02,	1000,	-0.1621604059,	0.1496085032E+01,	0.100E+01,	0.100E+01
0.099958,	.500000E-02,	1000,	-0.1737299526,	0.1439660173E+01,	0.100E+00,	0.100E+01
0.099958,	.500000E-02,	1000,	-0.1620696579,	0.1431042173E+01,	0.100E-01,	0.100E+01
0.099958,	.500000E-02,	1000,	-0.1579013288,	0.1429701038E+01,	0.100E-02,	0.100E+01
0.099958,	.500000E-02,	1000,	-0.1572720567,	0.1429533012E+01,	0.100E-03,	0.100E+01
0.099958,	.500000E-02,	1000,	-0.1572052233,	0.1429515584E+01,	0.100E-04,	0.100E+01
0.099958,	.500000E-02,	1000,	-0.1571984974,	0.1429513834E+01,	0.100E-05,	0.100E+01
0.099958,	.500000E-02,	1000,	-0.1571977496,	0.1429513640E+01,	0.000E+00,	0.100E+01

Rotation Results:CRAY X-MP

alpha	eps	n	force	torque	beta	betap
0.044718,	.100000E-02,	1500,	-0.1668064482,	0.1730846772E+01,	0.100E+01,	0.100E+01
0.044718,	.100000E-02,	2000,	-0.1668064497,	0.1730846772E+01,	0.100E+01,	0.100E+01
0.044718,	.100000E-02,	2500,	-0.1668064498,	0.1730846772E+01,	0.100E+01,	0.100E+01
0.044718,	.100000E-02,	2000,	0.6654824597,	0.3137983757E+01,	0.100E+01,	0.000E+00
0.044718,	.100000E-02,	2000,	0.6654692748,	0.3137944106E+01,	0.100E+01,	0.100E-06
0.044718,	.100000E-02,	2000,	0.6653505630,	0.3137587559E+01,	0.100E+01,	0.100E-05
0.044718,	.100000E-02,	2000,	0.6641589491,	0.3134051886E+01,	0.100E+01,	0.100E-04
0.044718,	.100000E-02,	2000,	0.6519830709,	0.3101324497E+01,	0.100E+01,	0.100E-03
0.044718,	.100000E-02,	2000,	0.5480656589,	0.2900254407E+01,	0.100E+01,	0.100E-02
0.044718,	.100000E-02,	2000,	0.2498365544,	0.2433080389E+01,	0.100E+01,	0.100E-01
0.044718,	.100000E-02,	2000,	-0.0323463963,	0.1971652027E+01,	0.100E+01,	0.100E+00
0.044718,	.100000E-02,	2000,	-0.1668064497,	0.1730846772E+01,	0.100E+01,	0.100E+01
0.044718,	.100000E-02,	2000,	-0.1750961627,	0.1674712297E+01,	0.100E+00,	0.100E+01
0.044718,	.100000E-02,	2000,	-0.1629063828,	0.1666099767E+01,	0.100E-01,	0.100E+01
0.044718,	.100000E-02,	2000,	-0.1586931240,	0.1664757947E+01,	0.100E-02,	0.100E+01
0.044718,	.100000E-02,	2000,	-0.1580731893,	0.1664591904E+01,	0.100E-03,	0.100E+01
0.044718,	.100000E-02,	2000,	-0.1580077135,	0.1664574740E+01,	0.100E-04,	0.100E+01
0.044718,	.100000E-02,	2000,	-0.1580011284,	0.1664573017E+01,	0.100E-05,	0.100E+01
0.044718,	.100000E-02,	2000,	-0.1580003963,	0.1664572826E+01,	0.000E+00,	0.100E+01
0.031621,	.500000E-03,	2200,	-0.1675204831,	0.1833800721E+01,	0.100E+01,	0.100E+01
0.031621,	.500000E-03,	2500,	-0.1675204839,	0.1833800721E+01,	0.100E+01,	0.100E+01
0.031621,	.500000E-03,	2500,	0.7571220818,	0.3413430693E+01,	0.100E+01,	0.000E+00
0.031621,	.500000E-03,	2500,	0.7570955778,	0.3413351089E+01,	0.100E+01,	0.100E-06
0.031621,	.500000E-03,	2500,	0.7568568520,	0.3412635876E+01,	0.100E+01,	0.100E-05
0.031621,	.500000E-03,	2500,	0.7544526645,	0.3405601229E+01,	0.100E+01,	0.100E-04
0.031621,	.500000E-03,	2500,	0.7299202028,	0.3344603542E+01,	0.100E+01,	0.100E-03
0.031621,	.500000E-03,	2500,	0.5634107691,	0.3051613682E+01,	0.100E+01,	0.100E-02
0.031621,	.500000E-03,	2500,	0.2376045077,	0.2538600396E+01,	0.100E+01,	0.100E-01
0.031621,	.500000E-03,	2500,	-0.0360571070,	0.2074391641E+01,	0.100E+01,	0.100E+00
0.031621,	.500000E-03,	2500,	-0.1675204839,	0.1833800721E+01,	0.100E+01,	0.100E+01
0.031621,	.500000E-03,	2500,	-0.1752775353,	0.1777720524E+01,	0.100E+00,	0.100E+01
0.031621,	.500000E-03,	2500,	-0.1629657304,	0.1769103208E+01,	0.100E-01,	0.100E+01
0.031621,	.500000E-03,	2500,	-0.1587732318,	0.1767766062E+01,	0.100E-02,	0.100E+01
0.031621,	.500000E-03,	2500,	-0.1581712920,	0.1767603062E+01,	0.100E-03,	0.100E+01
0.031621,	.500000E-03,	2500,	-0.1581080487,	0.1767586272E+01,	0.100E-04,	0.100E+01
0.031621,	.500000E-03,	2500,	-0.1581016917,	0.1767584588E+01,	0.100E-05,	0.100E+01
0.031621,	.500000E-03,	2500,	-0.1581009850,	0.1767584401E+01,	0.000E+00,	0.100E+01
0.014142,	.100000E-03,	2500,	-0.1681703851,	0.2074290757E+01,	0.100E+01,	0.100E+01
0.014142,	.100000E-03,	5000,	-0.1681707005,	0.2074290829E+01,	0.100E+01,	0.100E+01
0.014142,	.100000E-03,	7500,	-0.1681707015,	0.2074290830E+01,	0.100E+01,	0.100E+01
0.014142,	.100000E-03,	5000,	0.9709996963,	0.4055549051E+01,	0.100E+01,	0.000E+00
0.014142,	.100000E-03,	5000,	0.9708665117,	0.4055149858E+01,	0.100E+01,	0.100E-06
0.014142,	.100000E-03,	5000,	0.9696633187,	0.4051587256E+01,	0.100E+01,	0.100E-05
0.014142,	.100000E-03,	5000,	0.9573727238,	0.4018592949E+01,	0.100E+01,	0.100E-04
0.014142,	.100000E-03,	5000,	0.8523786739,	0.3815060343E+01,	0.100E+01,	0.100E-03
0.014142,	.100000E-03,	5000,	0.5460138938,	0.3330071634E+01,	0.100E+01,	0.100E-02
0.014142,	.100000E-03,	5000,	0.2203104263,	0.2779633368E+01,	0.100E+01,	0.100E-01
0.014142,	.100000E-03,	5000,	-0.0398176354,	0.2314592990E+01,	0.100E+01,	0.100E+00
0.014142,	.100000E-03,	5000,	-0.1681707005,	0.2074290829E+01,	0.100E+01,	0.100E+01
0.014142,	.100000E-03,	5000,	-0.1754286897,	0.2018264487E+01,	0.100E+00,	0.100E+01
0.014142,	.100000E-03,	5000,	-0.1630005708,	0.2009642496E+01,	0.100E-01,	0.100E+01
0.014142,	.100000E-03,	5000,	-0.1588346821,	0.2008310976E+01,	0.100E-02,	0.100E+01
0.014142,	.100000E-03,	5000,	-0.1582495421,	0.2008150829E+01,	0.100E-03,	0.100E+01
0.014142,	.100000E-03,	5000,	-0.1581883306,	0.2008134382E+01,	0.100E-04,	0.100E+01
0.014142,	.100000E-03,	5000,	-0.1581821808,	0.2008132732E+01,	0.100E-05,	0.100E+01
0.014142,	.100000E-03,	5000,	-0.1581814972,	0.2008132549E+01,	0.000E+00,	0.100E+01

Rotation Results:CRAY X-MP

alpha	eps	n	force	torque	beta	betap
0.010000,	.500000E-04,	7500,	-0.1682651840,	0.2178128610E+01,	0.100E+01,	0.100E+01
0.010000,	.500000E-04,	10000,	-0.1682651845,	0.2178128610E+01,	0.100E+01,	0.100E+01
0.010000,	.500000E-04,	7500,	1.0633149477,	0.4332566049E+01,	0.100E+01,	0.000E+00
0.010000,	.500000E-04,	7500,	1.0630482896,	0.4331767909E+01,	0.100E+01,	0.100E-06
0.010000,	.500000E-04,	7500,	1.0606312499,	0.4324703407E+01,	0.100E+01,	0.100E-05
0.010000,	.500000E-04,	7500,	1.0359722251,	0.4263411950E+01,	0.100E+01,	0.100E-04
0.010000,	.500000E-04,	7500,	0.8683136936,	0.3967819088E+01,	0.100E+01,	0.100E-03
0.010000,	.500000E-04,	7500,	0.5342121819,	0.3436746052E+01,	0.100E+01,	0.100E-02
0.010000,	.500000E-04,	7500,	0.2168347794,	0.2883301837E+01,	0.100E+01,	0.100E-01
0.010000,	.500000E-04,	7500,	-0.0404200705,	0.2418375991E+01,	0.100E+01,	0.100E+00
0.010000,	.500000E-04,	7500,	-0.1682651840,	0.2178128610E+01,	0.100E+01,	0.100E+01
0.010000,	.500000E-04,	7500,	-0.1754520109,	0.2122111343E+01,	0.100E+00,	0.100E+01
0.010000,	.500000E-04,	7500,	-0.1630418227,	0.2113494471E+01,	0.100E-01,	0.100E+01
0.010000,	.500000E-04,	7500,	-0.1588555074,	0.2112159743E+01,	0.100E-02,	0.100E+01
0.010000,	.500000E-04,	7500,	-0.1582608681,	0.2111998056E+01,	0.100E-03,	0.100E+01
0.010000,	.500000E-04,	7500,	-0.1581985252,	0.2111981425E+01,	0.100E-04,	0.100E+01
0.010000,	.500000E-04,	7500,	-0.1581922602,	0.2111979757E+01,	0.100E-05,	0.100E+01
0.010000,	.500000E-04,	7500,	-0.1581915638,	0.2111979572E+01,	0.000E+00,	0.100E+01
0.003162,	.500000E-05,	9000,	-0.1683589816,	0.2523380836E+01,	0.100E+01,	0.100E+01
0.003162,	.500000E-05,	10000,	-0.1683597098,	0.2523381002E+01,	0.100E+01,	0.100E+01
0.003162,	.500000E-05,	15000,	-0.1683603727,	0.2523381154E+01,	0.100E+01,	0.100E+01
0.003162,	.500000E-05,	10000,	1.3702207241,	0.5253355551E+01,	0.100E+01,	0.000E+00
0.003162,	.500000E-05,	10000,	1.3675351266,	0.5245488497E+01,	0.100E+01,	0.100E-06
0.003162,	.500000E-05,	10000,	1.3428591870,	0.5184157827E+01,	0.100E+01,	0.100E-05
0.003162,	.500000E-05,	10000,	1.1750429698,	0.4888206173E+01,	0.100E+01,	0.100E-04
0.003162,	.500000E-05,	10000,	0.8396854786,	0.4354343928E+01,	0.100E+01,	0.100E-03
0.003162,	.500000E-05,	10000,	0.5138394847,	0.3782603244E+01,	0.100E+01,	0.100E-02
0.003162,	.500000E-05,	10000,	0.2126845946,	0.3228237270E+01,	0.100E+01,	0.100E-01
0.003162,	.500000E-05,	10000,	-0.0410641505,	0.2763565280E+01,	0.100E+01,	0.100E+00
0.003162,	.500000E-05,	10000,	-0.1683597094,	0.2523381002E+01,	0.100E+01,	0.100E+01
0.003162,	.500000E-05,	10000,	-0.1752892504,	0.2467340570E+01,	0.100E+00,	0.100E+01
0.003162,	.500000E-05,	10000,	-0.1623589649,	0.2458642288E+01,	0.100E-01,	0.100E+01
0.003162,	.500000E-05,	10000,	-0.1586987895,	0.2457394966E+01,	0.100E-02,	0.100E+01
0.003162,	.500000E-05,	10000,	-0.1582514811,	0.2457257432E+01,	0.100E-03,	0.100E+01
0.003162,	.500000E-05,	10000,	-0.1582057205,	0.2457243516E+01,	0.100E-04,	0.100E+01
0.003162,	.500000E-05,	10000,	-0.1582011339,	0.2457242123E+01,	0.100E-05,	0.100E+01
0.003162,	.500000E-05,	10000,	-0.1582006241,	0.2457241968E+01,	0.000E+00,	0.100E+01

Rotation Results:CRAY X-MP

alpha	eps	n	force	torque	beta	betap
0.001000,	.500000E-06,	10000,	-0.1678451033,	0.2868633642E+01,	0.100E+01,	0.100E+01
0.001000,	.500000E-06,	15000,	-0.1683063425,	0.2868737537E+01,	0.100E+01,	0.100E+01
0.001000,	.500000E-06,	15000,	1.6772197815,	0.6174359634E+01,	0.100E+01,	0.000E+00
0.001000,	.500000E-06,	15000,	1.6772197815,	0.6174359634E+01,	0.100E+01,	0.000E+00
0.001000,	.500000E-06,	15000,	1.6498558618,	0.6105156497E+01,	0.100E+01,	0.100E-06
0.001000,	.500000E-06,	15000,	1.4820198722,	0.5809158978E+01,	0.100E+01,	0.100E-05
0.001000,	.500000E-06,	15000,	1.1464939454,	0.5274919219E+01,	0.100E+01,	0.100E-04
0.001000,	.500000E-06,	15000,	0.8193750863,	0.4700364349E+01,	0.100E+01,	0.100E-03
0.001000,	.500000E-06,	15000,	0.5097302136,	0.4127678002E+01,	0.100E+01,	0.100E-02
0.001000,	.500000E-06,	15000,	0.2120618552,	0.3573545129E+01,	0.100E+01,	0.100E-01
0.001000,	.500000E-06,	15000,	-0.0411491840,	0.3108927423E+01,	0.100E+01,	0.100E+00
0.001000,	.500000E-06,	15000,	-0.1683063436,	0.2868737539E+01,	0.100E+01,	0.100E+01
0.001000,	.500000E-06,	15000,	-0.1740445868,	0.2812492738E+01,	0.100E+00,	0.100E+01
0.001000,	.500000E-06,	15000,	-0.1612856359,	0.2803837894E+01,	0.100E-01,	0.100E+01
0.001000,	.500000E-06,	15000,	-0.1585418754,	0.2802741791E+01,	0.100E-02,	0.100E+01
0.001000,	.500000E-06,	15000,	-0.1582359218,	0.2802627356E+01,	0.100E-03,	0.100E+01
0.001000,	.500000E-06,	15000,	-0.1582049729,	0.2802615857E+01,	0.100E-04,	0.100E+01
0.001000,	.500000E-06,	15000,	-0.1582018744,	0.2802614706E+01,	0.100E-05,	0.100E+01
0.001000,	.500000E-06,	15000,	-0.1582015298,	0.2802614576E+01,	0.000E+00,	0.100E+01
0.000447,	.100000E-06,	14000,	-0.1637052354,	0.3109051603E+01,	0.100E+01,	0.100E+01
0.000047,	.111456E-08,	15000,	0.0892584195,	0.3270136071E+01,	0.100E+01,	0.100E+01
0.000447,	.100000E-06,	15000,	1.8918871023,	0.6818074388E+01,	0.100E+01,	0.000E+00
0.000447,	.100000E-06,	15000,	1.7730755352,	0.6577144653E+01,	0.100E+01,	0.100E-06
0.000447,	.100000E-06,	15000,	1.4652855413,	0.6088970534E+01,	0.100E+01,	0.100E-05
0.000447,	.100000E-06,	15000,	1.1296990001,	0.5517067892E+01,	0.100E+01,	0.100E-04
0.000447,	.100000E-06,	15000,	0.8159372687,	0.4941477876E+01,	0.100E+01,	0.100E-03
0.000447,	.100000E-06,	15000,	0.5092865126,	0.4368967048E+01,	0.100E+01,	0.100E-02
0.000447,	.100000E-06,	15000,	0.2120724627,	0.3814890728E+01,	0.100E+01,	0.100E-01
0.000447,	.100000E-06,	15000,	-0.0409863533,	0.3350256549E+01,	0.100E+01,	0.100E+00
0.000447,	.100000E-06,	15000,	-0.1649573826,	0.3109371074E+01,	0.100E+01,	0.100E+01
0.000447,	.100000E-06,	15000,	-0.1674742993,	0.3052733999E+01,	0.100E+00,	0.100E+01
0.000447,	.100000E-06,	15000,	-0.1595024529,	0.3044919417E+01,	0.100E-01,	0.100E+01
0.000447,	.100000E-06,	15000,	-0.1582672786,	0.3044067855E+01,	0.100E-02,	0.100E+01
0.000447,	.100000E-06,	15000,	-0.1581374417,	0.3043981755E+01,	0.100E-03,	0.100E+01
0.000447,	.100000E-06,	15000,	-0.1581243921,	0.3043973120E+01,	0.100E-04,	0.100E+01
0.000447,	.100000E-06,	15000,	-0.1581230865,	0.3043972260E+01,	0.100E-05,	0.100E+01
0.000447,	.100000E-06,	15000,	-0.1581229406,	0.3043972160E+01,	0.000E+00,	0.100E+01
0.000316,	.500000E-07,	15000,	-0.1563046897,	0.3146412849E+01,	0.000E+00,	0.100E+01

Bibliography

[1] A. Ambari, B. Gauthier-Manuel and E. Guyon. Wall effects on a sphere translating at constant velocity. *Journal of Fluid Mechanics*, 1984, Vol. 149, pp. 235-253.

[2] A. Ambari, B. Gauthier-Manuel and E. Guyon. Effect of a plane wall on a sphere moving parallel to it. *Le Journal De Physique - Lettres*, 1983, Vol. 44, pp. L143-146.

[3] H. Brenner. The slow motion of a sphere through a viscous fluid towards a plane surface. *Chemical Engineering Science*, 1961, Vol. 166, pp. 242-251.

[4] J. J. Carty, Jr. Resistance coefficients for spheres on a plane boundary. B.S. Thesis, Massachusetts Institute of Technology, Cambridge, Massachusetts, 1957.

[5] M. Chen and J. B. McLaughlin. Optical meaurements of gap in the lubrication limit. Presented at the American Institute of Chemical Engineers 1991 Summer National Meeting, August 18, 1991, Pittsburgh, Pennsylvania.

[6] R. G. Cox and H. Brenner. Slow viscous motion of a sphere parallel to a plane wall - II Small gap widths, including inertial effects. *Chemical Engineering Science*, 1967, Vol. 22, pp. 1753-1777.

[7] W. R. Dean and M. E. O'Neill. A slow motion of viscous liquid caused by the rotation of a solid sphere. *Mathematika*, 1963, Vol. 10, pp. 13-24.

[8] A. J. Goldman. Investigations in low Reynolds number fluid-particle dynamics, Volume II, Motion of a spherical particle in the presence of a plane subject to

a shear velocity at low Reynolds number. Ph.D. Thesis, New York University, New York, New York, 1965.

[9] A. J. Goldman, R. G. Cox and H. Brenner. The slow motion of two identical arbitrarily oriented spheres through a viscous fluid. *Chemical Engineering Science*, 1966, Vol. 21, pp. 1151-1170.

[10] A. J. Goldman, R. G. Cox and H. Brenner. Slow viscous motion of a sphere parallel to a plane wall - I Motion of a quiescent fluid. *Chemical Engineering Science*, 1967, Vol. 22, pp. 637-651.

[11] S. L. Goren. The hydrodynamic force resisting the approach of a sphere to a plane wall in slip flow. *Journal of Colloid and Interface Science*, 1973, Vol. 44, No. 2, pp. 356-360.

[12] S. L. Goren. The hydrodynamic force resisting the approach of a sphere to a plane permeable wall. *Journal of Colloid and Interface Science*, 1979, Vol. 69, pp. 78-85.

[13] J. Happel and H. Brenner *Low Reynolds Number Hydrodynamics.* Martinus Nijhoff Publishers, Dordrecht, The Netherlands, 1983.

[14] F. B. Hildebrand *Advanced Calculus for Applications.* Prentice Hall, Inc., Englewood Cliffs, New Jersey, 1976.

[15] G. B. Jeffrey. On a form solution of Laplace's equation suitable for problems relating to two spheres. *Proceedings of the Royal Society of London, A: Mathematical and Physical Sciences*, ,Vol 87, pp. 109-120.

[16] H. E. King, Jr., R. L. Cook, and E. Herbolzheimer. Wall-effect drag on a rolling sphere in a diamond-anvil cell. Presented at the American Institute of Chemical Engineers 1991 Summer National Meeting, August 18, 1991, Pittsburgh, Pennsylvania.

[17] A. C. Li, M. H. Kim, T. Jiang and J. C. Slattery. Flows of neutrally buoyant suspensions in several viscometers. *Chemical Engineering Communications*, 1988, Vol. 73, pp. 95-119.

[18] S. H. Lee, R. S. Chadwick and L. G. Leal. Motion of a sphere in the presence of a plane interface. Part 1. An approximate solution by generalization of the method of Lorentz. *Journal of Fluid Mechanics*, 1979, Vol. 93, part 4, pp. 705-726.

[19] S. H. Lee and L. G. Leal. Motion of a sphere in the presence of a plane interface. Part 2. An exact solution in bipolar co-ordinates. *Journal of Fluid Mechanics*, 1980, Vol. 98, part 1, pp. 193-224.

[20] G. D. M. MacKay and S. G. Mason. Approach of a solid sphere to a rigid plane interface. *Journal of Colloid Science*, 1961, Vol. 16, No. 6, pp. 632-635.

[21] G. D. M. MacKay, Suzuki and S. G. Mason. Approach of a solid sphere to a rigid plane interface. Part 2 *Journal of Colloid Science*, 1961, Vol. 18, No. 6, pp. 103-104

[22] K. Małysa, T. Dąbroś and T. G. M. Van de Ven. The sedimentation of one sphere past a 2nd attached to a wall. *Journal of Fluid Mechanics*, 1986, Vol. 162, No. 1, pp. 157-170.

[23] K. Małysa and T. G. M. Van de Ven. Hydrodynamic resistance of aggregates approaching a s solid surface. *Journal of Colloid and Interface Science*, 1985, Vol. 107, No. 2, pp. 477-487.

[24] K. Małysa and T. G. M. Van de Ven. Rotational and translational motion of a sphere parallel to a wall. *International Journal of Multiphase Flow*, 1986, Vol. 12, No. 3, pp. 459-468.

[25] A. D. Maude. End effects in a falling sphere viscometer. *British Journal of Applied Physics*, 1961, Vol. 12, pp. 293-295.

[26] J. L. Mege, C. Capo, A. M. Benoliel and P. Bongrand. Determination of binding strength and kinetics of binding initiation. A model study made on the adhesive properties of P388D1 macrophage-like cells. *Cell Biophysics*, 1986, Vol. 8, No. 2, pp. 141-160.

[27] K. Muhle. Particle adhesion in coagulation and bridging flocculation. *Colloid and Polymer Science*, 1985, Vol. 263, pp. 660-672.

[28] A. Nir. On the slow viscous rolling of a sphere in contact with a permeable surface. *Mathematika*, 1980, Vol. 27, pp. 104-112.

[29] A. Nir. On the departure of a sphere from contact with a permeable membrane. *Journal of Engineering Mathematics*, 1981, Vol. 15, pp. 65-75.

[30] M. E. O'Neill. A slow motion of viscous liquid caused by a slowly moving solid sphere. *Mathematika*, 1964, Vol. 11, pp. 67-74.

[31] M. E. O'Neill. A slow motion of viscous liquid caused by a slowly moving solid sphere: An addendum. *Mathematika*, 1967, Vol. 14, pp. 170-172.

[32] M. E. O'Neill, K. B. Ranger and H. Brenner. Slip at the surface of a translating-rotating sphere bisected by a free surface bounding a semi-infinite viscous fluied: Removal of the contact-line singularity. *Physics of Fluids*, 1986, Vol. 29, No. 4, pp. 913-923.

[33] M. E. O'Neill and K. Stewartson. On the slow motion of a sphere parallel to a nearby plane wall. *Journal of Fluid Mechanics*, 1967, Vol. 27, part 4, pp. 705-724.

[34] A. C. Payatakes and G. Dassios. Creeping flow around and through a permeable sphere moving with constant velocity towards a solid wall. *Chemical Engineering Communications*, 1987, Vol. 58, pp. 119-138.

[35] J. R. Smart and D. T. Leighton, Jr. Measurement of the hydrodynamic surface roughness of noncolloidal spheres. *Physics of Fluids A: Fluid Dynamics*, 1989, Vol. 1, pp. 52-60.

[36] M. Stimson and G. B. Jeffery. The motion of two spheres in a viscous fluid. *Proceedings of the Royal Society of London, A: Mathematical and Physical Sciences*, 1926, Vol. 111, pp. 110-126.

[37] J. R. Turner, H. J. Fissan and D. K. Liguras. Clean room applications of particle deposition from stagnation flow - Electrostatic effects. *Journal of Aerosol Science*, 1989, Vol. 20, No. 4, pp. 403-417.

[38] Y. Ye, D. Y. H. Pui, B. Y. H. Liu, S. Opiolka, S. Blumhorst and H. Fissan. Thermophoretic effect of particle deposition on a free standing semiconductor wafer in a clean room. *Journal of Aerosol Science*, 1991, Vol. 22, No. 1, pp. 63-72.